

Digital Fabrication Techniques for 3D Printing with Everyday Materials

Michael L. Rivera
mlrivera@alumni.cmu.edu

Human-Computer Interaction Institute
School of Computer Science
Carnegie Mellon University
Pittsburgh, Pennsylvania, USA

Thesis Committee

Scott E. Hudson (Chair), Carnegie Mellon University
Lining Yao, Carnegie Mellon University
Jeffrey P. Bigham, Carnegie Mellon University
Stefanie Mueller, Massachusetts Institute of Technology

*Submitted in partial fulfillment of the requirements
for the degree of Doctor of Philosophy*

October 2021

CMU-HCII-21-105

IMPRINT

*Digital Fabrication Techniques for 3D Printing
with Everyday Materials*

Copyright © 2021 by Michael L. Rivera.

All rights reserved.

COLOPHON

This thesis document was typeset using \LaTeX and the memoir documentclass. It is a modified version of Friedrich Wiemer’s thesis template¹. That template is based on Aaron Turon’s thesis *Understanding and expressing scalable concurrency*², which is a mixture of classicthesis³ by André Miede and tufte-latex⁴, based on Edward Tufte’s *Beautiful Evidence*.

The bibliography was processed by Biblalex. The text and display typeface is Matthew Carter’s Charter. Monospaced text uses Jim Lyles’s Bitstream Vera Mono (“Bera Mono”).

FUNDING SPONSORS

The work presented in this dissertation was made possible with funding from the National Science Foundation (IIS-1464377, IIS-1718651), the United States Department of Defense (Contract No. FA8721-05-C-0003), Google, H.P. Labs, Estée Lauder Companies Inc., a Google - Center for Minorities and People with Disabilities in Computing and Information Technology (CMD-IT) Diversifying Future Leadership in the Professoriate (LEAP) Alliance Dissertation Fellowship, a Carnegie Mellon University Sansom Endowed Presidential Fellowship, an Adobe Research Fellowship Honorable Mention award, and a Xerox Technical Minority Scholarship.

KEYWORDS

Human-Computer Interaction, Personal Fabrication, Digital Fabrication, 3D Printing, Electrospinning, Textiles, Hydrogels, Environmental Sustainability, Biodegradable Materials, Spent Coffee Grounds

¹https://github.com/pfasante/phd_thesis

²<https://people.mpi-sws.org/~turon/turon-thesis.pdf>

³<https://bitbucket.org/amiede/classicthesis/>

⁴<https://github.com/Tufte-LaTeX/tufte-latex>

Abstract

The recent proliferation of low-cost digital fabrication machines has promised a future of personal fabrication, where individuals have an unprecedented ability to design and produce their own custom physical objects. 3D printing, in particular, has emerged as one of the most promising technologies. The technology enables a wide range of objects to be produced from digital designs. However, most consumer 3D printing processes can only produce objects that are made of a single material, which is typically rigid plastic. In contrast, if we examine the world around us, nearly every object that we interact with daily (e.g., clothes, electronics), is made of a combination of many different types of material. These materials may be hard, soft, conductive, flexible, and even absorbent to meet different structural, functional and aesthetic needs.

Within the context of 3D printing (and more generally digital fabrication), "materials" usually refer to engineering materials—raw bulk materials like plastics that can be shaped in construction or manufacturing for a particular engineering purpose. In this dissertation, we investigate the use of materials with which we generally have interactions (e.g., the textiles that we wear daily), those that we can readily obtain (e.g., in nature) and those that we can make in a kitchen at home as inputs and outputs for digital fabrication. These so-called *everyday materials* extend the capabilities of 3D printing for personal fabrication, and offer new design possibilities with and beyond rigid plastic.

To this end, this dissertation introduces (1) digital fabrication techniques for embedding, creating, and controlling everyday materials with a consumer-grade 3D printing process; and (2) low-cost accessible material formulations, printer modifications (open-source parts, electronic circuits, etc.), and software that extend the material capabilities of current 3D printing set-ups. For each technique, a series of proof-of-concept objects and applications is presented to demonstrate a broadened design space for personal fabrication. This dissertation concludes with a discussion of digital fabrication techniques with everyday materials, and opportunities to lower design barriers, create new design possibilities, and tackle forthcoming challenges with growing access to digital fabrication technologies.

Acknowledgements

Throughout my academic career, I have had the honor of being supported, mentored and inspired by many wonderful people. They have been instrumental in my success as researcher and throughout my doctoral program.

My advisor, Scott Hudson, has provided invaluable mentorship throughout my doctoral program. He gave me the intellectual and financial freedom to pursue research challenges that piqued my interests, even when those challenges required stepping outside of my comfort zone. And when the research took longer than expected, Scott was patient and supportive. I am extremely grateful to Scott for his guidance over the last six years.

I would also like to express my deepest appreciation to my committee members: Lining Yao, Jeffrey Bigham and Stefanie Mueller. Lining has been a tremendous source of support and inspiration. Over the years, she has challenged me to re-think my work and encouraged me to explore new areas and collaborations. My discussions with her have often pushed the boundaries of my imagination. Jeff helped me see my work from new perspectives and encouraged me to think about its impact. Stefanie has been an academic role model for me. She has been a source of encouragement and has provided invaluable feedback and support throughout my dissertation journey. It has been a pleasure to work with all of them.

I am thankful to have received the mentorship and support of Jennifer Mankoff early in my doctoral program, and Norman Badler when I was undergraduate student. I am also indebted to all of my collaborators and research colleagues including Daniel Ashbrook, Melissa Moukperian, Tico Ballagas, Saiganesh Swaminathan, Anhong Guo, Jeeun Kim, Yang Zhang, Gierad Laput, Stephanie Valenica-Valencia, Jack Forman, Yiyuan Wang, Aditi Dhabalia, Joanna McAllister, Junhan Kong, Jonathan Fagert, Joselyn McDonald, Runchang Kang, Zheng Luo, Jen Liu, Kayla Yew, and Andrew Cao. They have given me opportunities to learn, be creative, and grow as a researcher.

The Human-Computer Interaction Institute (HCII) has been a second home to me during my doctoral program. I have been fortunate to work with great friends in two wonderful research labs. From the DevLab, I am immensely grateful to Saiganesh

Swaminathan, Lea Albaugh, Kristin Williams, Jesse Gonzalez, and Megan Hofmann. They have brought joy to my work and life during the doctoral program. I also want to thank my friends in the Morphing Matter Lab: Guanyun Wang, Danli Luo, Jianzhe Gu, Humphrey Yang, Youngwook Do, and Fang Qin. They kept me inspired me and pushed the boundaries of my knowledge.

Words cannot express how grateful I am to Queenie Kravitz for her endless support. She has been a guiding light through the darkest of times as I navigated my way through the PhD program. She has always believed in me and has continually instilled a sense of hope and belonging for me. Without her, I would have never completed the program.

I would also like to extend my gratitude to the all of the faculty, students, and colleagues who I have been lucky to meet, laugh, share meals, and work alongside including Geoff Kaufman, Mayank Goel, Laura Dabbish, Jason Hong, Patrick Carrington, Chris Harrison, Alexandra Ion, Raelin Musuraca, Chinmay Kulkarni, Steven Dang, Franceska Xhakaj, Fannie Liu, Felicia Ng, Toby Li, Mary Beth Kery, Julian Ramos Rojas, Ken Holstein, Judith Uchidiuno, Cole Gleason, Michael Madaio, Alexandra To, Joseph Seering, Nicholas Diana, Rushil Khurana, Alex Sciuto, Abdelkareem Bedri, Haojian Jin, Lynn Kirabo, Nur Yilirum, Zheng Yao, Tianshi Li, Julia Cambre, Samantha Reig, Alex Cabrera, Karan Ahuja, Tianying Chen, Vikram Kamath Cannanure, Alexandria Vail, Cori Faklaris, Anna Kasunic, Amy Cook, Xu Wang, Nathan Hahn, Qian Yang, Beka Gulotta, Dan Tasse, Nikola Banovic, Sauvik Das, Chris MacLellan, Nesra Yannier, Samantha Finkelstein, David Gerritsen, Brandon Taylor, Adrian de Freitas, and anyone who I may have missed. Each of you has made the HCII a very special place for me.

Thank you to Eric Davidson, Ebony Dickey, Marian D'Amico, Carolyn Buzzelli-Stumpf and Lindsay Olshenske for providing administrative support that made my work possible. I am also grateful to Karen Harlan for publicizing my research and generally being excited about the work that is done at the HCII.

Chapter 7 would not have been possible without the generous support of the lovely folks at Arriviste Coffee in Pittsburgh, PA, USA. I am grateful to Kim, Andy, Cole, Cassy, Johanna, and Ethan for providing spent coffee grounds and being excited about the work.

As an undergraduate at the University of Pennsylvania (Penn), I was incredibly lucky to be supported by two of the most caring people that I have ever met. Dr. Theresa Suriano of the Pennsylvania College Achievement Program (PENNCAP) gave me countless

advice, encouraged me to get involved in research, and saw my potential well before I could. She later introduced me to Dr. Bob Lane, who ran the McNair Scholars / Pre-Doctoral Initiative (PDI) Program at Penn. Dr. Bob has an unmatched level of enthusiasm and drive to see students succeed. His mentorship was a huge reason why I attended graduate school. As part of the McNair/PDI program, he helped me gain my first experience presenting research at a conference, prepare graduate school applications, and receive financial support to cover the prohibitively expensive application fees. I owe a huge debt of gratitude to Dr. Theresa Suriano and Dr. Bob Lane. As a doctoral student, I have also received crucial support through the Diversifying Future Leadership in the Professoriate (LEAP) Alliance and the Center for Minorities and People with Disabilities in Information Technology (CMD-IT). I deeply appreciate PENNCAP, the McNair Scholars/PDI program, the LEAP Alliance, and CMD-IT for providing critical mentorship and assistance that have led to my continued success in higher education.

I am eternally grateful to my parents who paved the way for me and my brother to become first-generation college graduates. I want to thank my parents, my brother and my parents-in-law for their unwavering belief in my ability to succeed. I also want to thank my dear friends, Nicholas McGill and Malori Holloman, for being in my corner and supporting me from a far.

This dissertation is dedicated to my life partner, Siyan Zhao. She is the most patient, kind, and supportive person that I have ever known. She has never lost faith in me and continually lifted me up in one of the most trying times of our both of our lives. I have been the luckiest person to work closely and have immeasurable amounts of fun with her over the last six years. She is a constant reminder that there is much more to life than work. As I look back to the start of the PhD program when we shared a cold, dark cubicle in Newell Simon Hall, there is no other person that I could imagine sharing this journey.

CONTENT ATTRIBUTION

I would like to acknowledge the following icons that are used under Creative Commons Attribution (CC-BY 3.0) license from [the Noun Project](#): "axis" by LAFS, "pattern" by Marta Ambrosetti, "water" by eragon, "liquid" by Mask Icon, "shapes" by mambu, and "textile" by Olena Panasovska are used in [Chapter 5](#); and "coffee beans" by Creative Stall, "particle" by Ilsur Aptukov, "handdrawn salt" by Littledecos, "Spoon" by Yazmin Alanis, "coffee beans & grounds" by Ella Jenkins, "3D Printer" by felix, "Recycle" by nailil jamila, "Cylinder" by Colourcreatype, "Garbage" by Kevin, "Gardener" by Gan Khoon Lay, and "composting" by Al D are used in [Chapter 7](#).

Contents

| | |
|---|-------|
| ABSTRACT | iii |
| ACKNOWLEDGEMENTS | v |
| CONTENTS | ix |
| LIST OF FIGURES | xiv |
| LIST OF TABLES | xxiii |
| PUBLICATIONS | xxv |
| 1 INTRODUCTION | 1 |
| 1.1 Motivation | 1 |
| 1.2 Thesis Contributions | 3 |
| 1.3 Document Structure | 4 |
| 2 OVERVIEW OF 3D PRINTING | 7 |
| 2.1 Vat Photopolymerization | 8 |
| 2.2 Powder Bed Fusion | 9 |
| 2.3 Laminated Object Manufacturing | 10 |
| 2.4 Material Deposition | 11 |
| 2.5 Comparison of 3D Printing Processes | 12 |
| 3 RELATED WORK | 13 |
| 3.1 Computational Design | 14 |
| 3.1.1 Mechanical Properties | 15 |
| 3.1.2 Optical Properties | 17 |
| 3.1.3 Acoustic Properties | 19 |
| 3.1.4 Thermal Properties | 20 |
| 3.1.5 Electrical and Magnetic Properties | 20 |
| 3.1.6 Perceptual Properties | 21 |
| 3.1.7 Summary | 22 |
| 3.2 Mixed Approaches | 22 |
| 3.2.1 Reducing Fabrication Time | 22 |
| 3.2.2 Repair, Adaptation and Augmentation | 23 |

| | | |
|-------|--|----|
| 3.2.3 | Fabricating Large-Scale Objects | 24 |
| 3.2.4 | Enabling Custom Interactive Devices | 24 |
| 3.2.5 | Summary | 26 |
| 3.3 | New Materials and Processes | 26 |
| 3.3.1 | Rapid and Large-Scale Printing | 26 |
| 3.3.2 | Composite Materials | 27 |
| 3.3.3 | Interactive Capabilities | 27 |
| 3.3.4 | Soft Materials | 27 |
| 3.3.5 | Summary | 28 |
| 3.4 | Discussion | 29 |
| 4 | 3D PRINTING WITH EMBEDDED TEXTILES | 33 |
| 4.1 | Introduction | 33 |
| 4.2 | Background | 34 |
| 4.3 | Basic Techniques for 3D Printing with Textiles | 36 |
| 4.3.1 | Adherence | 37 |
| 4.3.2 | Stabilization | 41 |
| 4.3.3 | Printing Beyond a Single Layer | 43 |
| 4.4 | Design Primitives | 43 |
| 4.4.1 | Selective Stiffening | 43 |
| 4.4.2 | Selective Adherence | 45 |
| 4.4.3 | Mechanical Action | 46 |
| 4.4.4 | Fast Production | 46 |
| 4.4.5 | Large Objects | 46 |
| 4.4.6 | Textile Reconfiguration | 47 |
| 4.4.7 | Summary | 47 |
| 4.5 | Input Devices | 48 |
| 4.5.1 | Slider | 50 |
| 4.5.2 | Knob | 50 |
| 4.5.3 | Button | 50 |
| 4.6 | Applications | 51 |
| 4.6.1 | Actuated Box with Interactive Control | 51 |
| 4.6.2 | Six-Panel Fabric Lampshade | 52 |
| 4.6.3 | Folding Polyhedron | 53 |
| 4.6.4 | Crown | 53 |
| 4.6.5 | Flex Watchband | 54 |
| 4.7 | Discussion and Limitations | 55 |

| | | |
|-------|---|----|
| 4.8 | Conclusion | 56 |
| 5 | 3D PRINTING WITH HYDROGEL AND EMBEDDED TEXTILES | 57 |
| 5.1 | Introduction | 57 |
| 5.2 | Background | 57 |
| 5.3 | Fabrication Technique | 58 |
| 5.3.1 | Hydrogel Preparation | 58 |
| 5.3.2 | Printer Construction | 59 |
| 5.3.3 | Hydrogel Printing Parameters | 60 |
| 5.4 | Exploration of Hydrogel-Textile Composites | 60 |
| 5.5 | Software Design Tool | 64 |
| 5.5.1 | Mesh Generation | 64 |
| 5.5.2 | Material Model | 65 |
| 5.5.3 | Physically-based Simulation | 67 |
| 5.6 | Example Applications | 67 |
| 5.6.1 | Weather-Responsive Direction Indicator | 67 |
| 5.6.2 | Texture-Changing Garment | 68 |
| 5.6.3 | Responsive Plant Watering Reminder | 68 |
| 5.7 | Discussion And Limitations | 69 |
| 5.8 | Conclusion | 69 |
| 6 | A 3D PRINTER FOR ELECTROSPUN TEXTILES | 71 |
| 6.1 | Introduction | 71 |
| 6.2 | Background | 71 |
| 6.2.1 | Electrospinning | 72 |
| 6.3 | Electrospinning 3D Printer Construction | 74 |
| 6.3.1 | 3D Printer Firmware | 78 |
| 6.3.2 | 3D Printing of PLA and Electrospun PLA Fibers | 78 |
| 6.4 | Electrospinning Process Parameters | 79 |
| 6.4.1 | Extrusion Rate | 79 |
| 6.4.2 | Temperature | 80 |
| 6.4.3 | Infill Density | 80 |
| 6.5 | Soft Sensor Fabrication | 82 |
| 6.5.1 | Capacitive Sensing | 83 |
| 6.5.2 | Piezoresistive Sensing | 83 |
| 6.5.3 | Liquid Absorption Sensing | 83 |
| 6.6 | Applications | 85 |

| | | |
|-------|---|-----|
| 6.6.1 | Water Me: Actuated Flower Reminder | 85 |
| 6.6.2 | Interactive Woolly the Sheep Comic | 86 |
| 6.6.3 | Foldaway Phone Stand | 87 |
| 6.6.4 | Textile Origami Lamp and Controls | 88 |
| 6.7 | Discussion and Limitations | 88 |
| 6.8 | Conclusion | 89 |
| 7 | 3D PRINTING WITH A NOVEL BIODEGRADABLE MATERIAL | 91 |
| 7.1 | Introduction | 91 |
| 7.2 | Background | 91 |
| 7.3 | Material Design | 95 |
| 7.3.1 | Spent Coffee Grounds | 97 |
| 7.3.2 | Carboxymethyl Cellulose | 97 |
| 7.3.3 | Xanthan Gum | 97 |
| 7.3.4 | Water | 98 |
| 7.4 | Fabrication Technique | 98 |
| 7.4.1 | Material Preparation | 98 |
| 7.4.2 | 3D Printer Set-Up | 99 |
| 7.5 | Workflows and Examples | 100 |
| 7.5.1 | Material Recycling for No-Waste Prototyping | 100 |
| 7.5.2 | Degradation During Use | 100 |
| 7.5.3 | Degradation After Use | 102 |
| 7.6 | Material Characterization | 104 |
| 7.6.1 | Shrinkage Characterization and Mitigation . | 104 |
| 7.6.2 | Strength Characterization | 106 |
| 7.6.3 | Surface Texture Characterization | 108 |
| 7.6.4 | Composting Study | 108 |
| 7.7 | Discussion and Limitations | 111 |
| 7.7.1 | Strength and Resolution of Printed Objects . | 111 |
| 7.7.2 | Material Shrinkage and Drying | 112 |
| 7.7.3 | Material Biodegradability and Compostability | 113 |
| 7.7.4 | Life-Cycle Assessment, Prototyping, and Beyond | 113 |
| 7.8 | Conclusion | 114 |
| 8 | CONCLUSION | 115 |
| 8.1 | Summary | 115 |
| 8.2 | Future Directions | 116 |

| | | |
|-------|---|-----|
| 8.2.1 | Designing Behaviors Around Everyday Materials | 116 |
| 8.2.2 | Modular Machines for Digital Fabrication . . | 117 |
| 8.2.3 | Sustainable Personal Fabrication | 117 |
| 8.3 | Final Remarks | 118 |
| | REFERENCES | 119 |

List of Figures

| | | |
|-----|---|----|
| 1.1 | Examples of everyday objects ranging from textiles, clothing, shoes, mobile devices, paper, wood, chairs, vases, furniture, etc. | 2 |
| 1.2 | Examples new design possibilities enabled when combining digital fabrication techniques with everyday materials including a linked watch band with embedded textiles that absorb sweat; a custom designed crown; and origami lamp with soft input controls; a moisture-responsive plant watering indicator; and two biodegradable espresso cups made from spent coffee grounds. | 3 |
| 4.1 | A range of textile-embedded 3D printed objects fabricated using our techniques—a box with a rolling lid containing a mesh of polyester and strings for actuation (A); a functional watchband printed on a polyester mesh (B); a figure with a pressure-sensitive head that controls an embedded displacement sensor containing a mesh of nylon and spandex fibers (C); a 22-inch (56 cm) crown printed on a single piece of felt that is larger than the print bed (D). | 34 |
| 4.2 | Primitives for stiffening in a single dimension by adding plastic (gray) to fabric (blue). Closely spaced elements printed onto the fabric can prevent it from bending up while allowing it to relax down (A); widely spaced top elements coupled with closely spaced bottom elements enforce the opposite motion (B). Using widely spaced elements allow the fabric to flex in both directions (C), while a solid bar prevents flexing entirely (D). | 36 |
| 4.3 | Plastic extruded onto a textile with a fuzzy surface creates very strong adherence. The plastic seen here is difficult to separate from a piece of felt. | 37 |
| 4.4 | Instron adhesion test setup. Left: attachment of fabric and plastic sample to test column; right: fabric anchor (yellow) with test in progress. | 39 |

| | | |
|------|---|----|
| 4.5 | Photo of the fabrics used in the adhesion test in order of Table 4.1 (A–F) from left to right. The top ruler is in centimeters; the bottom is in inches. | 40 |
| 4.6 | Results of the adhesion test showing force exerted for a given extension. Both graphs are on the same scale; the left is for ABS and the right is for PLA. | 40 |
| 4.7 | Stabilization problems and solutions. Textiles can shift, sag and tilt/twist if not properly secured with tape before printing. | 42 |
| 4.8 | Plastic segments that restrict the bend angles of a textile. | 43 |
| 4.9 | A textile that is only capable of rolling or flexing along the axis parallel to the plastic segments. | 44 |
| 4.10 | Textile-embedded, string actuated mechanical arms with variable bend angles—(A) and (B) show straight segments of plastic lead to a simple roll that aligns with the axis of the channel; (C) and (D) show angled segments of plastic cause the roll to skew to the left. | 45 |
| 4.11 | A shell printed triangular prism first printed flat and then folded to its 3D form. | 47 |
| 4.12 | Snaps printed onto a fabric. | 48 |
| 4.13 | Custom-shaped grommets printed onto a polyester mesh. The centers of the grommets were cut out after printing. | 48 |
| 4.14 | Cross-section of a textile-embedded displacement sensor. The tape is inserted with electrical components during the printing process. The tape acts as temporary support for printing the plunger. It is later removed using an opening on the underside of the object (Figure 4.16). | 49 |
| 4.15 | The displacement sensor’s principle of operation showing maximum light reaching the photoresistor when the plunger is not depressed (A) and reduced light as the plunger is pressed (B). | 49 |
| 4.16 | The displacement sensor’s underside showing the suspended plunger. | 49 |
| 4.17 | Process for fabricating a pressure sensitive button with stretchy fabric | 50 |
| 4.18 | Input devices with embedded textiles—our displacement sensor (A); a retractable slider (B); a knob (C); and a pressure sensitive button (D). | 51 |

| | | |
|------|--|----|
| 4.19 | Textile-embedded box fabricated <i>via</i> controlled bending. The box lid contains a polyester mesh and embedded strings that allow the lid to roll open and unroll closed. | 52 |
| 4.20 | The shell printed lampshade was constructed by gluing together six panels printed onto fabric (A). The top panel incorporated a custom grommet to accommodate a light bulb (B). | 52 |
| 4.21 | A shell-based dodecahedron fabricated by printing through a polyester mesh. The faces of the object were printed flat on a single sheet of mesh that was trimmed after fabrication (A). Rubber bands we used to actuate the shells into final 3D form (B). | 53 |
| 4.22 | A 22-inch crown fabricated by printing in rectangular sections on a single sheet of felt. | 54 |
| 4.23 | A watchband that supports hinging to a watch face (A). Stiffeners on the mesh fabric afford flexibility similar to a linked watchband (B). | 55 |
| | | |
| 5.1 | Hydrogel-textile composites are fabricated by 3D printing hydrogel patterns onto textile substrates. | 57 |
| 5.2 | Hydrogel-textile composites actuate in response to water. As they dehydrate, or dry, they reverse their actuation. | 57 |
| 5.3 | Hydrogel-Textile composite actuator design space. . . | 59 |
| 5.4 | Component view of our hot-end mount design showing the PC4-M6 connector threaded into the hot-end. (A). Our hydrogel hot-end and radial fan mounted onto a 3D printer to the left of a rigid plastic extruder (B). . | 60 |
| 5.5 | Test showing variations in hydrogel patterning produce different actuation states. | 61 |
| 5.8 | The structure of woven textiles gives rise to anisotropic behavior when the textile is stretched. The straight grain has the strongest resistance to deformation followed by the cross grain, and then the bias. | 61 |
| 5.6 | Test showing different actuation is produced based on the type of textile substrate. | 62 |
| 5.7 | Resistance to shape-change with hydrogel printed across the different grains of a woven cotton textile. | 62 |

| | | |
|------|---|----|
| 5.9 | The software design tool for hydrogel-textile composites. The user sketches the desired substrate and hydrogel pattern (A). The tool generates a mesh for the object (B) and begins simulating the actuation behavior (C). | 63 |
| 5.10 | The finished simulation of a hydrogel-textile composite (A) and the result when fabricated (B). | 64 |
| 5.11 | The process of generating a mesh for simulation. A user draws a gel center-lines and substrate boundary curve (1). Using the extrusion width for 3D printing, a gel boundary curve is generated (2). The substrate and gel boundary curves are discretized as a series of vertices (3). Delaunay triangulation is performed with the vertices to generate the mesh for the substrate and gel. | 65 |
| 5.12 | Comparison of actuation behavior of designs when simulated (A) and fabricated (B). | 66 |
| 5.13 | A weather-responsive direction indicator simulated in the design tool and after fabricated. When it is raining outside, the arrow remains flat pointing straight ahead (A/B). When its hydrogel is dry, the arrow bends upwards (C/D). | 67 |
| 5.14 | A moisture-responsive wrist garment that has a spiky texture when the garment is dry (A). The garment is worn around a user's wrist (B). | 68 |
| 5.15 | A flower-shaped hydrogel-textile composite that reminds a user when their living plant needs water. When the soil is dry, the petals are curled up (A). When the plant is watered, the flower petals actuate open to a flat state (B). | 68 |
| 6.1 | A range of objects fabricated on our new 3D printer using rigid plastic and electrospun textiles: (A) a close-up of our printer electrospinning; (B) an origami-style folding lamp with a soft piezoresistive brightness control and a soft capacitive toggle switch; (C) an actuated flower that opens when an electrospun liquid sensor detects sufficient water in the soil; (D) an sheep comic uses capacitive sensing to create an interactive tactile experience. | 72 |

6.2 A simple hinge fabricated with our 3D printer using rigid plastic printing and melt electrospinning on the same extruder. 73

6.3 A typical melt electrospinning setup uses a heated polymer fed into a spinneret. A high electric potential is applied between spinneret tip and the metal collector to propel (typically micron-level) fibers down to the collector. 74

6.4 A simplified representation of how rigid plastic 3D printing and electrospinning are accomplished on our printer. In rigid plastic mode (A), the disabled IR LED triggers the build plate to be connected to the high voltage ground and the high voltage power supply (HVPS) is off. In electrospinning mode (B), the enabled IR LED triggers the build plate to be disconnected from the high voltage ground and the high voltage power supply is enabled. 75

6.5 Our 3D printer that supports melt electrospinning and rigid plastic printing using only the left extruder (A). A close-up of the extruder shows the high voltage ground wire connected to hot-end nozzle (B). We note that (A) shows an additional extruder on the right, which was added to explore printing conductive filament as a third material type. 77

6.6 A series of tests we performed on extrusion rate (A-E), temperature (F-J), and infill density (K-O) to determine melt electrospinning process parameters for our 3D printer. Tool-paths were generated from the geometry of a 30x30mm square swatch using a 3D printer slicer engine. Scale bar: 20mm. 81

6.7 Infill density is positively correlated with the size of fabricated electrospun objects (A). The inverse of this relationship determines a geometry scale factor that when applied to objects prior to slicing will result in an electrospun object of desired size. 82

6.8 Electrospun fibers can be patterned onto conductive materials then bound together with rigid plastic to create custom-shaped capacitive sensors (A). The electrospun textile offers soft touch affordances and compliance to a capacitive sensor (B). 83

- 6.9 Electrospun fibers coated in conductive paint become a piezoresistive sensor (A), changing electrical resistance based on applied pressure (B). 84
- 6.10 Experimental setup (A) and results (B) for evaluating electrospun fibers as a liquid absorption sensor. Each additional drop of water added to the fibers causes an increase in the sensed voltage between the two electrodes fixed at opposite ends of the fibers. 85
- 6.11 A custom-shaped flower made of electrospun textile and rigid plastic that actuates based on the soil's water level sensed using an electrospun liquid absorption sensor. When the soil is dry, the flower closes its petals (A). When the soil is moist, the flower actuates open. 86
- 6.12 An interactive comic featuring a cartoon sheep whose body is made of a custom-shaped electrospun textile for soft capacitive sensing and tactile experience (A). Touching the sheep in various regions of its body produces different sound effects from a "Baaaah" to a giggle (B). 87
- 6.13 A foldaway phone stand fabricated using rigid plastic and electrospun textile. The phone stand is affixed to a phone case (A) and can be deployed when needed to obtain a preferred view angle for watching videos. 87
- 6.14 A custom-shaped origami-style lamp printed using rigid plastic and electrospun textile (A). Once folded into its final form, the lamp is paired with a soft, star-shaped capacitive toggle switch, and an electrospun piezoresistive capsule sensor to control the lamp's brightness (B). 88
- 7.1 Examples of biodegradable objects fabricated using our new 3D printing material: an ornament necklace, two custom-shaped planter pots, and two espresso cups coated in beeswax. 92

7.2 Overview of the personal fabrication workflows enabled with our spent coffee ground material: (1) Previously printed objects can be easily recycled at home to form new printing material; (2) Objects made with our material can readily biodegrade during their use such as a flower planter pot once placed into soil; (3) Objects and printing material that have completed their usage-cycle can be composted at home to create a fertilizer for gardening. These workflows minimize waste output and avoid disposal in landfills. 93

7.3 A biodegradable planter pot being printed using our spent coffee ground material. 95

7.4 After drying, objects made with our material are primarily composed of spent coffee grounds (84.46%). The remaining composition is of carboxymethyl cellulose (13.51%) and xanthan gum (2.03%). 96

7.5 The extrusion set-up used to print our spent coffee ground material on a modified FDM/FFF 3D printer. 99

7.6 Material Recycling Workflow. Objects printed with our SCG material such as prototypes and failed prints (A) can be ground up using a basic coffee grinder at home (B). The resulting granules (C), once weighed, can then be mixed with a proportional amount of water (D) to produce our SCG material again for printing (E). This recycling approach is useful in minimizing waste when printing errors occur as highlighted in the green circle. 101

7.7 A biodegradable ornament necklace that was prototyped and printed with our SCG material (A). The ornament has a printed hoop for attaching a necklace and features the infinity symbol at its center (B). 102

7.8 Biodegradable planter pots printed with our SCG material and their flowering plants (A). The first pot has a hexagonal-shape (B). The second pot is cylindrical with a ribbed pattern (C). 103

7.9 Composting Workflow. Objects made with our SCG material such as prototypes and failed prints (A) can be inserted into a compost box at home (B) with other food scraps (C). Within a few days, microorganisms like mold will grow and begin breaking the material down into compost (D). 103

| | | |
|------|--|-----|
| 7.10 | Biodegradable espresso cups made with our SCG material (A). The cups hold liquid once beeswax is applied either on the inside of the cup (B, left) or around the cup entirely (B, right). | 104 |
| 7.11 | Shrinkage characterization. The average error in dimensional accuracy for five printed samples (30 mm x 30 mm x 5.6 mm) once dried is -14.53% (SD=1.94). | 105 |
| 7.12 | After uniformly scaling the geometry of samples by 15.0% before printing, the average error in dimensional accuracy caused by shrinkage for five printed samples reduced to -1.05% (SD=0.60). | 105 |
| 7.13 | The tensile strength test set-up showing a hook printed with the SCG material holding 1.7 kg of mass (A) before breaking into two separate parts (B). | 107 |
| 7.14 | Results of the tensile strength test. On average, hooks printed with newly made SCG material had a higher maximum stable mass (1.43 kg) and failure mass (1.58 kg) than hooks printed with recycled SCG material with a difference of (0.43 kg). | 107 |
| 7.15 | Comparison of layer lines on test specimens printed with (1) newly made SCG material and (2) material that been recycled from previously printed objects. The surface texture of the recycled material appears less smooth than that of the freshly made material. Scale bar: 5 mm. | 109 |
| 7.16 | Compost Study Results. Material inserted into our home compost box consistently resulted in increased soil temperature relative to ambient temperature, indicating the material's decomposition by microorganisms. This trend of increased temperature continued for more than 80 hours after the material's insertion. The mean ambient and soil temperatures for five occurrences of material insertion are depicted in the bold orange and blue solid lines, respectively. The standard deviation is depicted as shaded regions around the each line. | 110 |
| 7.17 | A few small pieces of SCG material recovered after 3 weeks of composting, distinguishable by the color of the coffee grounds highlighted in the pink rectangular outline above. The recovered pieces were brittle and showed significant mold growth (highlighted in green circles) indicating their decomposition. | 110 |

7.18 A single layer square printed flat with our SCG material morphed into a saddle shape as a result of shrinkage during drying. 112

List of Tables

- 4.1 Properties of the fabrics used in the adhesion test. All fabrics tested were plain weave. Thread count is threads per square inch and weight is grams per square meter. 40
- 7.1 Proportions of the different components that are used to prepare our material for 3D printing. 96

Publications

Much of work appearing in this dissertation has been adapted from the following publications:

1. Michael L. Rivera, Melissa Moukperian, Daniel Ashbrook, Jennifer Mankoff, and Scott E. Hudson. “Stretching the Bounds of 3D Printing with Embedded Textiles”. In: *Proceedings of the 2017 CHI Conference on Human Factors in Computing Systems*. CHI ’17. Denver, Colorado, USA: ACM, 2017, pp. 497–508. DOI: [10.1145/3025453.3025460](https://doi.org/10.1145/3025453.3025460)
2. Michael L. Rivera and Scott E. Hudson. “Desktop Electrospinning: A Single Extruder 3D Printer for Producing Rigid Plastic and Electrospun Textiles”. In: *Proceedings of the 2019 CHI Conference on Human Factors in Computing Systems*. CHI ’19. Glasgow, Scotland Uk: ACM, 2019, 204:1–204:12. DOI: [10.1145/3290605.3300434](https://doi.org/10.1145/3290605.3300434)
3. Michael L. Rivera, Jack Forman, Scott E. Hudson, and Lining Yao. “Hydrogel-Textile Composites: Actuators for Shape-Changing Interfaces”. In: *Extended Abstracts of the 2020 CHI Conference on Human Factors in Computing Systems Extended Abstracts*. CHI ’20. Honolulu, HI, USA: Association for Computing Machinery, 2020, pp. 1–9. DOI: [10.1145/3334480.3382788](https://doi.org/10.1145/3334480.3382788)

1

Introduction

The last two decades have seen a proliferation of low-cost digital fabrication machines. Machines like laser cutters, computer numerical control (CNC) mills, and 3D printers that were previously tools for manufacturing are now entering the homes of consumers and small businesses. The democratization of these technologies promises a future of personal fabrication, where individuals have an unprecedented ability to design and produce their own custom physical objects. Motivated by this vision, research on personal fabrication [21, 86, 195] has sought to broaden access to digital fabrication and expand its capabilities for the masses.

1.1 MOTIVATION

Additive manufacturing, or more commonly referred to as 3D printing, has emerged as one of the most promising technologies for personal fabrication. The technology facilitates placing material freely in space, allowing objects to take on forms that would be difficult or impossible to manufacture in other ways. It is also versatile—a wide range of objects can be produced from digital designs without the need for machines specialized to each manufacturing task.

After key patents on the technology expired, open-source movements like Fab@Home [181] and RepRap [132] propelled low-cost 3D printers into the consumer market. Since then adoption has been steadily growing powered by decreased cost [242]. However, the vision of users being able to design and produce their own custom physical objects has not been fully realized.

Designing objects remains a difficult task that often requires engineering expertise. Thus, many users resort to remixing and



FIGURE 1.1: Examples of everyday objects ranging from textiles, clothing, shoes, mobile devices, paper, wood, chairs, vases, furniture, etc.

printing existing designs from 3D modeling repositories like Thingiverse [114, 206]. Furthermore, most consumer 3D printing processes can only produce objects that are made of a single material [195, 242], which is typically rigid plastic. In contrast, if we examine the world around us, nearly every object that we interact with daily (e.g., clothes, electronics), is made of a combination of many different types of material. These materials may be hard, soft, conductive, flexible, and even absorbent to meet different structural, functional and aesthetic needs (Figure 1.1).

This dissertation is primarily concerned with the challenge of materials. Within the context of digital fabrication machines, "materials" usually refer to *engineering materials* [9] such as plastics and metals—raw bulk materials that can be shaped in construction or manufacturing for a particular engineering purpose. The work here uses a much more expansive definition of materials. Namely, materials are anything with which we can manipulate, shape, and combine for the purpose of making something. We place a particular emphasis on *everyday materials* [346] as inputs and outputs for digital fabrication techniques.

Clement Zheng defines everyday materials as "materials that are common and familiar to the designer and maker" and typically found in their design environments such as paper and pencils [346]. Building on this definition, the work in this thesis captures materials with which we generally have interactions (e.g., the textiles that we wear daily), those that we can readily obtain, for example,



FIGURE 1.2: Examples new design possibilities enabled when combining digital fabrication techniques with everyday materials including a linked watch band with embedded textiles that absorb sweat; a custom designed crown; and origami lamp with soft input controls; a moisture-responsive plant watering indicator; and two biodegradable espresso cups made from spent coffee grounds.

in a supermarket, craft store or nature, and those that we can make in a kitchen at home. This work purposefully uses the lens of everyday materials to devise accessible digital fabrication techniques that extend the capabilities of 3D printing for personal fabrication and offer new design possibilities with and beyond rigid plastic (Figure 1.2).

1.2 THESIS CONTRIBUTIONS

This thesis makes the following contributions:

1. New digital fabrication techniques for embedding, creating, and controlling everyday materials such as textiles with a

consumer-grade 3D printing process.

2. Low-cost accessible material formulations, printer modifications (open-source parts, electronic circuits, etc.), and software that extend the material capabilities of current 3D printing set-ups.
3. A series of proof-of-concept objects, interactive devices, and applications that demonstrate a broadened design space for personal fabrication.
4. A discussion of digital fabrication techniques with everyday materials and opportunities to lower design barriers, create new design possibilities, and tackle forthcoming challenges with growing access to digital fabrication technology.

1.3 DOCUMENT STRUCTURE

This dissertation is structured as follows:

Chapter 2 provides an overview of 3D printing processes with the goal of familiarizing the reader with aspects of the technology and related terminology. A brief comparison of the different processes is provided to motivate the use of material deposition processes throughout this thesis.

Chapter 3 reviews related research on personal fabrication. An emphasis is placed on work in the Human-Computer Interaction and Computer Graphics communities that have sought to broaden access to and extend the capabilities of digital fabrication technologies, and in particular 3D printing.

Chapter 4 introduces new techniques for embedding everyday materials, and in particular textiles, during a consumer-grade 3D printing process. It provides an empirical study of bonding performance between textiles and printed plastic and an exploration of the design space opened by combining the two. Various applications are demonstrated including input devices and objects that can be worn on the body.

Chapter 5 continues examination of textiles, but further introduces a food-grade hydrogel as a printing material. Controlling the deposition of this material with 3D printing enables different substrates to become water-responsive interfaces that actuate in response to moisture. Alongside the material description and fabrication technique, a software design tool is presented to support the creation of such objects.

Chapter 6 demonstrates a new 3D printing process that can fabricate textiles and rigid plastic from a single material. This approach enables control over common textile properties like softness and supports fabricating objects with new capabilities like moisture absorption and light diffusion. Hardware modifications for a consumer 3D printer are described and a series of proof-of-concept applications are presented.

Chapter 7 introduces a new biodegradable material for printing that can serve functional and aesthetic purposes. The material primarily consists of cellulose, hemi-cellulose, and lignin—supplied by spent coffee grounds. As a natural material, it is renewable and more ecologically-friendly than typical plastics. Its biodegradability enables the fabrication objects that are designed to degrade during or after their intended use. A kitchen-friendly material recipe is described, and workflows for rapid prototyping and the design of biodegradable objects are presented.

Finally, **Chapter 8** discusses the contributions of thesis and offers future directions in digital fabrication techniques for/with everyday materials, and more generally in personal fabrication.

2

Overview of 3D Printing

This chapter serves to familiarize the reader with knowledge of the various types of additive manufacturing, or more commonly 3D printing, processes and engineering materials that are currently available. Note that the focus here is not to survey the entire history of 3D printing (for this see [333]). To this end, a brief description of these processes and occasional supporting references are provided. More comprehensive overviews of these additive manufacturing processes, materials, and applications can be found in [31, 204].

One of the first recorded objects to be 3D printed is a model of house from 1981 [144]. Hideo Kodama fabricated the object with a process that he developed to photopolymerize a liquid resin in a layer-by-layer manner. Each layer of the object was represented by a physical mask pattern. As ultraviolet light shined down through a pattern, the non-masked regions of the liquid resin solidified at the surface. By repeatedly changing the pattern and lowering the previously solidified layers into the liquid resin, the final 3D object was formed.

Since then several different 3D printing processes have been developed. Not surprisingly, each of these processes fabricates an object by combining material together, as opposed to removing it as is done in subtractive manufacturing like milling. A digital model (i.e., geometry) of a 3D object that is made in computer-aided design (CAD) software is typically processed by a slicer program. The slicer's job is to convert the model into instructions for a particular 3D printing process. There are some free-form 3D [36, 106] and volumetric processes [138]; however, most processes are layer-based. The slicer divides the model into layers, or cross-sections, of a particular height. Each layer is converted into paths or images that then form machine instructions (e.g., Gcode). The manner in

which the object is produced (e.g., in layers by connecting small amounts of material in paths), and how the material is combined into an object (e.g., light) delineates these various 3D printing processes. Processes for 3D printing can roughly be divided into four major categories: Vat photopolymerization, Powdered Bed Fusion, Lamination Object Manufacturing, and Material Deposition.

2.1 VAT PHOTOPOLYMERIZATION

Vat photopolymerization 3D printing consists of different variations and advancements of Kodama's process [144] for selectively curing a liquid resin, or photopolymer, in a vat using light. Exposure to light (typically ultraviolet) causes the resin to harden through *polymerization*. Stereolithography (SLA), invented by Charles Hull in 1984 [116], closely resembles Kodama's process with one key difference. SLA uses computer control to position and activate the light source (e.g., laser) at areas of interest instead of relying on placement of physical masks. This path-based tracing of layer is in contrast to hardening an entire cross-section with a light-projected mask as in done in digital light processing (DLP) 3D printers [131]. DLP 3D printers typically produce rougher surface textures than SLA printers¹. This is caused by pixelation artifacts in representing contours of an object as pixels in the light projection output.

Both DLP and SLA are limited by the resolution of the light source (either pixel size or laser spot size). Their speed is comparable depending on the size of the output object. Though a recent development in DLP 3D printing, called *Continuous Liquid Interface Production* (CLIP) [298], enables faster fabrication times by enabling continuous elevation of an object during fabrication (instead of pausing to polymerize discrete layers). Another speed advancement, called *Computed Axial Lithography* (CAL), circumvents the typical "layer-by-layer" approach by representing the volume of an object as a light field and dynamically adjusting the light onto a rotating vat of material [138].

Depending on the chosen resin, a produced object may be rigid, flexible, elastic, or have relatively high-temperature stability (238°C)². For engineering-focused applications that require extremely high thermal stability (1000 °C) and high resistance to corrosion and wear, recent research has examined *preceramic polymers* for 3D printing [322]. Preceramic polymers form ceramics after undergoing pyrolysis [262], or thermal decomposition,

¹SLA vs. DLP: Guide to Resin 3D Printers: <https://formlabs.com/blog/resin-3d-printer-comparison-sla-vs-dlp/>

²FormLabs - Choosing the Right Material: <https://support.formlabs.com/s/article/Choosing-the-Right-Material>

when fired (e.g., in a kiln) at high temperatures for an extended period of time. An experimental ceramic resin has recently reached consumer-grade SLA printers³.

Methods of incorporating different materials (non-resins) or properties in this type of process are not currently feasible. Mixing resins of different types (flexible and rigid) or colors (clear with black) is not advisable because the parameters for the printing process are calibrated for each specific resin (not mixtures). Swapping the resin material mid-print could theoretically be done but would require a laborious effort to drain the previous resin and clean the vat. Likewise, it may require re-calibration of the printing process (layer re-positioning and process parameters).

Finally, embedding materials (metals, electronics, etc.) during most vat photopolymerization processes (i.e., layer-by-layer approaches) is typically impractical. It can result in having uncured resin on the insertions, which would then have to be cleaned post-fabrication. Notably, the previously described volumetric light-field polymerization approach [138] demonstrates curing a polymeric handle around a metal screwdriver shaft. This appears to be a unique benefit of this approach but needs further exploration.

Objects made using vat photopolymerization need to be post-processed. This includes washing and soaking the object in a solvent like isopropyl alcohol to remove any uncured resin⁴. Some resins may also require a post-curing process in heat and ultraviolet light to improve the material's strength, stiffness and temperature resistance.

³Introducing Ceramic Resin for the Form 2: <https://formlabs.com/blog/introducing-ceramic-3d-printing-form-2/>

⁴SLA basic finishing steps: <https://support.formlabs.com/s/article/Form-2-Basic-Finishing-Steps>

2.2 POWDER BED FUSION

Powder bed fusion encompasses 3D printing processes that build objects from very thin layers of fine powder [204]. Powder is spread and closely packed by a roller before being selectively fused to form a layer. The build platform lowers, more powder is spread, and the process repeats until the object is formed. Fusion of the powder can be done with a laser or a binder.

The materials available depend on the fusion process. In Selective Laser Sintering (SLS), polymers (e.g., polyamide), metals and alloys may be fused together. While only some metals like steel, aluminum, and titanium can be melted using Selective Laser Melting (SLM). In liquid binder processes, the materials include polymers, ceramics and some metals [304].

Liquid binder processes are generally faster at producing objects than SLS/SLM as fusion occurs during area-wide sweeps instead of point-based sintering or melting. However, metals and ceramics produced with liquid binders may also need to be sintered after printing. Likewise, liquid binders are more likely to produce pores (micro-scale areas lacking material) in comparison to SLS/SLM which produce high density parts [304]. As a whole, objects made using powder bed fusion 3D printing require post-processing to remove excess powder and perform finishing.

2.3 LAMINATED OBJECT MANUFACTURING

The earliest commercial process of Laminated Object Manufacturing (LOM) appeared in 1991 from Helisys Incorporated [79]. In LOM, objects are formed by cutting and laminating its cross-sections from sheet or roll-based materials [80]. A layer profile can be cut mechanically or with a laser then bonded to a previous layer thermally, mechanically (e.g., clamping), or with an adhesive. Alternatively, full sheets of material can first be bonded and then cut to shape. Excess material (i.e., the non-laminated portions) are typically left in place as a support structure while the object is being manufactured. This excess material is then removed once the object is completed. The process is potentially wasteful if this material cannot be re-used or recycled. With sheet metal LOM, clamping instead of physical bonding may be used to support material re-use [88].

One of the benefits of LOM is that entire layers of an object can be fabricated using pre-existing material, which speeds up manufacturing time. However, objects require post-processing to remove excess material. Likewise, resolution of printed objects depends on the thickness of the material used and the cutting method (e.g., laser spot size).

To date, a number of different materials have been explored including plastics, metals (rolls and tapes), ceramics and paper [88, 204]. More recently, a process for fabric [217] was developed in the HCI community. Other objects (e.g., electronics, conductive elements) can potentially be embedded during an LOM processes (similar to [208]), if a cavity is incorporated into the object being fabricated. The excess material in the cavity would need to be removed (manually or potentially with laser cutting) at fabrication time. Though this may affect subsequent layers by reducing support

and surface area for bonding.

2.4 MATERIAL DEPOSITION

Material Deposition consists of processes in which material is placed down as small beads in lines or curves to form the layers of an object with each layer successively building on the previous one. The outer profile for a layer is usually printed first. Then inner area is then filled in with material using an infill pattern (connected lines, hexagonal, etc.). The most commonly used process is Fused Deposition Modeling (FDM) which was invented by S. Scott Crump in 1989 [53]. In FDM, a thermoplastic filament is pushed through a hot nozzle to deposit the material on to a build plate using 3-axes of motion.

After patents on the technology expired⁵, open-source movements like Fab@Home [181] and RepRap [132] propelled low-cost consumer-grade printers, new deposition techniques (e.g., syringe-based) and novel materials. Materials include thermoplastics, hydrogels, clay, silicone, food (e.g., chocolate) and bio-inks [181]. Though the most commonly used material are thermoplastics (i.e., PLA, ABS, PVA, etc.).

There are very few consumer-grade printers that support printing of different material types together. At most these machines print two to four materials of the same type—such as differently colored thermoplastics or composite filaments. Some printers rely on filament switching mechanisms with a single hot-end⁶. While others have dual extruder, or feeder, set-ups that can independently drive the different materials⁷.

Researchers in materials science and mechanical engineering have also been examining ways to control the low-level composition of a printed material by rapidly mixing different viscoelastic fluids at the nozzle [270]. Another promising area of work has looked at making material deposition processes more versatile through precise and fast tool-changing on the fly [307]. By quickly swapping extruders or tools, different material types can be printed together (e.g., thermoplastics and hydrogels). However, this type of set-up is expensive—costing roughly twenty times the amount of a typical thermoplastic 3D printer at \$170⁸—and requires expertise in machine building.

Material jetting (e.g., PolyJet⁹) is another approach for material deposition that builds objects by curing small droplets of

⁵There is still a trademark on name of FDM so this process is often called Fused Filament Fabrication (FFF).

⁶Original Prusa Multi Material Upgrade 2S: <https://www.prusa3d.com/original-prusa-i3-multi-material-2-0/>

⁷Ultimaker S3: <https://ultimaker.com/3d-printers/ultimaker-s3>

⁸2021 Best Cheap/Budget 3D Printers in 2021: <https://all3dp.com/1/best-cheap-budget-3d-printer-affordable-under-500-1000/>

⁹Stratasys - What is PolyJet Technology: <https://www.stratasys.com/polyjet-technology>

photo-sensitive resins. These printers can mix resins at a low-level, similar to how 2D ink-jet printers mix inks, to create different colors and material properties. Though these printers are generally more expensive and commonly used for industrial prototyping and applications.

2.5 COMPARISON OF 3D PRINTING PROCESSES

Material deposition has emerged as the most promising of 3D printing processes for personal/at-home use. From a material perspective, other forms of 3D printing like vat photopolymerization and powder-based rely on full containers and/or placement of the same material over the build area for the process to function properly. While material deposition is more amenable to having different types of materials (thermoplastics, clay, pastes etc.) being printed together at fabrication time. In addition, since the build area is generally clear of unused material, other materials and existing objects (e.g., textiles, electronics) can be inserted during the fabrication process. Material deposition is also generally the least expensive in terms of cost, time and effort (e.g., setting up and post-processing). Higher resolution (i.e., dimensional accuracy) objects can be obtained using SLA and powder bed fusion processes; however, for the majority of non-industrial use cases, material deposition is more than sufficient.

3

Related Work

Research on personal fabrication [21, 86, 195], and in particular 3D printing, spans across many disciplines including Computer Science, Mechanical Engineering, and Materials Science. This chapter reviews related work in the space with an emphasis on efforts in the Human-Computer Interaction and Computer Graphics communities. Much of the research on personal fabrication can roughly be classified into three areas:

1. **Computational Design:** Researchers have investigated using computational tools to reduce the burden designing such objects and to explore different functional capabilities. Notably, many of these tools use generative approaches to translate a user’s high-level functional specifications (e.g., this object should be strong enough to support the weight of a person) into geometry that can then be fabricated.
2. **Mixed Approaches:** Fabrication processes generally have constraints that limit what and how objects can be made. Many 3D printers are limited to printing a single material type (e.g., plastic), have small build volumes, and have slow fabrication speeds. Researchers have investigated combining different fabrication processes (e.g., mold-and-casting, laser cutting) and integrating existing objects (e.g., electronic circuits, metal wire, etc.) to mitigate these challenges. These approaches have also been explored to support rapid prototyping and enable the creation of objects with interactive capabilities.
3. **Novel Materials and Processes:** While 3D printing is perhaps the most versatile of digital fabrication technologies, many materials (and consequently, their various capabilities)

“We’re so busy watching out for what’s just ahead of us that we don’t take time to enjoy where we are.”
—Bill Watterson, *Calvin & Hobbes*

cannot currently be 3D printed. Researchers have developed new material formulations and processes to expand what can be made with 3D printing.

These areas are discussed with a focus on how they expand the design space of 3D printing, and more broadly personal fabrication. This chapter concludes with discussion of these different areas and their relationship to the work presented subsequent chapters.

3.1 COMPUTATIONAL DESIGN

There is a long line of work in the Computer Graphics and HCI communities that leverage computational tools to support interactive design. Beginning as early 1963 with Ivan Sutherland's Sketchpad [279], works have examined how to construct drawings and 3D models from sketches using constraints [68, 90], suggested actions [119], similar images [297], and automation [120]. Likewise, much effort has focused on numerically simulating the physics and interactions of real-world objects in the digital realm including cloth [18, 38], rigid bodies [17, 98], fluids [198], deformable bodies [58, 133], and even skin [32].

With the advent of low-cost digital fabrication technologies, these methods are now being applied to facilitate designing objects with desired shapes, motions and functional properties from a variety of different materials [21]. In particular, *generative design* approaches that combine design, simulation, and optimization take user-specified high-level functionality and optimize an object's geometry to meet it. From a user's perspective, this mitigates engineering challenges, for example, in deciding how to design an object that is strong in real-world use. Thus, these tools can enable a broad set of people to use digital fabrication technology beyond engineers.

Likewise, generative design enables exploration of design possibilities by producing many solutions (including those would be difficult to design by hand) for a given functional specification. However, the mapping between the input specification and output geometry is typically not intuitive, making user-driven design iteration challenging. Recent approaches leverage mesh parameterization and interpolation strategies to support interactive design space exploration [256, 257]. Another approach by Chen *et al.* allows for interactive control over design deviation and local edits with 2D topological optimization [49]. This approach can, for ex-

ample, allow a user to design a 3D printable object that is optimized to bear weight (e.g., a shoe) while maintaining agency over the object’s aesthetic qualities.

Researchers have developed generative approaches to optimize the shape of soft and flexible materials for plush toys [25, 194], rubber balloons [267], inflated structures [269], zippable fabric [254], sewn garments [301] and knitted structures [135, 203]. Others have examined optimizing linkages in mechanical characterizes to meet motion path requirements [13, 52, 290]. In addition, high strength and structural stability has been achieved for custom tensegrity structures [85] and laser-cut objects such as furniture made from optimized interlocking pieces [244, 259].

For a more comprehensive survey of research that explores interactive design, simulation and optimization for fabrication, see the review by Bermano *et al.* [24]. Of particular interest to this dissertation are works that have applied these techniques in the context of 3D printing. The geometry of an object is optimized at design time—before the 3D model is prepared for printing—to meet structural and functional specifications. Once fabricated, these objects can also have *emergent properties*, or characteristics that are difficult to design through any other means (i.e., by hand), and not necessarily innate to the bulk materials from which the objects are made.

3.1.1 *Mechanical Properties*

Early efforts in this space leverage the ability to freely place material with 3D printing to enable post-print mechanical properties and interactions. *Build-to-last* [173] uses honeycomb infill patterning to minimize material cost while providing high tensile strength in the produced objects. Similarly, printing portions of an object with frame structures can maintain structural stability while decreasing material use [320] and speeding up fabrication time [196, 334]. Others have examined how the orientation of an object during printing results in anisotropic strength. The orientation can be optimized to increase strength at the weakest areas of an object [300, 302]. Alternatively, regions of an object can be automatically thickened to maintain structural stability [277]. Material placement inside of an object has also been optimized to enable the object to balance (i.e., not fall over) with respect to gravity [226], float along a particular axis when placed in water [319], and spin along a stable axis [15].

Along with structural integrity, generative approaches have been examined to support 3D printed objects tightly fitting with other parts and items. Objects larger than a typical 3D printer's build volume (e.g., a chair) can be computationally divided into structurally stable and printable components that can be assembled post-fabrication [174, 274]. Existing objects, if captured as 3D models, can also be joined with auto-generated 3D printable connectors [149] and adaptations [48]. Researchers have also sought to support constrained motion by translating user-specified joint locations and motion paths on 3D models into printable designs [12, 41]. Notably, such joints, when printed on high resolution 3D printers, can be fabricated *in-place* using small voids and/or breakable connections.

Others have examined using generative approaches to create printable mechanisms with joints [303] and linkages [290]. In both cases, generative design reduces modeling challenges (e.g., manipulating low-level geometry of joints) while providing valid design suggestions based on user-specified parameters. Building on these efforts, others have demonstrated interactive tools to re-target [344] and combine [236] mechanism designs in an object while maintaining printability.

While rigid material is typically used for high strength applications and mechanical joints, controlled material placement on a small-scale can make otherwise rigid objects become *elastic*. Elastic objects deform predictably when a force is applied. Within certain limits, once the force is removed, the object returns to its original shape. Optimizing the patterning of microstructures [258] and open-cell foams [184], has been enabled rigid objects to have elastic deformation behavior. The extent of the elastic response can be smoothly varied across an object by tiling variations of these microstructures [258]. This approach has also been used to grade elastic response of objects made from flexible materials [33, 213, 296, 341] and mixed material objects [318]. Macro-scale tessellation and material placement can similarly cause flexible objects to bend and deform in prescribed ways [176, 220, 221, 268].

Elasticity can support mechanical motion with many benefits over traditional rigid kinematics. *Compliant mechanisms* [111] can achieve high precision motion with low weight, low friction and compactness, though they are difficult to design [110]. Within the domain of 3D printing, generative design has been used to alleviate some of this difficulty. Megaro *et al.* demonstrate a design tool that takes a conventional, rigidly-articulated mechanism as input and

uses optimization to output printable geometry for a corresponding compliant mechanism [188].

A related approach has examined *metamaterials*—artificial structures that derive their properties and functionality through the organization of usually repetitive cellular patterns [27, 229]. Computational patterning of cells can create mechanical metamaterials that support motion when printed in flexible materials [124]. Ion *et al.* demonstrate metamaterial mechanisms, such as a door handle and latch, that can function without assembly or additional parts and be printed on consumer-grade FDM/FFF printers [122]. Such mechanisms have also enabled printed objects to change shape and texture—for example, a shoe sole may transition from flat to treads when compressed [123]. Similarly, printed metamaterial cells made of rigid materials (PLA and ABS) can function as bi-stable springs that perform mechanical computation, such as unlocking a door once the correct sequence of cells are engaged [125]. Ruffles of paper, though not 3D printed, have also been optimized to create elastic metamaterial structures [265].

At the object-scale, researchers have computationally replaced areas of an otherwise rigid object with helical spring structures to support constrained elastic motion (e.g., bending or twisting) for interactivity [102]. Notably, the substitution ensures that the spring shape conforms to the replaced region and maintains the object's printability. Finally, substituting elastic material in place of rigid material in areas intended to interface with other existing objects—for example, the inner ring of a cup holder—has been used to ease some design time challenges for novice 3D modelers. Once fabricated, these elastic regions can offset poor fit caused by human-related measurement errors [139].

3.1.2 *Optical Properties*

Researchers have also investigated using generative approaches to enable interactions with light. Perhaps the simplest of these interactions is *color* which may be used for aesthetic and functional purposes (e.g., distinguishing parts of an object for assembly).

With traditional 2D ink-jet printers, color reproduction is accomplished with halftoning, or grading of small dots of ink to simulate color continuity. Most 3D printing processes produce objects in a single color. Material jetting printers can produce colors with different colored resins by halftoning *voxels*, or the discrete volumetric elements that correspond to the resolution of the printer.

Because these materials are generally translucent, inner layers can cause the object's surface color to be poorly represented or diminished. Brunton *et al.* enable 3D printed objects to achieve full color representation with *layered halftoning*—in which color data is algorithmically transferred from the surface to additional layers of voxels within the object [40]. This technique can produce realistic appearances for printed skin and even fruit. Other approaches have examined varying the thickness of printed layers that contain different colored inks [11] and filaments [271]

Achieving realistic appearances for many objects requires matching how light scatters below their surface. To this end, researchers have computationally printed materials of different translucency to mimic subsurface scattering present in real-world objects like marble, wax, and salmon skin [65, 101]. Similar to full color reproduction, realistic subsurface scattering in printed objects is currently only possible with high-end industrial 3D printers.

Apart from visual realism and aesthetic preferences, optical properties can be manipulated for interactive purposes. Researchers have leveraged multi-material 3D printing to produce optical fibers within objects [219, 331]. A material with a high index of refraction is printed as the *core* of the fiber, which is then shielded by *cladding*, a material with a relatively low refractive index. The difference in indices of the two materials allows light to propagate along the core with low loss through *total internal reflection*.

Computationally designing the geometry and placement of these fibers enables routing of light across arbitrary surfaces, for example, to create back-lit face-shaped displays [219]. Other forms of interactive objects with printed optical fibers include custom input sensors (e.g., buttons and sliders that block the passage of light) and chess pieces that display their location on the chessboard [331].

Patterning the internal geometry of objects with voids and materials of different translucency can also embed information that can be optically decoded. Each layer can encode parts of a multi-layer *gray code* pattern that is visible with terahertz imaging [332]. These printed objects support applications in pose estimation, data storage and authentication.

Along similar lines, Maia *et al.* demonstrate approaches to embedding information by alternating material color and varying layer thickness with FDM/FFF and SLA printers [179]. Selective placement of a resin material mixed with an near-infrared dye can also be used and preserve an object's outward appearance. Another approach, *G-ID*, uses infill patterning and extrusion width as opti-

cal tags [64] Notably, all of these approaches maintain the object's underlying geometry and can be decoded using a camera.

3.1.3 *Acoustic Properties*

The form of an object strongly influences the sound that it produces when struck, and how it interacts with other sounds. Researchers have computationally tuned the form and internal structure of objects to alter their the acoustic properties. Bharaj *et al.* optimize the shape of metal cups based on user-specified frequencies and amplitudes to produce musical notes and overtones [29]. Similarly, Lamello [247] generates *tine* structures that encode different frequencies of sound within passive printed objects. When a user interacts with the object—for example, by pressing a button—a small striker hits the tines, producing uniquely identifiable sounds. When coupled with a microphone, these passive objects can act as input devices.

Rather than encoding sound production, other researchers have explored tuning geometry to control the resonance of objects for interactive purposes. Kubo *et al.* use different infill patterns and densities to change the resonance profile of objects for identification purposes [150]. Laput *et al.* print passive mechanisms (e.g., a knob and slider) to dampen and reflect ultrasonic frequency sweeps that are emitted from a mobile phone [154]. Changes in the acoustic response, though inaudible to the human ear, are detectable on the mobile phone's microphone. This can support interactive control of many different applications including an alarm clock and car racing game.

Other approaches manipulate geometry to change the quality of externally produced sound. Liu *et al.* adjust the spacing of small perforations in a printed thermoplastic panel to absorb frequencies associated with noise [171]. Others have investigated printing *acoustic metasurfaces*—objects with sub-millimeter length geometry that enable controllable reflection, transmission and absorption of sound [10, 72]. Lastly, *Acoustic Voxels* computationally patterns variations of hollow cell structures within custom objects to create complex acoustic filters [164]. These filters are optimized to turn objects (e.g., animal figurines) into wind instruments as well as embed acoustic signatures.

3.1.4 *Thermal Properties*

Thermal properties relate to how an object interacts with and responds to changes in temperature. Researchers have investigated how 3D printed geometry can influence these properties. Much like mechanical strength, thermal conductivity and response in printed objects is affected by build orientation and the object's geometry [70, 225]. In general, a layer-by-layer process causes anisotropic thermal response. Researchers have investigated manipulating geometry to control this response for space-based applications (e.g., satellites) [263].

Others have investigated how thermoplastics, the most commonly printed materials, shrink and warp in response to heat [343]. Van Manen *et al.* characterizes expansion of PLA in an FDM/FFF printing process based on print speed, layer height, and print temperature [182]. They demonstrate simple flat objects that, when triggered with high temperatures, change into a 3D shapes such as a rose.

Geometric control coupled with functional and/or shape transformation is otherwise known as *4D Printing* [291]. Within the HCI community, thermal-based transformation in 3D printed objects has been explored extensively using consumer-grade FDM/FFF printers and thermoplastic materials. Computational design has enabled flat patterns to transform into surfaces with double-curvature [95] and texture [278]. Others have examined morphing flat patterns into hollow objects (e.g., a bunny) by restricting the shape-memory response of PLA with regions of printed TPU [7]. Thermal transformation has also been used to produce structurally stable and deployable tensegrity structures [168] and non-developable mesh surfaces [316]. Finally, Wang *et al.* demonstrate line-based objects that fold into elastic mechanisms (i.e., a spring) and self-locking structures in response to heat [315].

3.1.5 *Electrical and Magnetic Properties*

Electrical and magnetic properties are the most relevant for creating personalized interactive objects with 3D printing. With the exception of metal, most 3D printed materials are electrical insulators. Early work explored incorporating conductive particles (i.e., carbon powder) into thermoplastic filaments to create conductive composite filaments for FDM/FFF 3D printing [161]. Though the electrical conductivity of this material is orders of magnitude lower than that of typical metal conductors like copper, this approach

opened capacitive and resistive sensing capabilities to printed objects without additional embedded circuitry. A microcontroller is still required to capture and process inputs.

Building on these efforts, researchers have optimized the geometry and routing of conductive material in custom-shaped objects to support sensing through touch [250], deformation [14, 252] and hovering [253].

In general, the low conductivity of composite filaments only lends itself to basic sensing and display purposes (e.g., turning on light-emitting diodes) when coupled with an embedded microcontroller and power source. Reducing the reliance of additional electronics, researchers have explored printing mechanisms that can be wirelessly sensed. Mechanisms, such as a ratchet and gear system, make contact with conductive- and ferromagnetic-plastic composite regions causing detectable changes to radio frequency backscatter in Wi-Fi signals [127, 128]. When designed into otherwise passive objects, such as a pill bottle, data about the object's use can be captured without the need for tethered electronics.

3.1.6 *Perceptual Properties*

In contrast to other computationally designed functionality that has been discussed, perceptual properties are directly related to how we experience objects from sensory input like touch and taste. With 3D printing, an object's geometry can be customized to offer different information or perceptual cues during interaction (e.g., for usability and accessibility). Researchers have demonstrated printed input devices (e.g., buttons, knobs) that produce haptic feedback using pneumatic input resistance [308], embedded magnets [207], and electro-tactile stimulation [94]. Others have introduced computational tools that create textures on objects, for example, to increase grip on objects like bike handles [123, 278, 281] and offer tactile affordances for input controls [292]. Computational texturing has also been adapted to create printable hair-like structures [155, 211] and tactile overlays (e.g., braille patterns) that support non-visual access to electronic devices like microwave ovens [97].

A recent thread of work, known as Digital Gastronomy [192, 349], seeks to enhance traditional cooking with new fabrication capabilities. With 3D printing, researchers have explored texture in edible items. Common printing process parameters (e.g., infill patterning and material density) have been used to change the texture of different foods including mashed potatoes [170] and

chocolate [160]. Printed cookies with the same caloric content, but different internal texture have been shown to influence chewing time and an individual's perceived satiety [167].

3.1.7 *Summary*

Interactive design, simulation and optimization are valuable tools that support users in the design and fabrication of custom objects with 3D printing. These tools can generally provide real-time feedback about how objects will behave once fabricated. Furthermore, generative design approaches can often reduce human effort in complex modeling tasks (e.g., mechanism design), while also suggesting novel design possibilities that would be difficult to manually create. At a low-level, these tools manipulate the geometry and/or placement of material to produce different user-specified functionality in fabricated objects. Beyond a single property or function, optimization becomes challenging. It requires a well-defined objective function and encompasses a large, non-linear parameter search space [255]. Recent efforts exploring programming pipelines [311] and interactive design [310] for spatially-varying different material properties (e.g., appearance, mechanical, optical) offer promising routes for expanding computational control and broadening the design space of 3D printing.

3.2 MIXED APPROACHES

Current 3D printing processes have a few key limitations. These processes are typically very slow at fabricating objects, tend to have small build volumes, and are generally limited to printing a single type of material (usually plastic). An inability to print different materials greatly narrows what can be made with the technology, particularly because nearly every human-made object is made from a mix of materials for different structural, functional and aesthetic purposes. In an effort to address some of these challenges and explore what can be made with 3D printing, researchers have investigated combining different fabrication approaches (e.g., laser cutting) and integrating existing objects (e.g., electronic circuits, metal wire, etc.).

3.2.1 *Reducing Fabrication Time*

One use of existing materials and other processes is to speed up fabrication of an object by reducing the amount of printed material—

only using 3D printing where custom and/or high-fidelity geometry is needed. Gao *et al.* replace a large internal volume of an object with hollow, laser-cut and assembled acrylic box [83]. This box provides structure and can be supplemented with electronics for product development and prototyping. Using a 5-axis rotational cuboid platform, custom shapes are printed on different sides of the box to create functional devices like a computer mouse. Alternatively, Song *et al.* optimize the shape of a laser-cut assembly to fit a non-rectangular volume inside of an object [273]. Their method incorporates holes for attaching high resolution surface geometry plates that can be fabricated on a typical 3D printer. Researchers have also investigated injecting resin into voids within an object, reducing the amount of printed material while significantly increasing the object's strength [338]. Others have examined substituting Lego-style blocks as low-fidelity parts in an object to speed up design iterations [197]. Another approach integrates CNC milling into a 3D printer to enable reuse of a previously printed object [287]. Portions of a stale design are milled off of the object. Then new design iterations are fabricated directly onto what remains, reducing material consumption and fabrication time.

Fabrication of solid objects can also be sped up by using 3D printing to create molds for casting different materials. Researchers have demonstrated variations of this technique to create objects made of rigid [180], flexible [45] materials. Objects with much more complex geometries can be cast using 3D printed molds than possible with traditional molding approaches [4]. Mold-and-cast approaches also allow multiple copies of an object to be fabricated more quickly than would otherwise be possible with 3D printing alone.

3.2.2 *Repair, Adaptation and Augmentation*

Researchers have investigated how 3D printing can be combined with existing objects to repair, adapt and augment objects for different use cases. Using 3D scanning and 3D printing, fractured objects (e.g., a vase) can be repaired with custom and/or aesthetically pleasing components [153, 348]. Household objects like a hot glue gun can be adapted with a stand or grips to support ease of use [47, 48]. In these examples, the adaptation is printed and then joined to an existing item (e.g., with glue). Researchers have also examined embedding and printing around existing objects at fabrication time [46, 47]. This includes mechanical parts such as

metal wire and nuts to provide strength and stability, for example, in a printed spoon and phone stand, respectively [46].

By embedding heating elements, Groeger *et al.* demonstrate a technique for post-print remodeling and customization [93]. Regions of a printed object such as a bracelet can be selectively heated to soften the plastic for re-forming around a user's wrist. Embedded heating elements coupled with heat-responsive thin-films also enables printing custom-shaped thermochromic displays.

3.2.3 *Fabricating Large-Scale Objects*

Printed objects are generally small because they are limited by a printer's build volume. Researchers have examined approaches to fabricate large-scale objects by combining 3D printing with existing objects. Custom adaptors can be fabricated to join wood [178], and polyethylene terephthalate (PET) bottles (i.e., plastic soda bottles) [147, 148] to make structurally-stable objects such as chairs and tables. When coupled with printed hinges and actuation mechanisms, these objects can also become interactive [147, 165].

3.2.4 *Enabling Custom Interactive Devices*

The ability to fabricate complex geometries with 3D printing offers great promise for supporting the creation of custom interactive objects. However, due to limitations in the types of materials that can be printed, objects made with 3D printing alone are generally passive and static. Researchers have explored embedding different materials to enable interactivity and facilitate functional prototyping. These materials include embedded wires [73, 248], circuit boards [246], and paper [57]. Others have created traces for embedded components by airbrushing conductive ink [243] and depositing conductive material [73, 222]. Likewise, Wu *et al.* inject liquid metal into printed forms to create simple electrical components including resistors, inductors, and capacitors [336].

Typically, deposition of conductive composite material results in high resistance circuits that are only suitable for low power electronics. Recently, Swaminathan *et al.* demonstrated laser-etching of printed carbon fiber epoxy composite to create highly conductive carbon fiber traces [282] in printed objects. These traces are combined with silver epoxy and electrical components to create functional objects such as a bicycle handlebar that has embedded touch-sensing capabilities.

Vasilevitsky and Zoran show custom machine elements (e.g., ball bearings and hinges) that are assembled from printed metal and plastic parts can function as basic electrical components (e.g., switches and variable capacitors) [305]. This functionality enables embedded sensing of their usage. Others have injected liquid (e.g., water) into printed objects to support *offline* sensing of interactions [249, 251]. The embedded liquid acts a capacitor between an object's conductive areas. Interactions, such as tilting, cause liquid to be pushed into interior channels, effectively changing the object's capacitance. This change can be sensed using a mobile phone's touch screen [249].

Along similar lines, researchers have examined embedding magnets in printed objects to prototype input devices [345], actuators [214], and low-fidelity physical models [280]. Printed objects with embedded magnets can also enable haptic feedback during interaction [207, 214, 345].

Researchers have also investigated combined 3D printing with mold-and-cast approaches to fabricate custom interactive objects. Ishiguro and Poupyrev create custom-shaped electrostatic speakers by coating printed objects in nickel, polyethylene, and silicone [126]. This combination forms a thin film diaphragm that produces sound when activated with a high voltage. Others have explored using printed molds to create custom conductive sensors and bellow actuators for applications in robotics and shape-changing interfaces [202].

Others have explored light-based interactions with 3D printing. Torres *et al.* optimize the geometry of 3D printed molds that are then cast with a mixture of resin and glass beads to create personalized light diffusers [293]. Other approaches use aerosol spraying of photochromic [130] and electroluminescent inks [100], and internal tubes filled with electroluminescent wire [248] to create custom interactive displays on printed objects. Finally, Savage *et al.* embed a camera and small mirrors into printed objects (e.g., a game controller) to passively sense different input actions like button presses [245]. Customized internal geometry is used at each input area so that it can be optically distinguished from inside using computer vision techniques. This approach enables otherwise passive printed objects to become interactive devices.

3.2.5 *Summary*

Mixed approaches aim to address current limitations and broaden the design space of 3D printing by combining existing materials and other fabrication processes. In comparison to 3D printing alone, these approaches can allow custom-shaped objects to be made more quickly and at larger scales. By integrating other materials (e.g., wires, conductive ink, magnets), printed objects can also support interactive capabilities such as input sensing and haptic feedback. However, designing printable objects around an existing material can be challenging because it requires having a digital representation, possibly produced from 3D scanning or human measurements. In addition, other fabrication processes may not be as accessible as 3D printing and may require a more hands-on approach during fabrication (e.g., to cast materials). As a whole, mixed approaches are a way of exploring and expanding what is possible with 3D printing in its current state.

3.3 NEW MATERIALS AND PROCESSES

The development of new materials and processes is another way researchers have expanded the versatility of 3D printing. This is a complementary approach as advancements can enable new computational design opportunities and mixed approaches.

3.3.1 *Rapid and Large-Scale Printing*

As discussed in [Chapter 2](#), many process developments for 3D printing have focused on addressing limited fabrication speed and object size. In vat photopolymerization processes (e.g., SLA), curing with continuous elevation instead of at discrete layer pauses increases fabrication speed [298]. Similarly, dynamic projection of light fields onto a rotating vat of material can rapidly cure whole volumes instead of individual layers [138]. In material deposition processes, hobbyists have designed Cartesian motion set-ups ¹ that reduce inertial mass and support rapid acceleration during prints. While researchers have examined fast and high precision switching of tools [307], and mixing of multiple viscoelastic materials through a single nozzle [270].

Another area of work has looked at large-scale material deposition, otherwise known as Big Area Additive Manufacturing (BAAM) [109]. Researchers have produced strong objects such as the chassis and body of a car [55]. However, strength in BAAM

¹Ilan E. Moyer. CoreXY: <https://corexy.com/index.html>

processes can be compromised by improper layer adhesion and void formation in printed materials [67].

3.3.2 *Composite Materials*

Owing to its popularity and support for many material types (e.g., inks, gels, clay and thermoplastics), efforts in new materials have primarily focused on deposition processes. Researchers have demonstrated combined printing of photopolymers and non-curing liquids to create hydraulically actuated robots [177]. Others have explored elastic [99] and conductive [199] materials that can be printed into gel baths. New material formulations have also enabled unique combinations of material properties. Researchers have demonstrated a ballistic gel that has both high elasticity and optical transmission for light manipulation [299]; a rigid thermoplastic composite filament with high dielectric permittivity for microwave devices [337]; and an elastic ferromagnetic ink [142] for soft actuation.

3.3.3 *Interactive Capabilities*

Within the HCI and Computer Graphics communities, many recent process and material developments have focused on enabling interactive capabilities. This includes incremental printing while 3D modeling [218] to support faster prototyping iterations, and using a 3D printer to fabricate and manipulate objects (e.g., for in-place assembly) [136]. Others have explored liquid deposition processes to create responsive clothing with Natto cells that change shape in response to moisture [317]; color-changing objects with photochromic inks [227]; and interactive paper from conductive and thermochromic cellulose gels [56]. A combined process for deposition of copper and iron wire alongside plastic printing has been used to create electromagnetic devices such as a solenoid, reluctance motor and coupling sensor [216].

3.3.4 *Soft Materials*

Soft materials are generally compliant making them advantageous in interactions that occur directly with and around humans (e.g., in soft robotics [140, 238]). These materials have seen a number of interactive use cases within the HCI community. Researchers have created soft sensors by mixing soft and conductive materials together such as coating sponges in conductive ink [201]; curing a

carbon-filled elastomer [339]; and embedding conductive ink into objects printed in flexible thermoplastic polyurethane (TPU) [14].

Among soft materials, textiles are the most prevalent in our everyday lives. Owing to this, another related line of work in the HCI community has explored the fabrication and design of “smart” textiles. These textiles have embedded sensing capabilities and support a rich interaction space on and around the body. Textiles have been explored as a means to sense human gesture input [143, 209, 224, 241, 260, 312, 325], and display information through light [209] and color change [22, 59]. Others have shown how smart textiles can augment musical performance [325] and enhance prosthetic limbs [162]. Researchers have also examined actuating textiles in response to external stimuli such as motor-driven tendons [3] and joule heating [66, 81, 200] to support applications in interactive clothing and shape-changing interfaces.

With respect to 3D printing, a recent thread of work has examined printing interactive objects made of textiles and textile-like structures. Inspired by weaving, Takahashi and Kim demonstrate using an FDM/FFF 3D printer to create woven-like sheet structures from plastic that are flexible and potentially conductive [286]. Hudson describes a new type of 3D printer that needle-felts yarn to enable the creation of new soft objects such as teddy bears [115]. In the process a length of yarn is continually felted on a single path (and potentially across multiple layers); however, the yarn must be manually cut for long movements that do not lay down more material. Additional existing items, such as electronics, can be embedded if an appropriate cavity is left in an object’s geometry.

Peng *et al.* demonstrate an LOM printing process in which a roll of fabric is positioned on the the build area, cut to size with a laser cutter, and then bonded together using with a heat-sensitive adhesive [217]. Similar to other LOM processes, this printer can combine two different rolls of fabric material (e.g., conductive). This done by orienting the second roll along the axis perpendicular to the first. By layering non-conductive and conductive fabric, soft touch sensors and interactive objects can be made.

3.3.5 Summary

Unlike computational design and mixed approaches, the development of new materials and processes aims to directly resolve limitations of current 3D printing technology. This includes enabling faster production, larger object sizes, and new material

capabilities. However, these advancements typically come with decreased access. New materials often need to be formulated in a laboratory setting [142, 227, 299, 317, 337]. Furthermore, new processes may require extensive hardware modifications (e.g., for wire [216] or textile deposition [115, 217]) or entirely new printer set-ups [109, 138, 307].

3.4 DISCUSSION

The previous sections discuss various ways that researchers explored and broadened the design space of 3D printing. Computational design techniques allow users to specify high-level functional goals that are met by optimizing an object's geometry for fabrication. Generative design, in particular, enables users to explore different design possibilities while reducing the burden of designing them. Moreover, it supports designing objects that have new material capabilities such as having a graded elastic response [33, 213, 296, 341]. Mixed approaches combine 3D printing with existing items (e.g., electronics, heating elements) and other fabrication processes to explore and broaden design possibilities including for functional prototyping and interactive purposes. Lastly, material and process developments resolve challenges with current 3D printing technology. This includes small build volumes, slow fabrication speed, and limited printable materials.

While this chapter has presented work in these areas as having clearly defined boundaries, in reality the boundaries are much more fluid. Work in this space often complements or spans across multiple areas, for example, a technique for embedding magnets can be supported with computational design to explore haptic feedback mechanisms for printed input devices [207]. The same is true of the work presented in this dissertation. The subsequent chapters introduce digital fabrication techniques for 3D printing that span across computational tools, mixed approaches, materials and printing processes.

Techniques in these areas open up new design possibilities but also come different challenges and trade-offs. Computational design can limit a user's control over the aesthetics of object and require entirely different design software. Mixed approaches may necessitate having 3D models of existing objects to design around or additional fabrication equipment beyond a 3D printer. Likewise, new materials and processes can be difficult to integrate into exist-

ing printer set-ups and/or require special equipment, for example, to synthesize a material for printing. These aspects limit the ability of users to adopt these techniques for personal fabrication. Accordingly, the work presented as part of this dissertation is aimed at reducing these barriers. In the subsequent chapters, new techniques that leverage everyday materials (as discussed in [Chapter 1](#)) are introduced to address challenges with 3D printing and expand design possibilities with and beyond typical rigid plastic printing. Importantly, the techniques presented are aimed at being approachable to end-users. The presented materials are familiar—they can be readily obtained (e.g., at home, in a supermarket, craft store), or made in a kitchen at home. Likewise, all of the techniques can be readily integrated into existing 3D printing set-ups and design workflows.

[Chapter 4](#) establishes basic techniques for embedding textiles, the most common material with which we interact, during an FDM/FFF 3D printing process. Textiles, including fabric, offer a variety of different material characteristics (e.g., elasticity, flexibility) and they can easily be manipulated through cutting, bending, and stretching. These capabilities enable printing objects more quickly and at larger sizes than typical printer build volumes. Embedded textiles can also support interactivity and custom objects that can be worn close to the body. To this end, examples of input devices and personalized objects are presented to showcase a broadened design space for 3D printing.

[Chapter 5](#) builds on techniques for embedding textiles and introduces a food-grade hydrogel as a material for printing. Hydrogels are polymer networks that swell in response to water. The interplay between this material and textiles enables the creation of interfaces that actuate and change shape in response to water. An interactive design tool that integrates into existing 3D modeling software is presented to facilitate the creation of such interfaces. The chapter concludes with a series of example applications.

[Chapter 6](#) presents a new 3D printing process that enables direct textile fabrication via melt electrospinning. The process produces both rigid plastic and soft textiles from the same plastic filament using a single hot-end. Notably, properties of these textiles (e.g., texture, porosity, flexibility) can be controlled with typical printing parameters like temperature. The versatility of this process is demonstrated through a series of example objects that are soft, flexible, and interactive.

[Chapter 7](#) introduces a new printing material that is primarily

made from cellulose, hemi-cellulose, and lignin—materials that form the cell walls of plants and trees. In contrast to plastic filaments typically used for 3D printing, this material is biodegradable and renewable. It can be easily recycled during prototyping sessions and supports creating objects that are intended to degrade during or after their intended use. Example workflows and applications are presented to demonstrate these design possibilities.

Finally, [Chapter 8](#) concludes this dissertation with a discussion of these different techniques and opportunities for future work in this space, and more broadly in personal fabrication.

4

3D Printing with Embedded Textiles

4.1 INTRODUCTION

Textiles are a very well developed technology: techniques for the construction, manipulation, and modification of textiles have been refined for millennia [19]. Textiles offer many desirable characteristics: they can be easily folded, twisted or deformed; some can maintain shape when placed under tension and preserve functional qualities when cut. These and other properties such as aesthetic appearance, warmth, and versatility have afforded textiles a rich history of practical uses extending from clothing and decoration to more functional objects such as furniture and even as parts of buildings [37].

In contrast, 3D printing is a relatively new technology that offers a means of fabricating items with precise custom geometries. While most 3D printing techniques create rigid objects—typically from plastic and more recently from metal—printed objects can benefit greatly from the flexibility, stretchability, and aesthetic qualities found in many textiles. Similarly, the utility of textiles can be augmented by the use of computer-aided design software and the accuracy and functional properties of 3D printing. As illustrated in [Figure 4.1](#), the combination of 3D printing and textiles creates a new design space for rigid objects with embedded flexibility and soft materials imbued with functionality.

This chapter introduces a set of techniques for successfully combining 3D printing and textiles, including details on adhering plastic to fabric and embedding fabric into a printed object. These techniques are supplemented by a series of design primitives to support the creation of customized objects and input devices with useful properties such as strength, elasticity and absorbency. Likewise,

*“There are no boundaries for what
can be fabric.”*
—Issey Miyake



FIGURE 4.1: A range of textile-embedded 3D printed objects fabricated using our techniques—a box with a rolling lid containing a mesh of polyester and strings for actuation (A); a functional watchband printed on a polyester mesh (B); a figure with a pressure-sensitive head that controls an embedded displacement sensor containing a mesh of nylon and spandex fibers (C); a 22-inch (56 cm) crown printed on a single piece of felt that is larger than the print bed (D).

these primitives can reduce fabrication time and support creating objects that are larger than a typical 3D printer’s build volume. Building on these primitives, a series of example objects that encompass these properties are presented—some of which are shown in Figure 4.1. As a whole, the work in this chapter brings the properties of textiles into printed objects to broaden the design space of 3D printing.

4.2 BACKGROUND

The properties of textiles have long been explored in the material science and textile manufacturing communities [69, 103, 104, 105]. Their structure of interlocking fibers—either natural or manufactured—gives textiles a breadth of characteristics that are useful beyond their appearance. Some textiles can absorb sound or moisture, and be engineered with specific stretchability [105, 294]. Others may be coated with polymers that block wind and water, or are sensitive to heat [261].

Fabric—the material produced by interlacing fibers through weaving, knitting, crocheting, or bonding—can also be designed

to provide further variations in properties such as stretchability and permeability. For example, fabric engineered with large spaces between fibers, or interstices, can facilitate faster diffusion of liquids such as water or hot plastic between the fibers [328].

The ability to add structure and manipulability to fabric has long been of interest in textile communities. Shaping and/or stiffening of fabric is accomplished by attaching it to rigid objects, draping it over rigid objects, sewing seams and darts, and layering fabrics. These are all fairly labor-intensive actions that require some skill and knowledge about sewing and textile-working.

Textiles have recently captured the imagination of the 3D printing community, which can benefit from aesthetic and other properties of textiles, while reducing the manual labor needed to create with them. For example, Hudson describes a new type of 3D printer that prints in needle-felted yarn, enabling the creation of new soft objects such as teddy bears [115]. Peng *et al.* created a layered fabric printer, which uses textiles as the printing medium, cut with a laser and adhered together with a heat-sensitive glue [217]. This printer can combine two different textiles, enabling, for example, the embedding of conductive material in a print.

Within the textile science community, there has been limited prior research into combining 3D printing with existing textiles. Pei *et al.* show that it is possible to directly 3D print plastic onto textiles [215], exploring structures such as a latch and hook. They also examine the quality of adhesion acceptability through visual surface inspection, suggesting PLA has strong adhesion with certain fabrics. However, they do not measure the force that can be held by a bond between plastic and fabric nor the extent to which a fabric will stretch before the bond breaks. Mikkonen *et al.* create flexible, 3D printed objects intended to be integrated with cloth [189]. However, they use standard methods for attaching hard objects to textiles, such as printing buttons and sewing them on, or inserting boning into a corset. Sabantina *et al.* demonstrate simple 3D printed forms combined with textile structures and their mechanical and geometric properties [239]. The current chapter extends theirs by realizing a set of usable techniques, design primitives, and exemplars that support combining textiles with 3D printed components to support a range functional, structural, and aesthetic use cases.

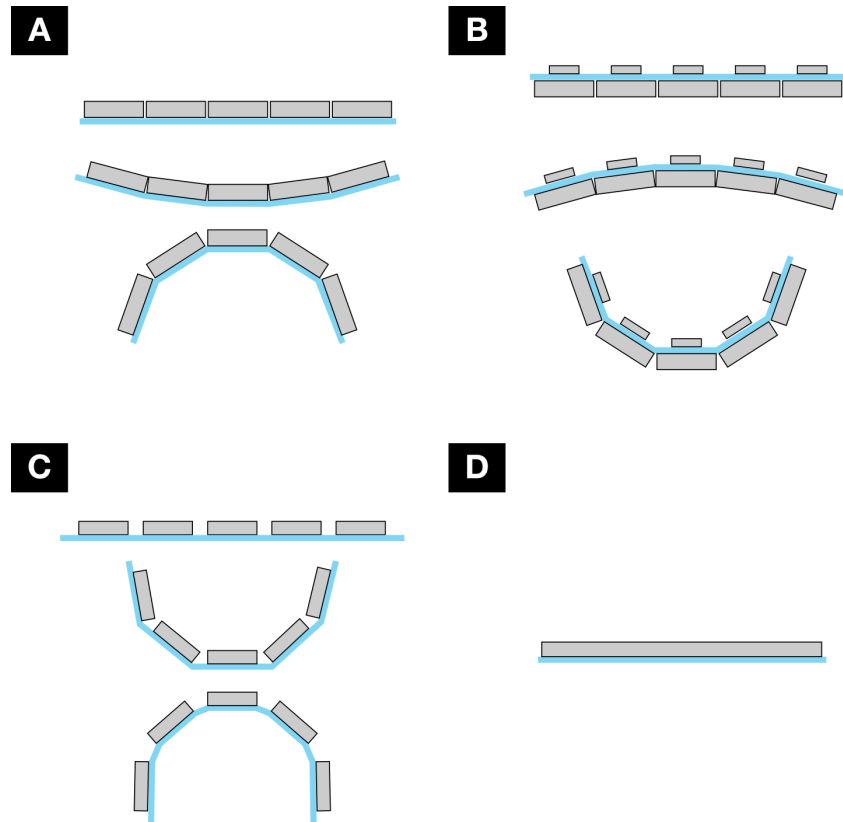


FIGURE 4.2: Primitives for stiffening in a single dimension by adding plastic (gray) to fabric (blue). Closely spaced elements printed onto the fabric can prevent it from bending up while allowing it to relax down (A); widely spaced top elements coupled with closely spaced bottom elements enforce the opposite motion (B). Using widely spaced elements allow the fabric to flex in both directions (C), while a solid bar prevents flexing entirely (D).

4.3 BASIC TECHNIQUES FOR 3D PRINTING WITH TEXTILES

Embedded textile 3D printing takes place at three different levels: low-level techniques for successfully 3D printing with textiles; design primitives for accomplishing specific higher level goals; and fully functional objects. This section discusses low-level techniques for embedding textiles into an FDM/FFF 3D printing process.

Strong adherence between textiles and 3D printed plastic is necessary to integrate their different properties. Extensive experiments—both informal and formal—were conducted to determine the best methods to achieve a strong bond, and support high-level design primitives for creating more complex structures.

Experiments were performed using an unmodified consumer-grade FDM/FFF 3D printer, PLA and ABS filament, and a variety



FIGURE 4.3: Plastic extruded onto a textile with a fuzzy surface creates very strong adherence. The plastic seen here is difficult to separate from a piece of felt.

of different textiles. Note that there is inherent variability in measurements related to a printing process. The temperature reading for 3D printing can vary based on the calibration of the 3D printer as well as the quality and type of filament used [5]. For example, the ideal print temperature of PLA is typically between 180–230°C. Similarly, coatings and variations in material make-up of textile fibers may alter how a textile interacts with printed plastic. Information about the presence and types of coatings on textiles is not easily available, particularly if textiles are purchased off the shelf. Thus some degree of experimentation around parameters such as extrusion temperature is required when attempting to print with embedded textiles.

The two main factors that were considered for successfully combining fabric and plastic are *adherence* and *stability*. Adherence refers to the ability of the plastic filament to attach to the textile, while stabilization of the fabric with respect to the printer is also necessary to achieve success, particularly when printing tall objects.

4.3.1 *Adherence*

Because FDM printing lays down print material in layers, it is critical that each layer bonds to the previous one. When incorporating textiles in an FDM/FFF print, the textile can be considered a “layer” as well. However, due to variability in factors such as print tem-

perature and textile coatings, experimentation is required to attain optimal adherence, such that the textile cannot not be easily separated from a printed object (Figure 4.3). PLA, for example, often adheres better to fabric when extruded at a slightly higher temperature than typical (210-220°C). The high temperature produces lower viscosity and facilitates a longer settling period for the plastic to cool and solidify, allowing it to partially seep into the fabric for a stronger bond.

For thin fabric, approximately less than 0.4mm thick, the best adherence resulted from simply securing the fabric and proceeding with printing without leaving extra space in the model for the fabric layer: the force and heat of the hot-end pressing into the fabric assisted in achieving a good bond between the plastic and textile. For thicker fabric, however, the hot-end can catch on the fabric, displacing it during the printing process. In this case, it is necessary to raise the height of the next layer of plastic to be printed, leaving adequate space for the fabric.

When a fabric is not used as the first layer of a print and is instead intended to adhere between two layers of plastic, it will not normally adhere to the layer below it. For this to occur, the fabric must have holes, or interstices, for the melted plastic to flow through. These openings may be an intrinsic part of the fabric, in the case of netting or other low-density textiles, or can be artificially created by cutting.

Adhesion Testing

Pei *et al.* examine the quality of adhesion between plastic and fabric through visual and surface inspection [215]. However, they do not provide quantitative insights about the bond strength. We performed a characterization of the bonding performance between plastic and fabric by measuring the force required to separate plastic printed onto different types of fabric with Instron model 5567 strain tester.

Figure 4.4 illustrates the test setup: a 1-inch (2.54 cm) diameter “plug” of plastic was printed onto a sample of fabric. The fabric was secured onto the lower arm of the Instron. The upper arm’s clamp was then attached to the plug. The machine then pulled the two arms apart until the plug separated from the fabric, measuring the amount of force required during the extension.

A baseline of performance was measured using basic materials and default printer configurations. The test was performed using

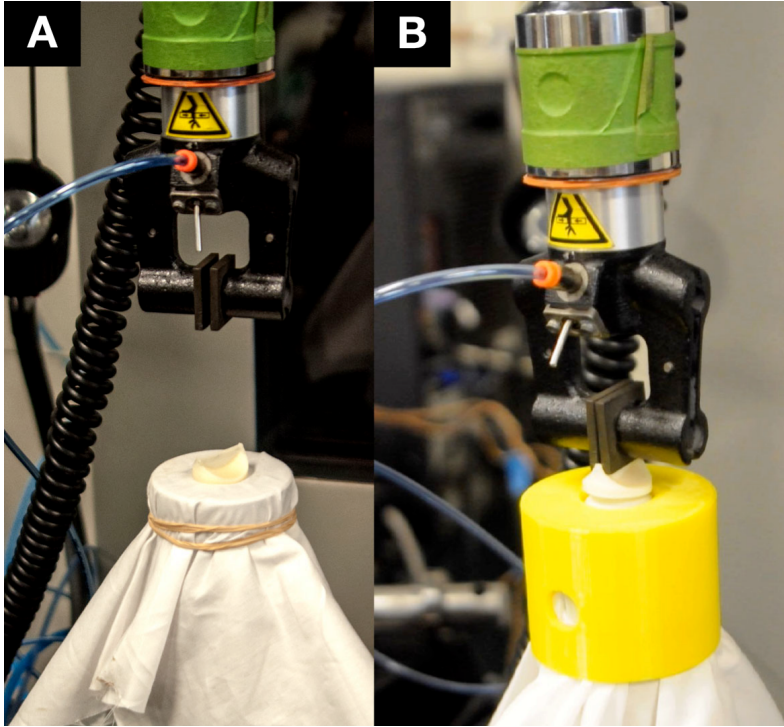


FIGURE 4.4: Instron adhesion test setup. Left: attachment of fabric and plastic sample to test column; right: fabric anchor (yellow) with test in progress.

two plastic types, ABS and PLA, both un-colored, from Mitus¹. Fabric samples were similarly un-dyed and, and determined to be un-coated. The plastic was printed at manufacturer-recommended temperatures (248°C for ABS and 210°C for PLA) on an Ultimaker 3D printer. Figure 4.6 illustrates the results of the adherence test. Table 4.1 describes the properties of the six fabrics that were tested, and Figure 4.5 shows images of each fabric.

¹<http://mitusbrand.com>

The results demonstrate that the adhesion capabilities can vary widely based on the composition of a fabric and the filament used for printing, which is useful in supporting different functionality. For example, the combination of Sew Essential fabric with PLA is capable of sustaining a weight of 50 N (11 pounds of force) which is equivalent to a grocery bag full of food. Similarly, the Voile fabric with PLA can extend about 1 cm in length with a small amount of force (approximately 10 N or 2 pounds of force) without adhesion failing.

| ID | Name | Composition | Thread Count | Weight |
|----|---------------------------|---------------------------|--------------|--------|
| A | Ripstop Nylon | 100% nylon | 196 | 68 |
| B | Sport Nylon | 100% nylon | 113 | 91 |
| C | Symphony Broadcloth | 65% polyester, 35% cotton | 208 | 112 |
| D | Voile | 65% polyester, 35% cotton | 120 | 53 |
| E | Premium Muslin (Bleached) | 100% cotton | 204 | 125 |
| F | Sew Essential (Bleached) | 100% cotton | 142 | 114 |

TABLE 4.1: Properties of the fabrics used in the adhesion test. All fabrics tested were plain weave. Thread count is threads per square inch and weight is grams per square meter.

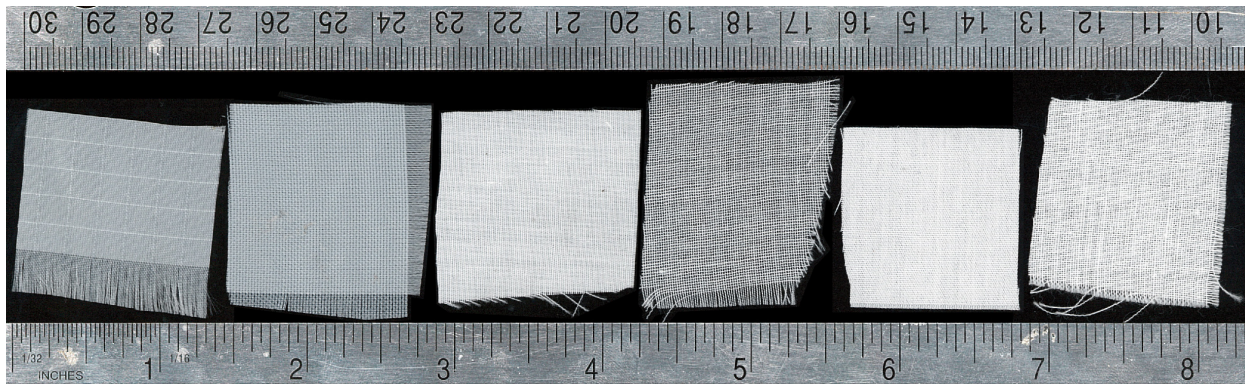


FIGURE 4.5: Photo of the fabrics used in the adhesion test in order of Table 4.1 (A–F) from left to right. The top ruler is in centimeters; the bottom is in inches.

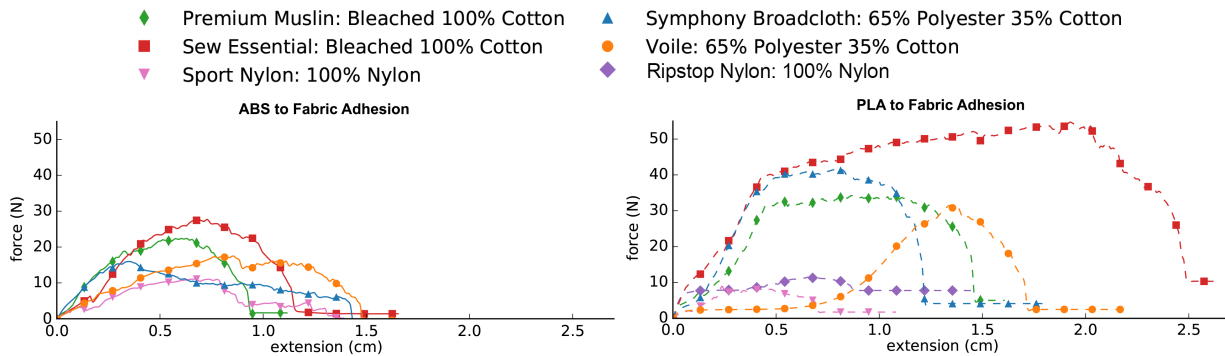


FIGURE 4.6: Results of the adhesion test showing force exerted for a given extension. Both graphs are on the same scale; the left is for ABS and the right is for PLA.

4.3.2 *Stabilization*

When 3D printing with plastic alone, as long as the printer is calibrated and the bed is appropriately prepared printed plastic will adhere providing a stable surface for subsequent layers of material. Unfortunately, the mechanical advantages of fabrics—their abilities to compress, flex, and stretch—are also potential disadvantages when it comes to the 3D printing process. For example, the relative motion between the hot-end nozzle and the fabric can cause lateral forces to be exerted on the fabric which can then shift or stretch; fabric placed across gaps can sag; and taller prints can tilt or twist as the fabric flexes. Extra steps that prevent these issues must be taken to provide a stable surface on which to print. Solutions to these challenges are discussed below and illustrated in [Figure 4.7](#).

Shifting

Unless a piece of fabric is secured to the print bed, it will simply be pushed around by the hot-end as it moves. As discussed in the [Adherence](#) Section, for thicker fabrics, the hot-end can be repositioned such that it does not catch, but this may decrease the strength of adherence. Textiles with a low degree of stretch may be fixed in place at the edges with tape or clamps similar to [121]. For fabric with a higher degree of stretch, it may be necessary to secure the underside as well to prevent shifting during the printing process. Double-sided tape is an effective solution for preventing this unwanted motion.

For fabric that is intended to be embedded as a middle layer of an object—for example, in a displacement sensor [Figure 4.14](#)—the same technique of fixing the fabric in place at the edges applies. Alternatively, if it is undesirable to drape the fabric over the edges of the object, another strategy is to use glue (e.g., gel-viscosity cyanoacrylate adhesive).

Stretching

The ability of some textiles to stretch creates new opportunities for 3D printed objects. For example, stretch can facilitate the creation of resizable objects and pressure-sensitive input devices ([Figure 4.1C](#)). However, stretch also introduces fabrication challenges such as movement that makes objects tilt as more layers added to them. Likewise, textiles made of nylon or spandex fibers may shift or melt due to contact with the hot-end. Adjusting the

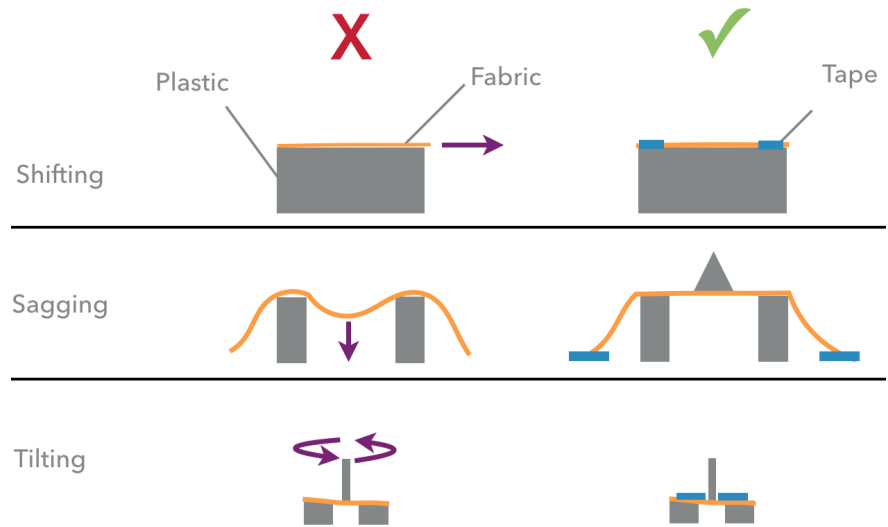


FIGURE 4.7: Stabilization problems and solutions. Textiles can shift, sag and tilt/twist if not properly secured with tape before printing.

hot-end position to be just above the surface of the textile and placing painter's tape over it can reduce stretching.

Sagging

An advantage of textiles is their ability to easily bridge large gaps in a print. However, they may sag if not well supported and printing may cause the fabric to dip, leading to improper layer alignment and poor adhesion of plastic. This problem can be reduced by first placing painter's tape over a gap to support the fabric (Figure 4.17C), or by using one of the shifting-reduction methods to keep the textile taut over the gap.

Tilting

Tilting occurs when the object being printed has a small contact area with a textile and a comparatively large height. As the height rises, it is more likely that the print head will be able to push the object aside causing inaccurate (or even in-air) printing. This effect is worsened by textiles that stretch. Tilting can be corrected by placing painter's tape directly on a textile near problem spots to reduce stretching, or by adding double-sided tape between the textile and the print bed and/or underlying printed material to hold it steady.

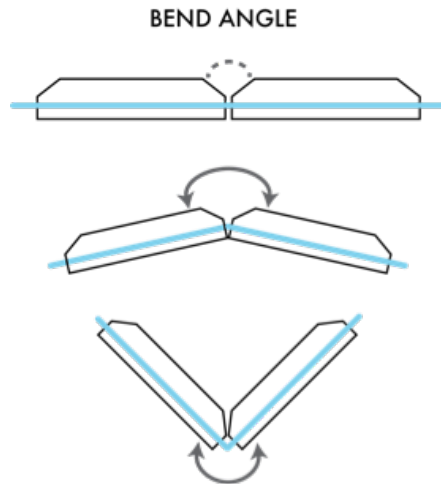


FIGURE 4.8: Plastic segments that restrict the bend angles of a textile.

4.3.3 *Printing Beyond a Single Layer*

A fundamental limitation of printing on fabric in an FDM/FFF process is that the fabric must lie horizontal to the print plane. Otherwise, it may obstruct the movement of the hot-end and prevent hot plastic from being properly laid down. Textiles intended to fold may be printed flat and then folded (such as those described in the [Design Primitives](#) Section). Fabric may also be folded up and around after some number of plastic layers are printed (e.g., by pausing the printing process). In many cases, excess fabric is small enough to fit on the print bed, and naturally remains out of the way as layers are added. In other cases, fabric can be folded or rolled and secured out of the way of any moving parts (e.g., the hot-end) during printing.

4.4 DESIGN PRIMITIVES

This section introduces design primitives that use low-level techniques to combine the different properties of textiles and printed plastic.

4.4.1 *Selective Stiffening*

Adding plastic to fabric enables selective stiffening of the fabric, controlling where and how the fabric can bend or stretch. This basic primitive can be used to build up a number of higher-level



FIGURE 4.9: A textile that is only capable of rolling or flexing along the axis parallel to the plastic segments.

primitives, including mechanically-actuated devices, sensor-based objects, and large-scale fabrication.

Printed plastic normally cannot bend unless hinges are included in its design, which often requires a level of precise design and and/or additional assembly steps. In contrast, most textiles are not normally rigid at all. Many techniques exist for adding stiffness to fabric, such as incorporating additional hard materials (e.g., cardboard or plastic whalebone); however, adding these materials can be labor-intensive and require considerable knowledge of, and skill in, sewing and textile shaping.

Printing plastic onto fabric can *selectively stiffen* different areas of the fabric, controlling the way in which the fabric is able to bend (Figure 4.9). Figure 4.2 illustrates the different ways we can control bending in a single dimension. Control of the spacing of between printed elements on top of fabric can also allow or prevent bending in the direction perpendicular to the fabric. Incorporating the fabric in between layers can restrict bending in the opposite direction as well.

In addition to direction, the *degree* of bending can be manipulated through the amount and shape of printed plastic. Specifically, the bend angle can be controlled by using closely spaced stiffeners with angled side cutoffs or explicit side braces. As illustrated in Figure 4.8, the bend angle will be approximately the sum of the two side angles in the bend direction, and will remain small in the opposite direction (unless additional bending support on the opposite side is provided). Note however, that the exact bend angle may depend on the stretch of the small section of fabric between

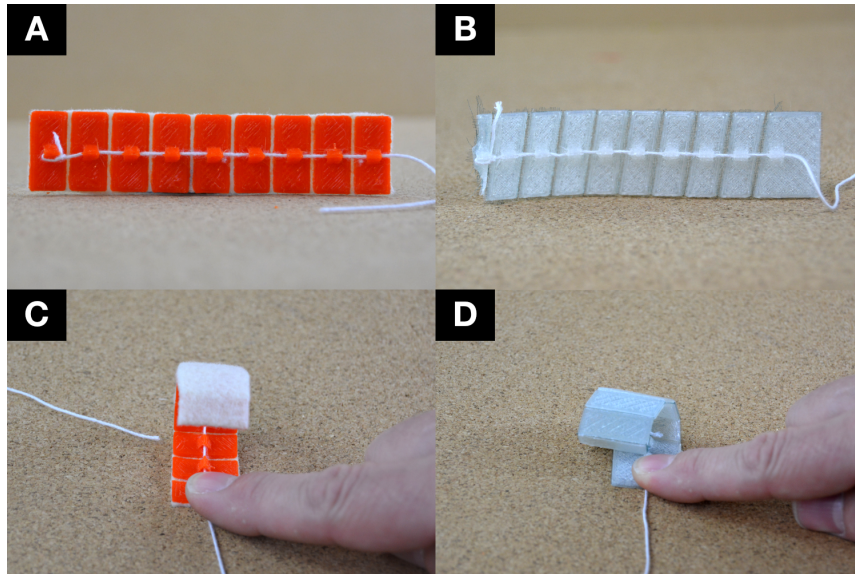


FIGURE 4.10: Textile-embedded, string actuated mechanical arms with variable bend angles—(A) and (B) show straight segments of plastic lead to a simple roll that aligns with the axis of the channel; (C) and (D) show angled segments of plastic cause the roll to skew to the left.

the stiffeners. Consequently, for fabrics with very high stretch it may be necessary to experiment to obtain an exact angle.

Individual one-dimensional bends can also be composed to create more complex shapes and motions. For example, [Figure 4.10](#) illustrates curling shapes produced using angled and straight stiffening segments. [Figure 4.21](#) illustrates the creation of a three-dimensional shape by folding from a flat printed object. The final shape is obtained by printing each edge in the polygonal model with a pair of braces that have a bend angle equal to half the dihedral angle for that edge.

4.4.2 *Selective Adherence*

By selectively adhering plastic to the fabric, the degree of flexing and stretching in the plane and bending out of it can be controlled. This behavior can be further customized by selectively manipulating the areas where plastic adheres to the fabric. For example, placement of painter's tape can be used over areas of the textile where plastic is to be printed but should not adhere. Printing can then proceed on and around the tape, which supports the hot plastic while preventing it from bonding with the surface below. After printing is complete, the fabric can shift or stretch while being in

contact with, but not adhered to, the plastic. This technique allows, for example, creating a mechanical slider which is free to move and retract using stretchy fabric (Figure 4.18B).

4.4.3 *Mechanical Action*

More complex interactive objects can be created using stiffening primitives. In particular, constraining the bend of fabric in specific ways also supports simple mechanisms. Figure 4.10 illustrates how a string affixed to one end of a strip of stiffening segments can create a rolling mechanism. By varying the angle at which the segments are placed next to each other (Figure 4.10B), the strip can be made to curl as it rolls up and (Figure 4.10D). Figure 4.1A illustrates a hybrid textile/printed box with a segmented lid. Controlled by a motor, the box's lid can automatically curl open and uncurl closed.

4.4.4 *Fast Production*

One of the key advantages of using textiles with 3D printing is that layers of fabric are pre-fabricated, opening up the possibility of reducing fabrication time by selectively replacing some of the printed plastic with fabric. However, to emulate the hard plastic it replaces, the fabric may need to be reinforced so that does not bend. Fabric can be stiffened with a small amount of printed plastic over its surface. Furthermore, the outer structure or *shell* of an object can be construct using textile-supported panels (Figure 4.11). There are several options for assembling a shell-printed object. Structures such as printed snaps and clips can fasten the shells together (Figure 4.12). Alternatively, shells can be glued together or sewn at their edges.

4.4.5 *Large Objects*

One advantage of printing on fabric is that it can be larger than the build plate. Once a portion of fabric is printed on, its unused sections can be aligned for further printing. The resulting object then consists of a series of printed sections that are all connected across the fabric. The only caveat of to this approach is that previously printed components must not obstruct movement of the hot-end during subsequent printing. For this, the gaps between each printed section should be larger than the size of the hot-end nozzle. Another challenge is that the textile must be properly aligned such that printing can accomplished where it is desired. One solution is

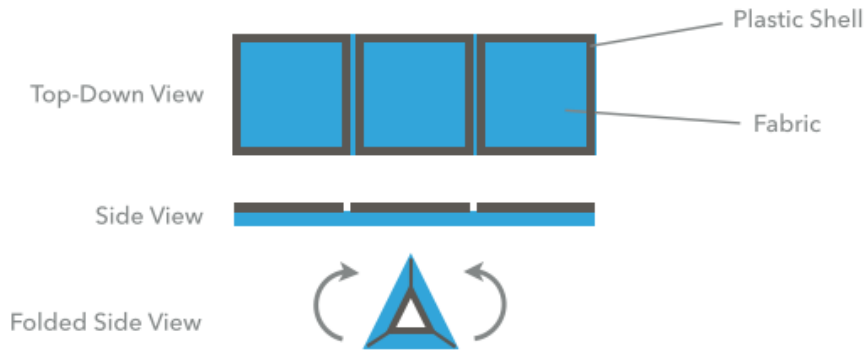


FIGURE 4.11: A shell printed triangular prism first printed flat and then folded to its 3D form.

to use a printed skirt layer to assist in positioning the textile on the print bed. A laser pointer attached to the hot-end can also guide alignment each time the fabric is adjusted. Figure 4.1D illustrates a large head crown fabricated with this approach.

4.4.6 Textile Reconfiguration

Textiles have many options for post processing. Assembly of a shell print can be done through printed snaps (Figure 4.12) or textile-working techniques like sewing. A textile can be cut to size or shape after printing to remove excess material; it can also be trimmed to size if the desired sizing was not known at design time. Reinforcing plastic structure can be printed around holes—creating grommets—to protect the fabric’s raw edges from fraying and provide passage for cords or strings. Figure 4.13 shows several examples of custom-shaped grommets enabled through 3D printing.

Augmentations such as snaps and grommets can be readily provided by more conventional means. However, printing these items in-place reduces the number of manufacturing steps needed to produce an object. Importantly, it also provides a flexible way to mix these conventional fixed form augmentations with highly customized structures that can be achieved with 3D printing.

4.4.7 Summary

Integration of textiles with 3D printing enables a set of design primitives that printed plastic alone cannot realize. With stiffening constructs, we can control how the fabric flexes. A composition of these constructs allows for more complex mechanical behaviors



FIGURE 4.12: Snaps printed onto a fabric.



FIGURE 4.13: Custom-shaped grommets printed onto a polyester mesh. The centers of the grommets were cut out after printing.

such as flexing, rolling and snapping. With basic materials like painter's tape, adherence of fabric to plastic can be manipulated to enable further movement possibilities such as with the input devices discussed in the next section.

4.5 INPUT DEVICES

The discussed design primitives can be used with stretchable textiles to quickly fabricate customized input devices. These input devices are supported by a reusable displacement sensor that has electrical components which are embedded during the printing process as illustrated in Figure 4.14. The displacement sensor allows custom input mechanisms to be quickly fabricated, snapped on top, and tested before deciding on a final design.

The principle of operation behind the displacement sensor is to sense the movement of a textile-suspended plunger (Figure 4.15). As the plunger moves, it occludes light produced by an LED in proportion to the amount of displacement. This change is detected using a photoresistor placed directly across from the LED inside of the object.

The inside of the displacement sensor is hollow to allow the plunger to move freely (Figure 4.16). During the printing process, the plunger is temporarily supported with tape (Figure 4.17C).

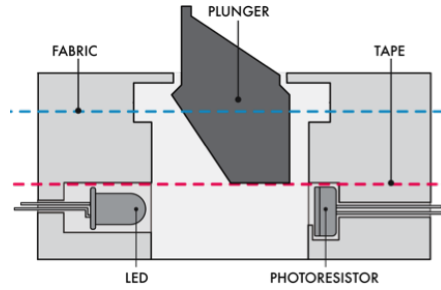


FIGURE 4.14: Cross-section of a textile-embedded displacement sensor. The tape is inserted with electrical components during the printing process. The tape acts as temporary support for printing the plunger. It is later removed using an opening on the underside of the object (Figure 4.16).

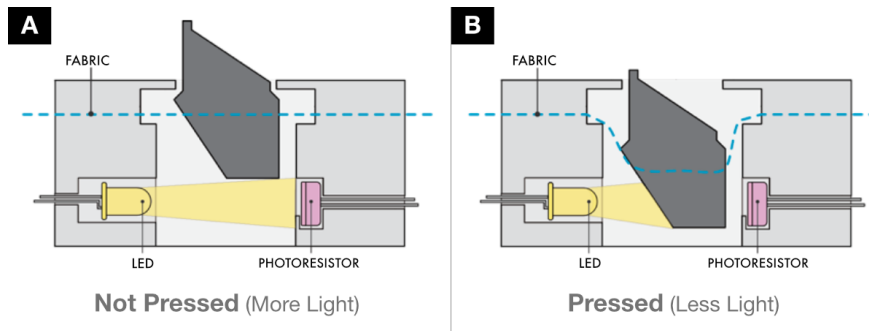


FIGURE 4.15: The displacement sensor’s principle of operation showing maximum light reaching the photoresistor when the plunger is not depressed (A) and reduced light as the plunger is pressed (B).

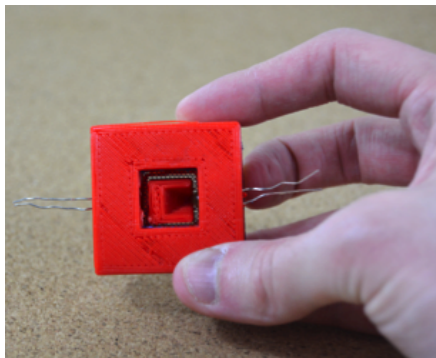


FIGURE 4.16: The displacement sensor’s underside showing the suspended plunger.

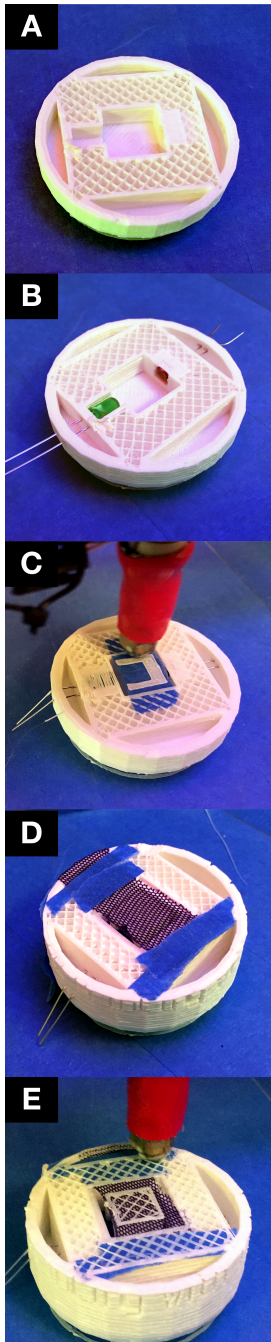


FIGURE 4.17: Process for fabricating a pressure sensitive button: inserting electrical components (A-B); using painter's tape to support printing the plunger (C); printing a portion of the plunger, then pausing the print to lay a stretchable fabric (D); and finally, printing the rest of the object (E).

Once enough layers of the plunger are printed, the printing process is paused and a thin stretchy fabric composed of nylon and spandex fibers is laid down (Figure 4.17D). The process is resumed to finish fabrication of the object (Figure 4.17E) and embed the fabric partially inside the plunger. After fabrication, the support tape is removed through an opening on the underside of the object (Figure 4.16). This leaves the plunger suspended in mid-air by the stretchy fabric. Once this displacement sensor is constructed, additional input mechanisms can be attached for testing including a slider, knob and button.

4.5.1 *Slider*

The slider thumb is constructed using a stretchable polyester mesh, which causes it to snap back to its position in the middle of the box shown in Figure 4.18B when released. As shown in Figure 4.14, the displacement sensor is wedge shaped. This causes its height to vary linearly as the slider thumb moves across it.

4.5.2 *Knob*

Rotation is converted into pressure on the displacement sensor using a 3D printed threaded screw and knob (Figure 4.18C). As the knob is turned, it gradually lowers to displace the plunger. The displacement of the plunger is proportional to the amount of rotation.

4.5.3 *Button*

The pressure-sensing button applies mechanical force to the top of the plunger (Figure 4.18D). Tension in the textile under the displacement sensor opposes downward motion while allowing the textile to slowly stretch. Once the pressure applied to the plunger is relieved, the textile retracts and the plunger and button return to their initial positions.

As a final example, a custom-shape is demonstrated around a pressure sensitive button. The “android” button illustrated in Figure 4.1C uses the design primitives of selective stiffening, selective adherence, and mechanical action. Fabric embedded in the android's body enables sensing while giving its head the aesthetic qualities of a bobble-head figure.

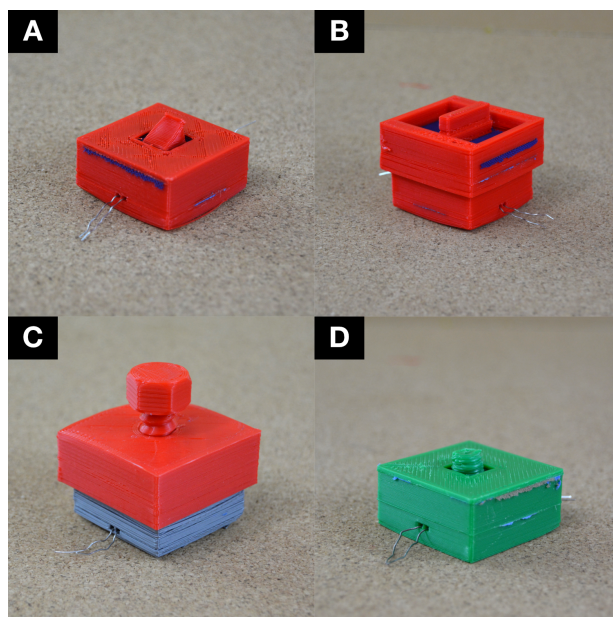


FIGURE 4.18: Input devices with embedded textiles—our displacement sensor (A); a retractable slider (B); a knob (C); and a pressure sensitive button (D).

4.6 APPLICATIONS

This section presents a series of examples objects with embedded textiles ranging from interactive devices to wearable objects. Each of these encompasses the previously discussed design primitives to combine the properties of textiles with 3D printing.

4.6.1 *Actuated Box with Interactive Control*

Textiles can facilitate the creation of functional objects that have variable stiffness and kinematics such as the box in [Figure 4.19](#). The box consists of a textile-embedded lid that rolls open upon actuation. The lid was printed with a flexible mesh made of polyester fibers and two strings fixed at one end of the lid for actuation. The button uses the fabric-embedded displacement sensor described in the previous section ([Figure 4.18A](#)).

The lid combines several design primitives. Plastic sections placed along the lid's diagonals demonstrate controlled bending and mechanical action with selective stiffening, resulting in restricting the lid to only rolling. Strings are placed through channels on top and bottom of the mesh and fixed to one end of the lid such that pulling one results in rolling and pulling the other results in unrolling.

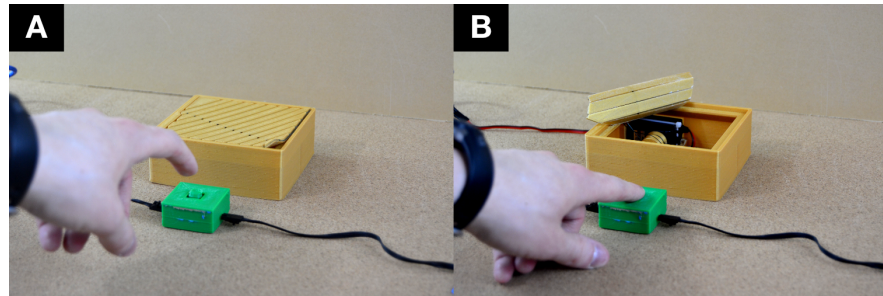


FIGURE 4.19: Textile-embedded box fabricated *via* controlled bending. The box lid contains a polyester mesh and embedded strings that allow the lid to roll open and unroll closed.

4.6.2 Six-Panel Fabric Lampshade

A six-inch (152 mm) cube-shaped lampshade (Figure 4.20A) was constructed out of five identical panels with a sixth panel that was modified with a custom-shaped grommet to accommodate the light bulb (Figure 4.20B). Each panel was printed separately as shells with with short tabs to support being glued to its neighboring panel. While we chose to glue the panels together, other options could include a cord through grommets (e.g., Figure 4.13) or press snaps (e.g., Figure 4.12) for easy access to the light bulb. Unused fabric was trimmed after fabrication.

Printing each panel took about 30 minutes and overall the lampshade took three hours from start to full assembly. Printing a full 6x6x6 inch plastic cube on our printer, in contrast, would take an order of magnitude longer (12 hours for a cube frame or 29 hours for a closed hollow cube). Such a printed design would also not provide the aesthetic and light diffusion qualities of the fabric.

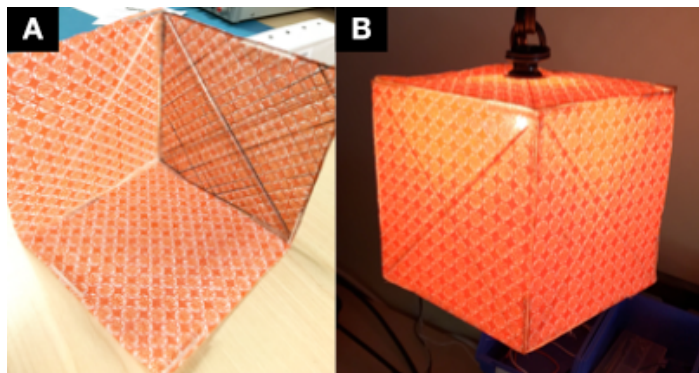


FIGURE 4.20: The shell printed lampshade was constructed by gluing together six panels printed onto fabric (A). The top panel incorporated a custom grommet to accommodate a light bulb (B).

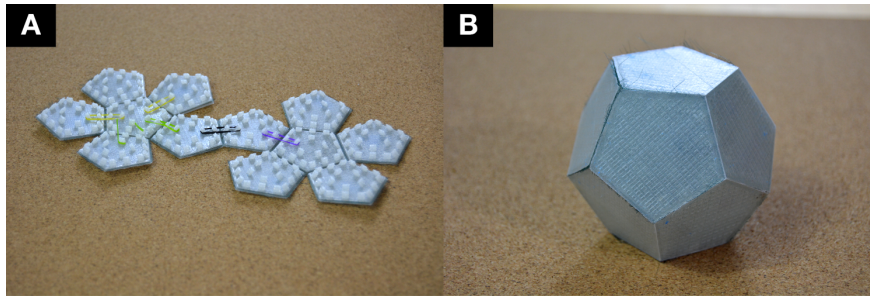


FIGURE 4.21: A shell-based dodecahedron fabricated by printing through a polyester mesh. The faces of the object were printed flat on a single sheet of mesh that was trimmed after fabrication (A). Rubber bands we used to actuate the shells into final 3D form (B).

4.6.3 *Folding Polyhedron*

Figure 4.21 illustrates a dodecahedron designed as a seven-inch (180 mm) flat sheet of pentagonal faces similar to how the shape would be created *via* origami. In its folded form, the shape measures three inches (76 mm) in height. The dodecahedron is secured in its assembled position by small rubber bands wrapped around the pegs visible in Figure 4.21A.

The dodecahedron demonstrates controlled bending using the technique shown at the bottom of Figure 4.8. A small gap was left between adjacent sides of the shape to create hinges and plastic was used to limit their bending to be close to the proper dihedral angle for a pentagonal dodecahedron (116.56°).

The object was fabricated by first printing a layer of plastic for the rigid shells of the dodecahedron. A low-density, flexible nylon fabric was then placed above the surface layer and fixed to the print bed. The printing process was resumed and the subsequent layers of plastic printed through the fabric adhering to the plastic layer beneath.

4.6.4 *Crown*

As an example of object much larger than a typical 3D printer's build volume, a 22-inch (56 cm) crown was fabricated as seen in Figure 4.22 and Figure 4.1D. The crown's decorations were printed as series of rectangular sections onto a single large piece of felt that extended the printer's build plate.

The geometry of the crown was pre-processed in modeling software to separate it into different sections. During the printing process, each section was aligned using a laser pointer that was



FIGURE 4.22: A 22-inch crown fabricated by printing in rectangular sections on a single sheet of felt.

attached to the hot-end. After a section was completed, the fabric was readjusted to print the next section. The crown makes use of decorative elements, grommets and a post-processing step that cuts the felt to the outer shape of the plastic.

4.6.5 *Flex Watchband*

The flexible watchband shown in [Figure 4.23](#) consists of two types of plastic, two layers of fabric, and a magnetic clasp. It is primarily constructed of layers of printed thermoplastic polyurethane (TPU), consisting of NinjaTek SemiFlex filaments, and two layers of polyester mesh fabric. The fabric is folded up and around at the end of the watchband to strengthen the connection around the metal pin that secures the watchband to the watch.

The watchband is constructed from bars of SemiFlex, with only fabric crossing the gaps between them (leading to controlled bending in the direction around the wrist). The fabric is folded up and around the SemiFlex to connect the two layers of fabric and provide extra strength.

The watchband went through several design iterations. Early iterations did not prove to be mechanically robust and lasted only a few days before fractures in the brittle material near the attachment pins occurred. Robustness was improved where the band connects to the watch—an area with less than 2 mm of material between the metal mounting pin and the watch body—by looping fabric around the end of the band, including the metal mounting pins inside the plastic of the band. The fibers of this polyester mesh have higher tensile strength than the printed plastic that they wrap around, and hence substantially strengthen it. The compliant nature of the SemiFlex plastic used for this part of the band eliminates most of the brittleness that would occur with a hard plastic such as PLA.

Printed PLA was used to provide complementary capabilities:

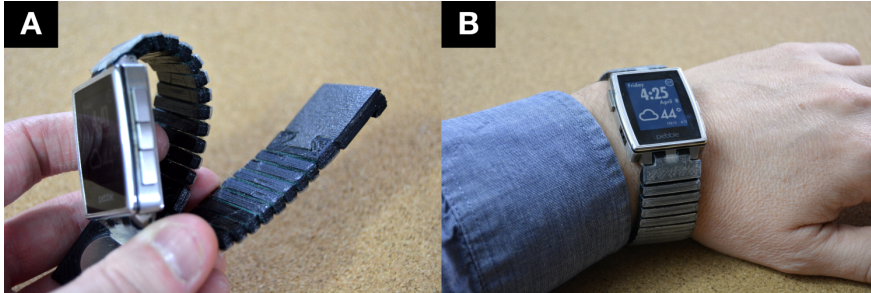


FIGURE 4.23: A watchband that supports hinging to a watch face (A). Stiffeners on the mesh fabric afford flexibility similar to a linked watchband (B).

this harder material was required for some of the functional parts of the magnetic latch. In addition, three separate colors of PLA were used for aesthetic purposes: translucent to give an overall silver tone to the band, and black and white for a logo on the latch.

After the design improvements outlined above, the band has proven to be much more robust. It was used daily for about four months (until the watch it was built for began to fail).

4.7 DISCUSSION AND LIMITATIONS

These examples demonstrate the range of possibilities enabled by combining 3D printing and textiles. However this combination also poses some limitations. Some textiles can experience permanent stretching over time. In the custom android button, this effect gave the button a "squishier" feel. The watchband also stretched slightly over the months it had been in use; choosing a different mesh for the interior of future bands may mitigate this issue.

The durability of textiles embedded in 3D printed objects can be limited as well. Towards the end of its testing period, the watchband experienced some fraying of the connecting fabric near non-flexible latch components; an extra reinforcing fabric layer in these problem spots would likely mitigate this issue. Similarly, durability can be an issue for the strings, such as in the actuated box, due to them rubbing each time the lid rolls and unrolls. Other materials such as braided gel-spun ultra-high molecular weight polyethylene fishing line can address this issue.

For printing objects larger than the printer's build plate, a limitation of the realignment approach is the need to leave large (hot-end wide) gaps between sections. Without sufficiently sized gaps, printing artifacts may be produced such as those visible in the rightmost

side of the crown in [Figure 4.22](#). Better software support for dividing up an object and possibly printing appropriate fiduciary markers would help with fabrication and reduce printing artifacts.

While this work showcases the use of textiles with 3D printing, these techniques are not mutually exclusive with other materials and approaches. As an example, the watchband used a flexible plastic (SemiFlex) because it was soft against the skin and reduced moisture absorption (e.g., from sweat) while fabric could have retained moisture. Similarly, fishing line was used for tendons within the actuated box to address durability issues with string. Different techniques afford different pros and cons— these should be considered when combining textiles with 3D printing.

4.8 CONCLUSION

This chapter has presented techniques to integrate textiles into a consumer 3D printing process. These techniques open new possibilities for fabricating rigid objects with embedded flexibility and soft materials imbued with functionality. Objects that are made using these techniques encompass more pleasing materials, and can be larger, softer, and more flexible than typical rigid plastic prints alone. As a whole, textiles offer a variety of properties that broaden the design space of 3D printing. The next chapter continues to expand this design space by examining how the structure, flexibility and absorbency of textiles combined with a new printing material can support the creation of water-responsive interfaces.

5

3D Printing with Hydrogel and Embedded Textiles

5.1 INTRODUCTION

The previous chapter introduced techniques for embedding materials (and particularly textiles) into 3D printing processes. These techniques support the creation of objects that can combine the structure and rigidity of printed plastic with the flexibility and softness of textiles. This chapter continues to examine textiles as an embedded material. However, it introduces a kitchen-friendly material known as κ -carrageenan hydrogel for 3D printing. By printing this hydrogel onto different textile substrates, we create interfaces that change shape in response to water. To this end, this chapter presents a fabrication technique and software tool that supports the creation of these hydrogel-textile composites (Figure 5.1), and explores interactions that can be achieved through variations in the printed hydrogel patterning and the textile substrate.

5.2 BACKGROUND

As indicated in the last two chapters, there has been growing interest in textiles as an interactive media because of their prevalence in our daily lives. Along with being used to sense human gesture input [143, 209, 224, 312, 325] and display information [59, 209], textiles have been explored as an actuation medium. Researchers have demonstrated changing the shape of textiles in response to external stimuli such as motor-driven tendons [3, 232] and joule heating [66, 81, 200]. This chapter demonstrates another technique

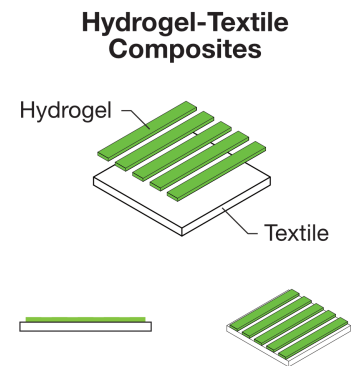


FIGURE 5.1: Hydrogel-textile composites are fabricated by 3D printing hydrogel patterns onto textile substrates.

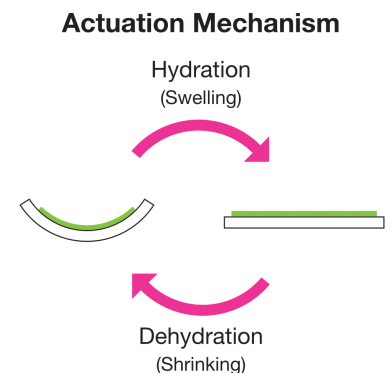


FIGURE 5.2: Hydrogel-textile composites actuate in response to water. As they dehydrate, or dry, they reverse their actuation.

for fabricating interactive textiles that can change shape. However, this transformation is achieved without the use of a power source. Instead, a human-safe hydrogel is printed onto textiles to form a composite that changes shape as the hydrogel swells in response to water.

¹Hydrogel: <https://wikipedia.com/hydrogel>

²N-isopropylacrylamide: <https://pubchem.ncbi.nlm.nih.gov/compound/16637>

³Carrageenan: <https://en.wikipedia.org/wiki/Carrageenan>

Hydrogels¹ are hydrophilic polymer networks that can absorb significant amounts of water. They have been engineered to respond to external stimuli such as pH [340], temperature [134, 205], and light [166]. In the HCI community, poly(N-isopropylacrylamide), or PNIPAM, hydrogel has previously been used to support stiffness- and opacity-changing interfaces [134, 191]. However, PNIPAM hydrogel is not recommended for direct contact with human skin and its synthesis requires the use of hazardous materials (i.e., N-isopropylacrylamide²). In contrast, the work in this chapter relies on κ -carrageenan³, a human-safe material that is extracted from red seaweed. Transformative Appetite [321] explores food made of gelatin-cellulose films that changes shape when cooked in water. However, these films only achieve one-time actuation. Finally, Gallegos *et al.* demonstrated using a 3D printer to extrude κ -carrageenan hydrogel [61]. We employ their material preparation procedure and explore how the hydrogel can be leveraged for interactive purposes. In particular, we print κ -carrageenan hydrogel onto textiles to create reversible water-responsive shape-change.

5.3 FABRICATION TECHNIQUE

This section describes how to prepare κ -carrageenan hydrogel for use in a consumer-grade 3D printing process. We provide open-source 3D printer modifications that are necessary to extrude the hydrogel.

5.3.1 Hydrogel Preparation

Prior efforts in Food Science literature have shown how to 3D print κ -carrageenan hydrogel with in situ polymerization [61]. We leverage their material preparation procedure in our work. We prepare a 3% solution of κ -carrageenan hydrogel by dispersing 3 grams of κ -carrageenan⁴ into 100 grams of cold water. The water is placed into in a beaker along with a magnetic stirring rod. We then slowly add κ -carrageenan, ensuring that the powder does not cake together. The dispersion is left to mix on the magnetic

⁴ κ -carrageenan: <https://www.sigmaaldrich.com/catalog/product/sigma/22048>

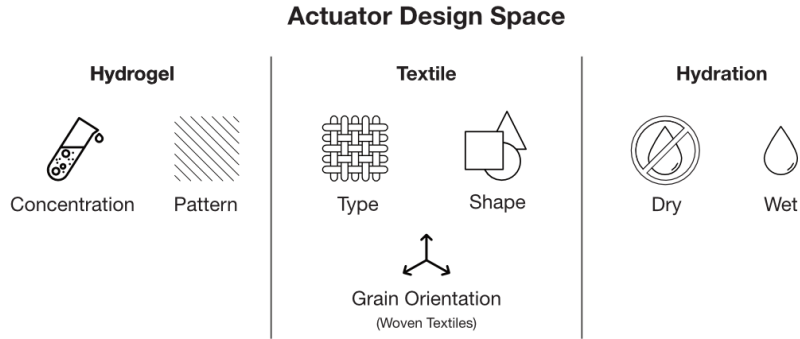


FIGURE 5.3: Hydrogel-Textile composite actuator design space.

stirrer plate for 30 minutes to create a homogeneous solution. The prepared gel is then transferred to a 60 mm syringe⁵.

We experimented with different concentrations of the hydrogel and found that 2% and 3% worked best. Higher concentrations ($\geq 4\%$) resulted in a significantly higher viscosity gel that was not able to be homogeneously mixed with our magnetic stirrer plate. Lower concentrations were obtainable, however, we chose a 3% solution to obtain a more robust and tough hydrogel without sacrificing too much swelling capacity for shape-changes.

5.3.2 Printer Construction

We modified an existing FDM/FFF 3D printer similar in design to the Prusa I3⁶ to support printing the κ -carrageenan hydrogel. Extrusion of the κ -carrageenan hydrogel is done using an open-source, large volume syringe pump design [228]. Initially, we connected the syringe pump to a bowden hot-end set-up⁷ that is typically used for rigid plastic printing. A similar approach was used by prior work [61]. However, we found that hydrogel would frequently dry in the cold region of the extruder (i.e., heat sink) during a print, blocking further extrusion.

Because the extrusion temperature of the hydrogel (50-80°C) is relatively low compared to printing rigid plastic filaments, the heat sink is not required and can be removed to reduce blockages. We replaced the heat sink with a PC4-M6⁸ fitting and directly connected the bowden tube from the syringe pump (Figure 5.4).

As a note, the threads of the PC4-M6 fitting and the hot-end nozzle (0.4 mm) must be wrapped in PTFE thread seal tape⁹ to ensure the connections are water-tight. Lastly, we designed a mount to hold the hot-end as seen in Figure 5.4A. We also designed an

⁵60 mL Syringe: <https://www.amazon.com/dp/B01MSWP002/>

⁶Prusa I3: https://reprap.org/wiki/Prusa_i3

⁷Bowden Hot-end: <https://www.amazon.com/dp/B07B4FHN72>

⁸PC4-M6 Fitting: <https://www.amazon.com/dp/B01NANKRTD/>

⁹PTFE Thread Seal Tape: <https://www.amazon.com/dp/B079T52ZYJ/>

¹⁰<https://github.com/mriveralee/hydrogel-textile-composite-parts>

adjustable radial fan mount to dry the hydrogel as it is extruded onto a textile. We have open-sourced both 3D printable mount designs¹⁰.

5.3.3 Hydrogel Printing Parameters

We print the κ -carrageenan hydrogel at 70°C with a print speed (i.e., feed rate) of 1200 mm/min. Our hot-end uses a nozzle with a 0.4 mm diameter. In our early investigations, we found that the hydrogel has a lower viscosity than rigid plastic filaments like PLA. Thus, as it is extruded, the hydrogel spreads, forming a wider extrusion width than expected. For a 0.4 mm extrusion width, we found the hydrogel's actual extrusion width to be roughly 2 mm. We calibrated the printing parameters to reflect this new extrusion width and ensure our designed patterns are printed correctly. In slicing software, we set the extrusion width to be 2 mm and the extrusion flow to 0.36 (matching the material volume output for an 0.4 mm extrusion width for rigid plastic).

5.4 EXPLORATION OF HYDROGEL-TEXTILE COMPOSITES

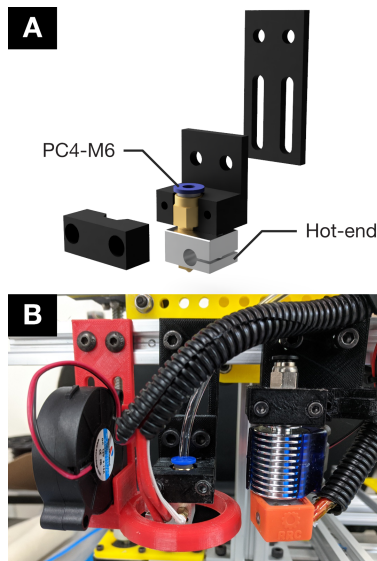


FIGURE 5.4: Component view of our hot-end mount design showing the PC4-M6 connector threaded into the hot-end. (A). Our hydrogel hot-end and radial fan mounted onto a 3D printer to the left of a rigid plastic extruder (B).

The hydrogel-textile composites presented here operate under the principle of a bilayer actuator (Figure 5.2). Prior work has shown that through manipulation of the bilayer's material composition and/or the placement of another material, different interactions such as controlled bending can be obtained [7, 108, 314]. These interactions are enabled when one material changes its underlying properties or organization based on some energy source. For example, polylactic acid (PLA) when 3D printed has stored internal stresses that can be released when the material is heated to its glass transition temperature, creating a controlled shape-change [7].

The bilayer mechanism used in this chapter is achieved through interactions between the κ -carrageenan hydrogel and a textile substrate as the hydrogel swells in response to water (Figure 5.2). In our explorations, we found that as the κ -carrageenan hydrogel dehydrates, it shrinks and pulls along the XY plane of a textile substrate. Decreasing the concentration of the hydrogel solution creates polymer networks that are less dense and increases the amount of shrinkage. Additionally, controlled placement (i.e., patterning) of the hydrogel onto a textile substrate can be used to obtain different shape changes (Figure 5.5).

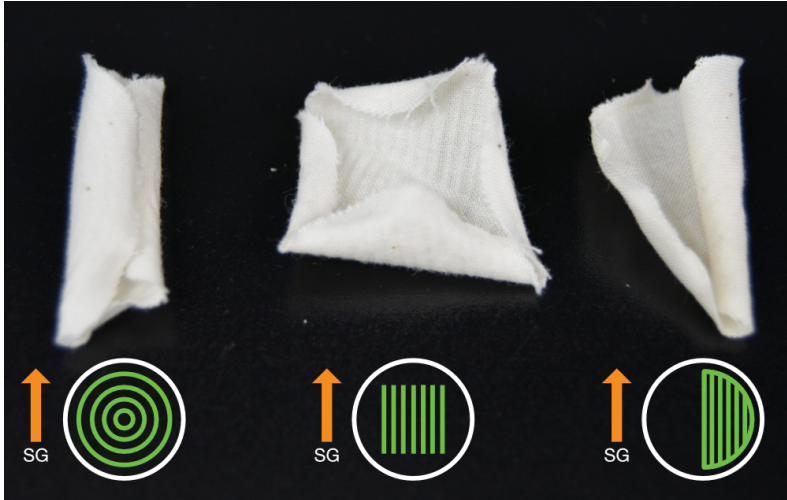


FIGURE 5.5: Test showing variations in hydrogel patterning produce different actuation states.

The textile's composition (i.e., how it was manufactured), its grain orientation during hydrogel printing, and its shape (once cut to size) also serve as parameters to control the interaction in the bilayer mechanism. Our explorations demonstrate that non-woven textiles, e.g., felt and polypropylene (PP), primarily respond to the hydrogel dehydration's along a single axis (either X or Y) causing bending of a textile substrate (Figure 5.6). While woven textiles, such as muslin cotton, tend to have interactions along both axes, resulting in twisting actuation.

Woven textiles have different bilayer interactions based on the anisotropy of their underlying grain structure (Figure 5.8). The straight grain of textile (parallel to the selvage) has the strongest resistance to deformation, followed by the cross grain, and then the bias (along the diagonal of the textile). In general, shrinking and swelling of a printed hydrogel is most likely to act on the bias as this direction has the most flexibility to respond to shrinkage. As seen in Figure 5.7, printing along the bias creates a twist and curling actuation. While printing along the straight grain introduces very little shape-change. Choosing the grain orientation of a woven textile during the printing process is thus important to ensure the desired actuated form is achieved. We have summarized the design space for hydrogel-textile composite actuators in Figure 5.3.

Woven Textile Grains

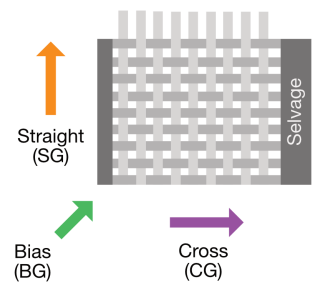


FIGURE 5.8: The structure of woven textiles gives rise to anisotropic behavior when the textile is stretched. The straight grain has the strongest resistance to deformation followed by the cross grain, and then the bias.

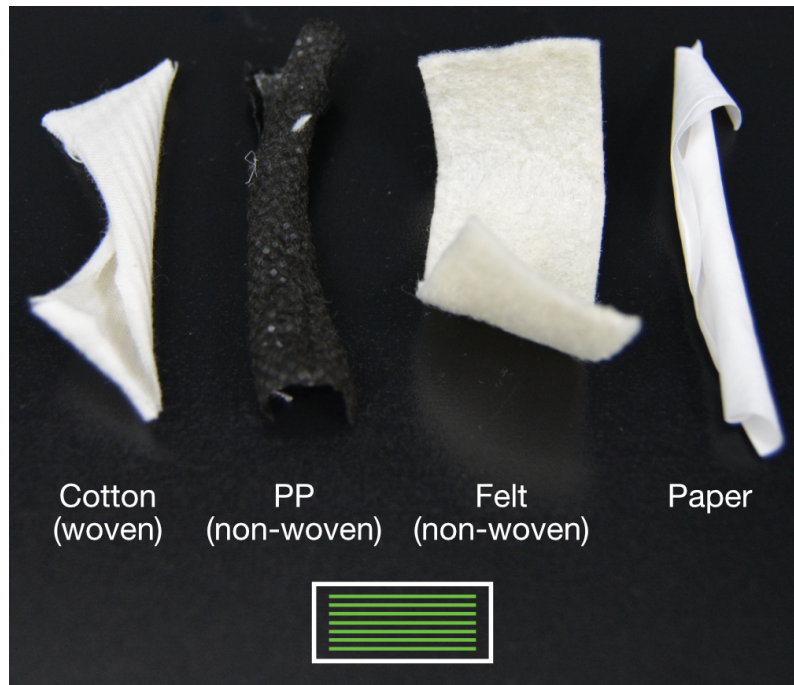


FIGURE 5.6: Test showing different actuation is produced based on the type of textile substrate.

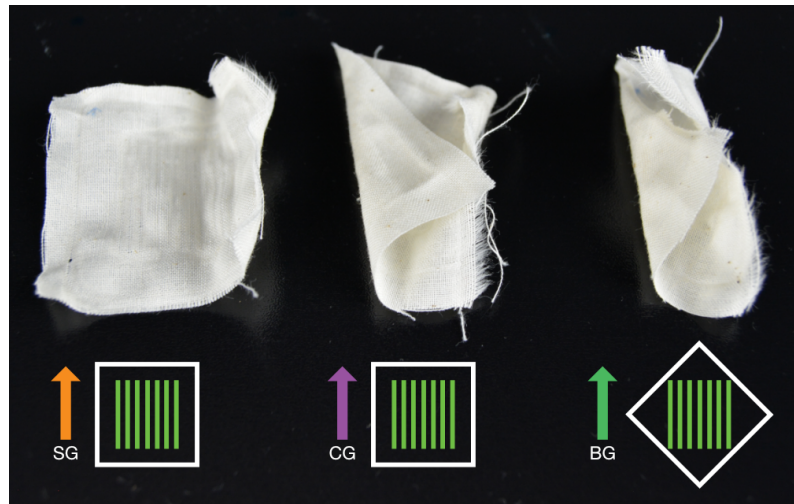


FIGURE 5.7: Resistance to shape-change with hydrogel printed across the different grains of a woven cotton textile.

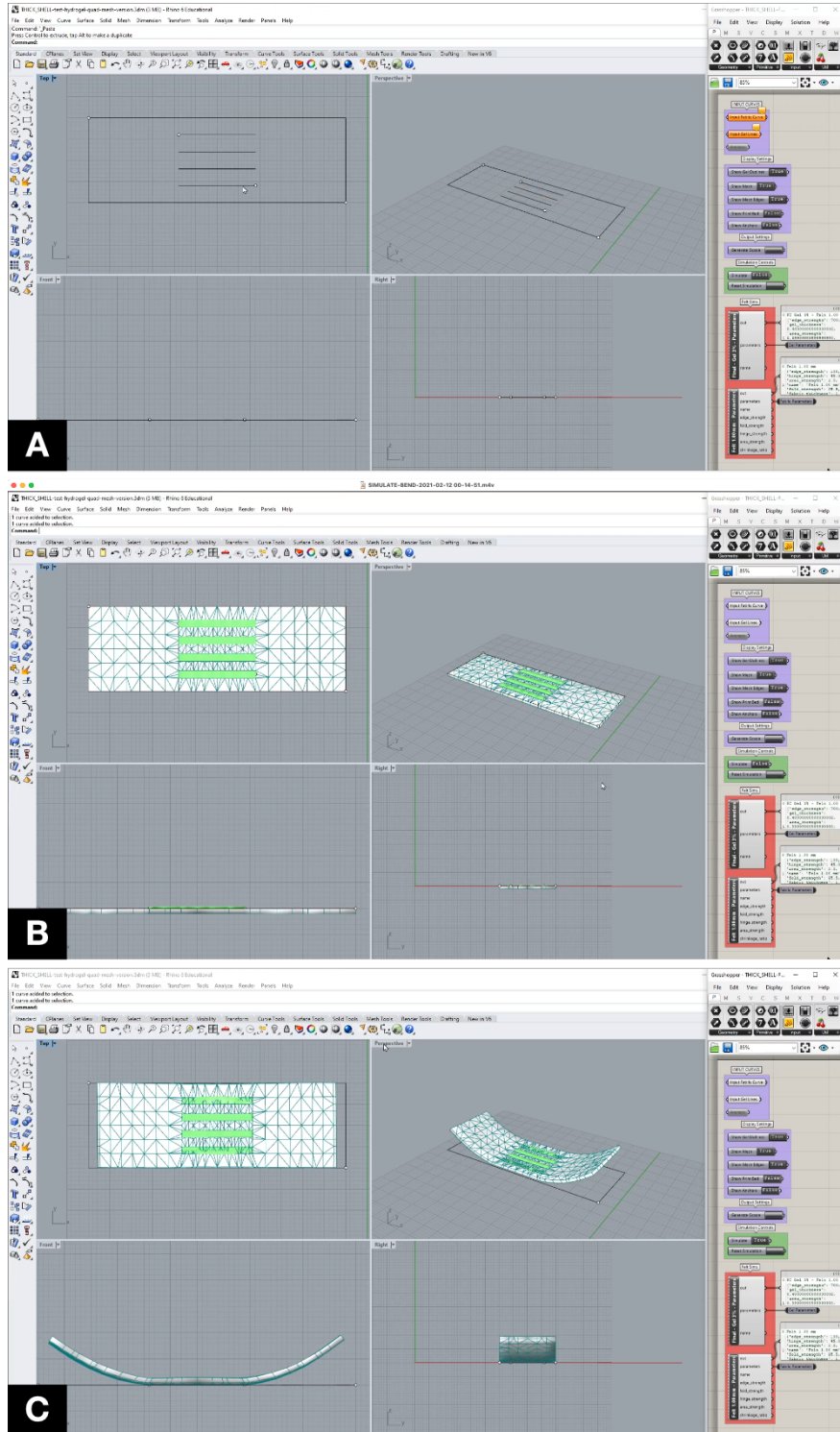


FIGURE 5.9: The software design tool for hydrogel-textile composites. The user sketches the desired substrate and hydrogel pattern (A). The tool generates a mesh for the object (B) and begins simulating the actuation behavior (C).

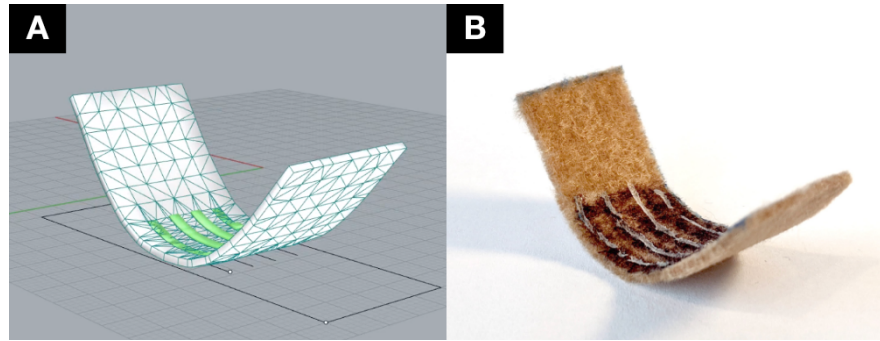


FIGURE 5.10: The finished simulation of a hydrogel-textile composite (A) and the result when fabricated (B).

5.5 SOFTWARE DESIGN TOOL

As discussed in the previous section (Section 5.4), the actuation behavior of a hydrogel-textile composite depends on a few different factors including the pattern of the hydrogel, the substrate's structure and the substrate's shape. Thus the actuation behavior can be difficult to design using traditional computer-aided design (CAD) software, which are generally material-agnostic and devoid of material-based interactions such as swelling/de-swelling. To assist users in creating hydrogel-textile composites, we developed a software tool that allows users to interactively design and preview different actuation behaviors.

The software tool is an extension of *Rhino 6*, a parametric 3D CAD program. It is built using *Grasshopper*¹¹, an algorithmic modeling environment and programming language. We use *Kangaroo 2* as the physics engine and constraint solver¹². Users interactively sketch the profile of a substrate and a pattern for where hydrogel should be printed (Figure 5.9A). The tool then constructs a mesh representation (Figure 5.9B) of the hydrogel-textile composite that is used to physically simulate the shrinking behavior of the hydrogel and its pulling interaction on the substrate (Figure 5.9C). Once the desired behavior is achieved, the user can export the 3D printing toolpath directly from the design tool and fabricate the result (Figure 5.10).

¹¹<https://www.grasshopper3d.com/>

¹²<https://www.food4rhino.com/en/app/kangaroo-physics>

5.5.1 Mesh Generation

As seen in Figure 5.11, the user-drawn substrate profile and hydrogel pattern are used as input for mesh generation. Each

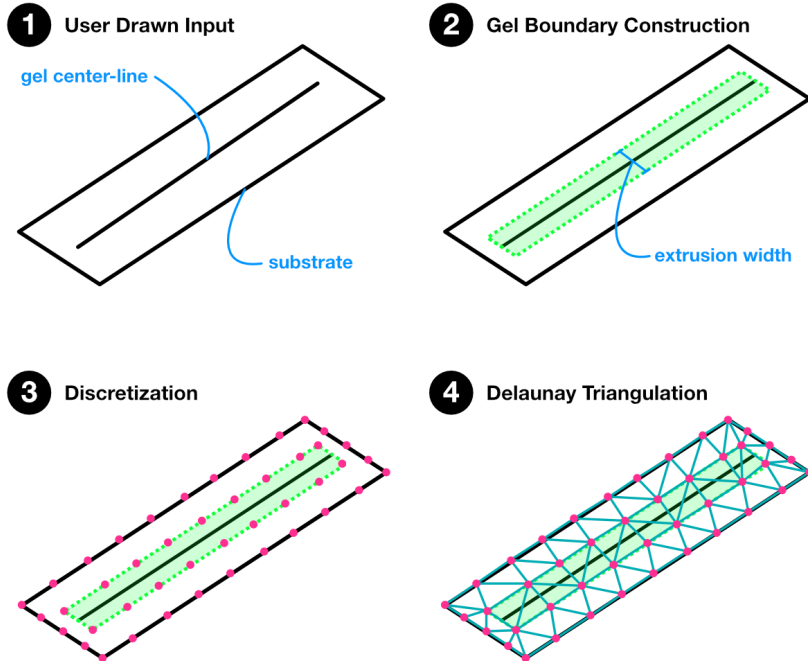


FIGURE 5.11: The process of generating a mesh for simulation. A user draws a gel center-lines and substrate boundary curve (1). Using the extrusion width for 3D printing, a gel boundary curve is generated (2). The substrate and gel boundary curves are discretized as a series of vertices (3). Delaunay triangulation is performed with the vertices to generate the mesh for the substrate and gel.

hydrogel pattern is drawn using a center-line representation. The geometry for the printed hydrogel is generated by constructing the boundary curve of the hydrogel from the center-lines and the user's desired extrusion width for 3D printing. The boundary for the hydrogel and the profile curve of the substrate are then discretized into a series of vertices. These vertices are triangulated into a mesh using Delaunay Triangulation¹³. Any mesh faces lying on the outside the original substrate profile curve are removed to produce a clean mesh for the material model.

¹³https://en.wikipedia.org/wiki/Delaunay_triangulation

5.5.2 Material Model

The material model for the simulation uses a variation of discrete shells [92]. The substrate mesh is modelled using inextensible shells where each mesh face has constraints for maintaining its edge lengths and its dihedral angle between adjoining neighbor faces. The hydrogel pattern mesh is obtained by selecting the subset of mesh faces that lie on the inside of the hydrogel boundary curve

as described in the previous section (Section 5.5.1). The hydrogel pattern mesh is modelled with shells that have edge length and triangular area constraints. However, we assume that the user-drawn hydrogel pattern is in a non-equilibrium (swelled) state. Thus, the rest length and rest area of the hydrogel constraints are scaled by a shrinkage factor (0.90), which was calibrated based on our concentration of hydrogel. Collocation of vertices is used to implicitly couple the hydrogel and substrate constraints.

The strength of the hydrogel and substrate constraints are calibrated by printing various amounts of lines along strips of a substrate. Notably, these strengths can be tuned based on the type of substrate being used and the hydrogel concentration. While our model does allow for anisotropic substrate structures to be simulated, for example, by reducing the strength of edge constraints that lie along the cross grain, we focus primarily on isotropic substrates (e.g., non-woven felt).

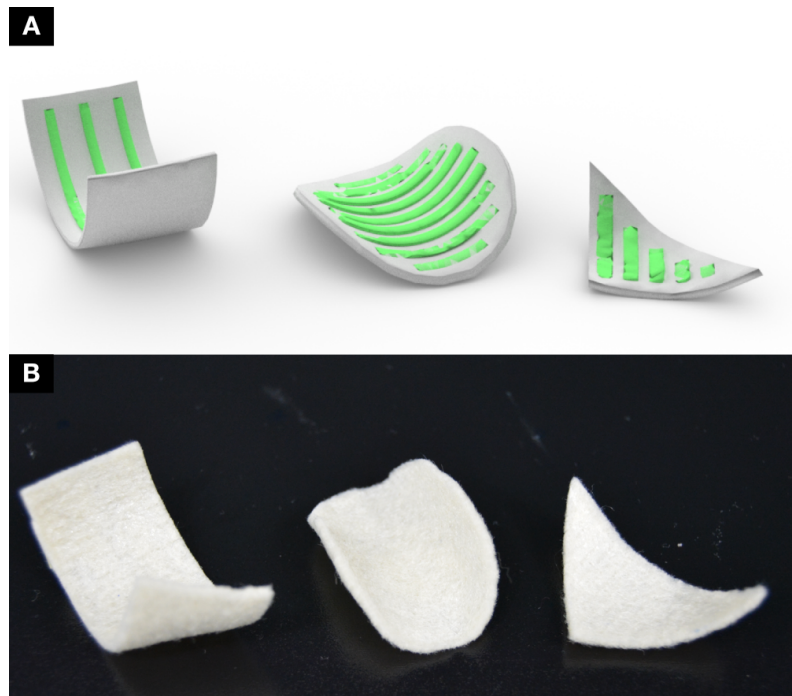


FIGURE 5.12: Comparison of actuation behavior of designs when simulated (A) and fabricated (B).

5.5.3 Physically-based Simulation

Simulation of the actuation behavior occurs as the competing constraints of hydrogel and the substrate attempt to reach an equilibrium state. In [Figure 5.12](#), we show some simulated composites and their corresponding physical prototypes.

5.6 EXAMPLE APPLICATIONS

5.6.1 Weather-Responsive Direction Indicator

We created a passive, weather-responsive direction indicator ([Figure 5.13](#)). Many events, such as music concerts, have venues that change their location (i.e., from outdoor to indoor) based on the weather at the time of the event. Using our software tool, we designed a hydrogel pattern on arrow-shaped piece of felt to create a direction indicator that points 90-degrees in one direction when the weather is dry. When it rains, the arrow changes to a flattened state to point in another direction. The fabricated result's behavior ([Figure 5.13B and D](#)) closely resembles the simulated design ([Figure 5.13A and C](#)).

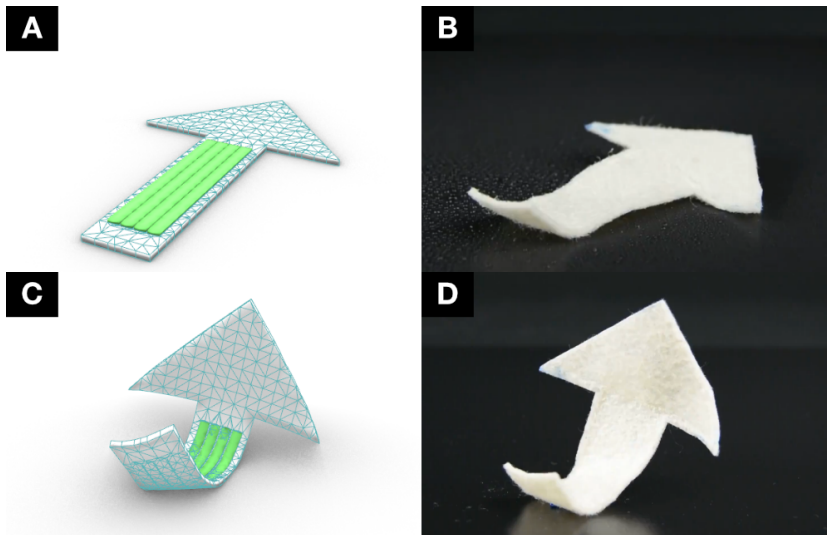


FIGURE 5.13: A weather-responsive direction indicator simulated in the design tool and after fabricated. When it is raining outside, the arrow remains flat pointing straight ahead (A/B). When its hydrogel is dry, the arrow bends upwards (C/D).

5.6.2 *Texture-Changing Garment*

We created a moisture-responsive wrist garment (Figure 5.14) that has a spiky texture when the garment is dry. As a user sweats, the garment absorbs the moisture and the spikes fold down. The garment is worn around a user's wrist (B). The spikes flatten as a user's sweat is absorbed.

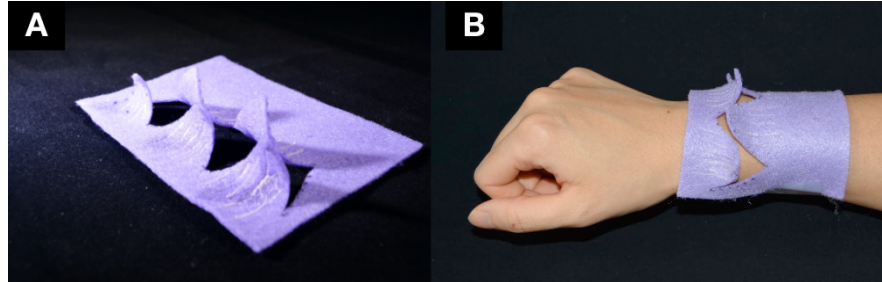


FIGURE 5.14: A moisture-responsive wrist garment that has a spiky texture when the garment is dry (A). The garment is worn around a user's wrist (B).

5.6.3 *Responsive Plant Watering Reminder*

We created a flower-shaped hydrogel-textile composite that is placed in a plant's pot and reminds a user when the plant needs water. Notably, this responsive flower does not require rigid electronics, motors, or sensors to indicate when the soil is dry. The flower's curled up petals indicate its dryness (Figure 5.15A). Once the soil is watered, the flower petals open to visually letting us know that it has enough water (Figure 5.15B).



FIGURE 5.15: A flower-shaped hydrogel-textile composite that reminds a user when their living plant needs water. When the soil is dry, the petals are curled up (A). When the plant is watered, the flower petals actuate open to a flat state (B).

5.7 DISCUSSION AND LIMITATIONS

Currently our software tool focuses on forward design, in which a user interactively designs a hydrogel pattern and textile substrate and simulates the composite's actuation behavior. While the simulation is useful for previewing different shape-changes, designing complex geometries can be cumbersome. Adding support for an inverse design approach could help reduce the design burden. Given some particular 3D geometry, the tool could use optimization techniques to determine the optimal textile substrate and hydrogel patterning that would actuate and fold to achieve the desired 3D geometry. Achieving much larger bending deformations may require printing with different hydrogel concentrations (i.e., to obtain differential shrinkage behavior). Similar approaches have been demonstrated with thermal shrinkage in PLA and TPU composites [7].

Hydrogel-textile composites change shape based on the amount of water present in the hydrogel. As the hydrogel dehydrates, it shrinks and pulls the substrate along its path of least resistance. Rehydration of the hydrogel causes the composite form to revert to its flat, neutral state. This change can occur in seconds depending on the mechanism in which the water is applied. We found using a spray bottle to hydrate the composite form achieved the fastest and most uniform actuation response when compared with an eye dropper.

The rate at which the textile substrate dehydrates can vary based on the amount of water present and the thickness of the textile substrate. Very thin textiles (e.g., muslin cotton, 0.3 mm in thickness) can dehydrate in a matter of minutes, while felt (1.3 mm in thickness) can take up to an hour. Exploring strategies to speed up dehydration, such as using hot air or joule heating with conductive textiles, could reduce the time required for each actuation cycle.

5.8 CONCLUSION

In this chapter we have demonstrated an approach to fabricating hydrogel-textile composites. Embedding textiles into a hydrogel 3D printing process adds a new dimension of interactivity allowing objects to become water-responsive interfaces.

6

A 3D Printer for Electrospun Textiles

6.1 INTRODUCTION

The current chapter investigates a new material production approach that incorporates the fabrication of textiles directly into a consumer-grade FDM/FFF 3D printing process. This approach supports both rigid plastic printing and melt electrospinning—a technique that uses an electrostatic forces to produce thin fibers from a molten polymer (e.g., PLA). The placement and properties of these fibers (e.g., texture and absorbency) can be computationally controlled, opening up new opportunities for fabricating interactive objects and sensors (Figure 6.1).

6.2 BACKGROUND

As discussed in previous chapters, researchers have demonstrated many approaches that use the flexibility and softness of materials for interactive purposes. Some create sensors by mixing soft and conductive materials together, such as coating sponges in conductive ink [201]; curing a carbon-filled elastomer [339]; and embedding conductive ink into 3D printed objects made of flexible thermoplastic polyurethane (TPU) [14]. Other have shown how computational design of an object's structure can control its flexibility either when printed in soft [188, 341] or rigid materials [33, 184, 220, 258]. The fabrication and design of “smart” textiles has also been examined to support interactivity on and around the body. For example, StretchEBand [312] investigates how various stitching patterns of conductive thread can create piezoresistive textile sensors. Similar approaches have been used to augment musical performance [325], enhance prosthetic limbs [162], and

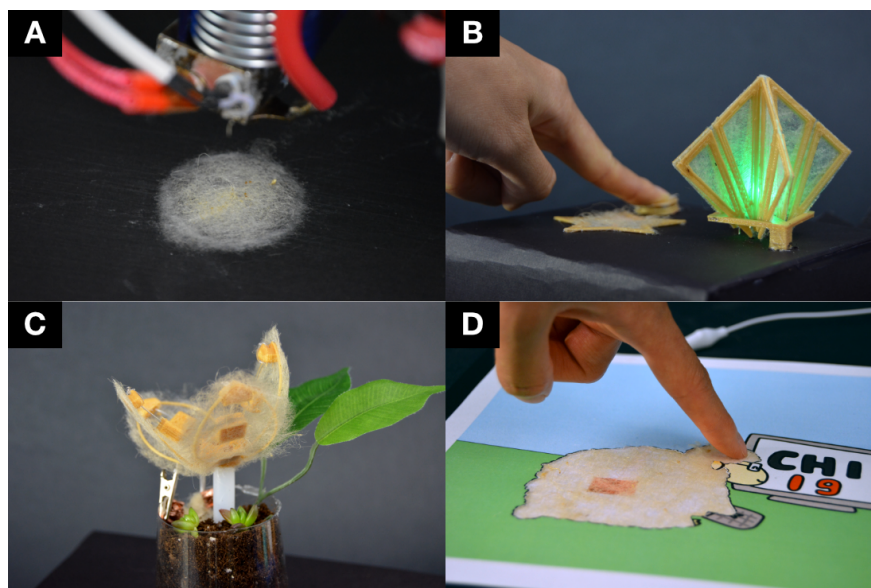


FIGURE 6.1: A range of objects fabricated on our new 3D printer using rigid plastic and electrospun textiles: (A) a close-up of our printer electrospinning; (B) an origami-style folding lamp with a soft piezoresistive brightness control and a soft capacitive toggle switch; (C) an actuated flower that opens when an electrospun liquid sensor detects sufficient water in the soil; (D) an sheep comic uses capacitive sensing to create an interactive tactile experience.

support on-body gesture sensing [224, 241, 260].

The current work differs from these prior efforts in that it focuses on in situ creation of textiles and rigid plastic objects in a single 3D printing process (i.e., using a single base material from a single extruder). Unlike existing work that either embeds pre-fabricated textiles into plastic objects or vice versa, textiles are directly fabricated using melt electrospinning (Figure 6.2). This combination of 3D printing and melt electrospinning enables properties such as texture, elasticity and absorbency to be computationally controlled in printed objects for interactive purposes.

6.2.1 *Electrospinning*

The current work builds on efforts in the material and polymer science communities that have long explored using electrostatic forces to produce polymer fibers with small diameters (nanometer to micrometer scale). Electrostatic spinning, or electrospinning, is accomplished by applying a high electric potential to a polymer that is either melted, or dissolved into a solution using a solvent. The process has been used to create biological tissue scaffolding [309],

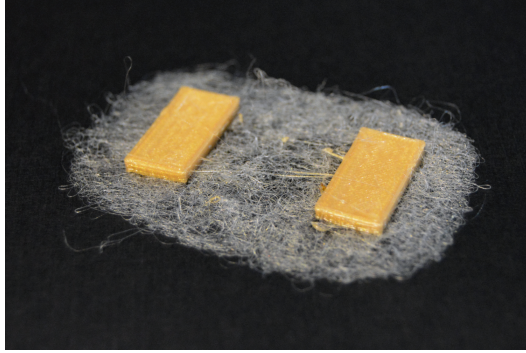


FIGURE 6.2: A simple hinge fabricated with our 3D printer using rigid plastic printing and melt electrospinning on the same extruder.

protective clothing for agricultural workers [159], and even selectively permeable membranes [89]. We briefly describe aspects of electrospinning below. For a more comprehensive overview of electrospinning and its applications, we refer readers to these literature surveys [30, 113, 118].

There are three major components to an electrospinning set-up: a high voltage power supply (5-50 kV), a spinneret (typically a syringe needle) and a collector (a metal plate) [30, 113, 118]. In this work, we focus on supporting melt electrospinning alongside rigid plastic 3D printing using a single extruder. Using a solvent-based approach typically requires a ventilation system, which is not easily accessible nor well-suited for typical consumer-grade 3D printer environments.

In melt electrospinning, a polymer is inserted into a spinneret and heated (e.g., with a heat gun or a hot circulating fluid). Once melted, a large charge differential is applied between the spinneret and the collector causing the melted material to be propelled out of the spinneret towards the collector (Figure 6.3).

Recently, a sub-field of the melt electrospinning community has emerged that explores direct writing of fibers [39]. In direct writing, the spinneret and collector move to support controlled electrospinning. Our work is heavily influenced by these efforts. We support melt electrospinning on a consumer-grade 3D printer that has three axes of movement. However, we focus on producing both rigid plastic and electrospun fibers in the same process, expanding the range of objects that can be 3D printed.

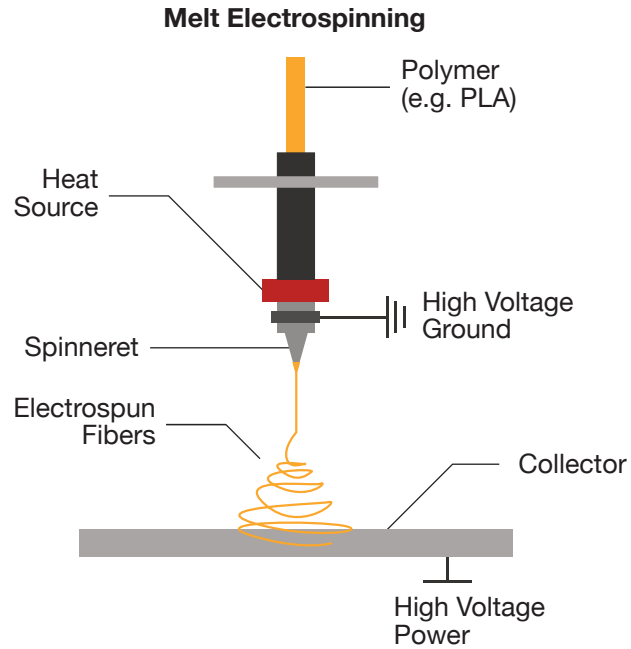


FIGURE 6.3: A typical melt electrospinning setup uses a heated polymer fed into a spinneret. A high electric potential is applied between spinneret tip and the metal collector to propel (typically micron-level) fibers down to the collector.

6.3 ELECTROSPINNING 3D PRINTER CONSTRUCTION

The supplied voltage in electrospinning can typically range between 5-50kV [30, 113, 118]. Such a large electric potential introduces difficulties that can prevent a 3D printer from operating properly. Firstly, high voltage can cause electrical breakdown¹ in which a material that is normally considered to be an electrical insulator (e.g., wire insulation or air) becomes conductive. Secondly, any voltage above the maximum rated voltage for a electronics can damage the electronics and cause malfunction during operation. Thirdly, high voltage can remain on the surface of a conductive material until it is discharged creating possible hazards for moving electronics (e.g., the hot-end heater and thermistor).

¹https://en.wikipedia.org/wiki/Electrical_breakdown

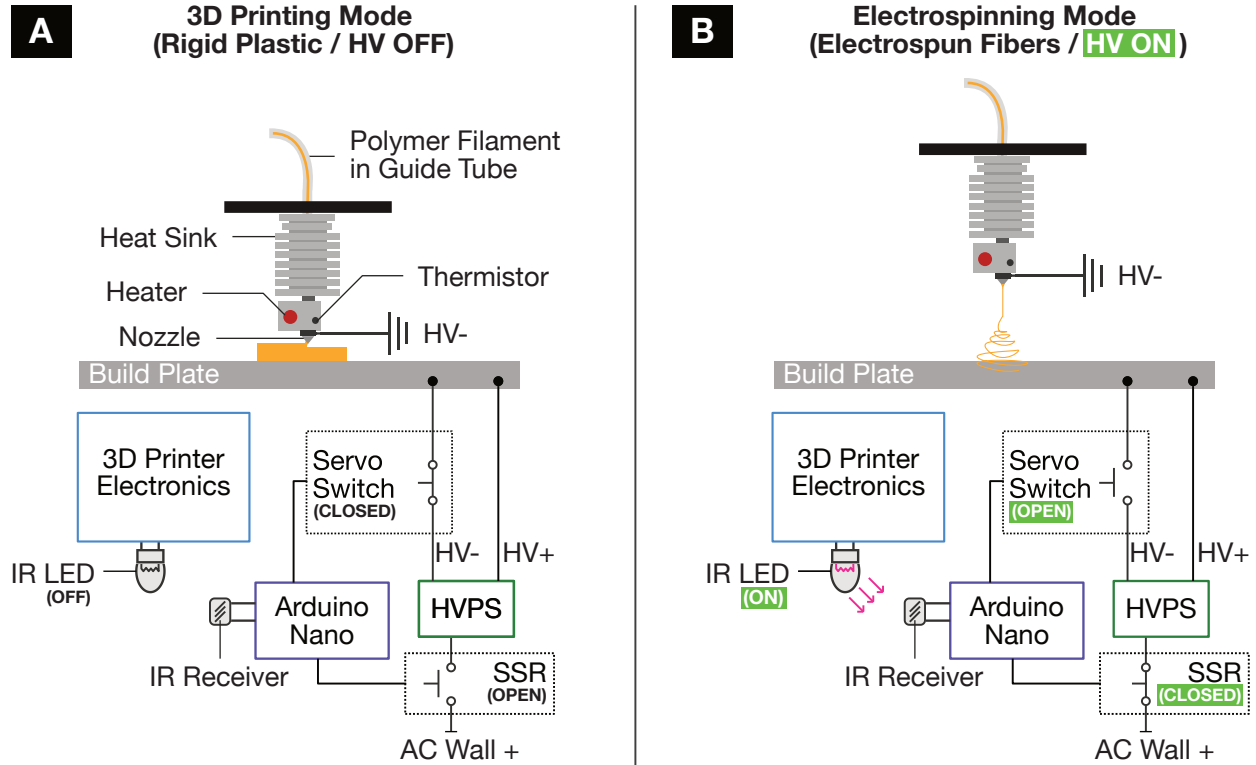


FIGURE 6.4: A simplified representation of how rigid plastic 3D printing and electrospinning are accomplished on our printer. In rigid plastic mode (A), the disabled IR LED triggers the build plate to be connected to the high voltage ground and the high voltage power supply (HVPS) is off. In electrospinning mode (B), the enabled IR LED triggers the build plate to be disconnected from the high voltage ground and the high voltage power supply is enabled.

Most consumer-grade 3D printers operate at comparatively low voltages in the range of 5-24V (two orders of magnitude less than the applied voltage in melt electrospinning). Our printer also operates in this range using a typical 12V power supply; we do not use any high voltage rated electronics apart from a high voltage power supply that is normally used in electrospinning. In the following section, we describe how we modified a consumer-grade 3D printer to support electrospinning by minimizing electrical breakdown, controlling electrical discharge, and isolating electronics.

²Similar to the Prusa I3: https://reprap.org/wiki/Prusa_i3

³<https://www.amazing1.com/hv-dc-power-supplies.html>

Our printer is a variation of an open-source, consumer-grade 3D printer² modified to support melt electrospinning. We note that the hot-end nozzle can be likened to the spinneret typically used in electrospinning, while the printer's metal (aluminum) build plate functions as the collector. We use a low current high voltage (1 mA; 5-35kV) power supply³ (HVPS) to create an electrostatic potential between the hot-end nozzle and build plate of the 3D printer (see [Figure 6.4A](#)) when we enable electrospinning during a print job. The HVPS is operated independently of the 12V power supply that we use to operate the 3D printer's electronics.

Prior work on electrospinning has shown that either the spinneret or the collector can be wired with the positive voltage as long as the other is wired with the high voltage ground [117, 118, 175, 347]. We experimented with both configurations and found that wiring the high voltage ground to the hot-end nozzle and the high voltage positive wire to the build plate allowed us to more readily isolate the electronics and reduce potential charge being stored on the printer's frame during operation.

As a precaution, we wire the printer's frame to the high voltage ground to discharge any high voltage that manages to reach the frame. We note that while this high voltage can cause the electronics of the 3D printer to malfunction, the low current rating of our HVPS poses minimal risk for humans. Touching a surface charged by the HVPS only produces a zap sensation akin to a static shock.

In our initial investigations, we found that a minimum air gap of 1.5 cm is needed to prevent the applied high voltage (7kV) from arcing across to the high voltage ground while the HVPS is on. To control when the HVPS is enabled while limiting any potential high voltage interactions with the 3D printer electronics, we use a separate electrical circuit consisting of an Arduino Nano, a solid-state relay (SSR), an IR receiver, and a servo mechanism (as described below). The SSR is connected to the HVPS power

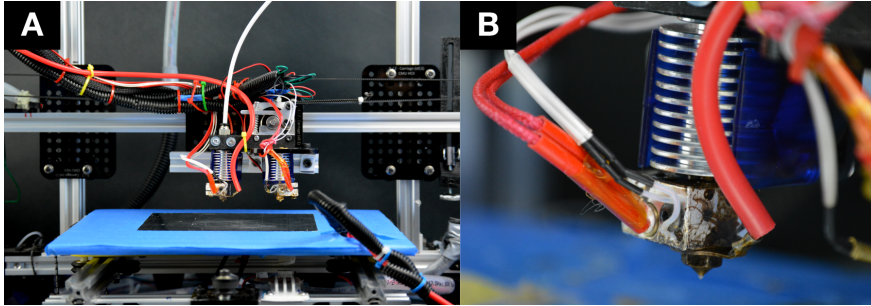


FIGURE 6.5: Our 3D printer that supports melt electrospinning and rigid plastic printing using only the left extruder (A). A close-up of the extruder shows the high voltage ground wire connected to hot-end nozzle (B). We note that (A) shows an additional extruder on the right, which was added to explore printing conductive filament as a third material type.

input from a wall outlet (120 VAC). The signal of the SSR and the IR receiver are wired to the Arduino Nano. The HVPS's state is toggled when an IR LED signal sent from our printer's electronics is received by the Arduino Nano (Figure 6.4).

As mentioned before, high voltage charges can be retained in the surface of objects until discharged. Our initial explorations found the metal build plate would hold enough charge to shutdown the entire printer when switching between print modes. To prevent charge from being held on the printer's build plate during operation, we use a servo mechanism connected to the Arduino Nano to mechanically open or close a switch connecting the metal build plate to the high voltage ground.

When the printer is in electrospinning mode, the servo opens the switch to disconnect the build plate from the high voltage ground (Figure 6.4B). When the printer is in normal plastic printing mode, the servo closes the switch to connect the build plate to the high voltage ground, discharging any remaining voltage (Figure 6.4A).

To ensure the servo motor is electrically isolated from the high voltage wires during operation, we maintain the minimum air gap distance between the servo motor, the high voltage wires and the build plate's contact terminals using a 3D printed plastic extension affixed to the servo. This ensures a safe distance is maintained for the wires and allows the contact terminals to touch without fear of arcing. The servo and SSR are operated by the Arduino Nano at the same time when the corresponding electrospinning mode on/off signal is received.

Because the hot-end nozzle maintains a safe working distance while the HVPS is activated and any electric potential applied to

the build plate is discharged once the HVPS is disabled, we are able to use a standard ceramic cartridge heater and thermistor to manage the temperature of the hot-end during printing.

⁴<https://www.amazon.com/Gulfcoast-Robotics-Extruder-Printer-Filament/dp/B07B4FHN72>

We note that we use an all-metal hot-end (without PTFE inserts) ⁴ to increase the range of print temperatures. hot-ends with PTFE liners can experience melting of the liner when the temperature rises above 265°C.

⁵<https://www.amazon.com/Ivelink-Stainless-Extruder-Filament-Printer/dp/B077M8Z91C/>

Lastly, we initially used a standard brass nozzle, however, we found that higher operation temperatures (>270°C) during melt electrospinning caused the nozzle to wear more quickly. Our printer design now uses a 0.4mm stainless steel hot-end nozzle⁵. This modification is consistent with prior literature on melt electrospinning that has used stainless steel syringe tips for extrusion. With these modifications, we have been able to successfully operate our 3D printer at high temperatures to support melt electrospinning.

6.3.1 3D Printer Firmware

⁶<https://github.com/repetier/Repetier-Firmware>

We modified the printer's base firmware⁶ to handle operations that enable the electrospinning mode, namely sending a signal *via* IR LED and adjusting the extruder's Z position offset to be at least the minimum air gap distance away from the build plate while electrospinning. When the normal plastic printing mode is enabled, the IR LED is disabled and the extruder's Z position offset returns to zero. Lastly, we support using a single extruder for both electrospinning and normal plastic printing by specifying there are two extruders in the firmware that share a heater and thermistor on a single hot-end. We have open-sourced the printer's firmware⁷.

⁷<https://github.com/mriveralee/desktop-electrospinning/>

6.3.2 3D Printing of PLA and Electrospun PLA Fibers

⁸<https://hatchbox3d.com/collections/pla/products/3d-pla-1kg1-75-gld>

We primarily use Hatchbox PLA 1.75mm filament⁸ in our 3D printer. We print rigid PLA at a temperature of 220°C with a combined movement and extrusion feed rate of 2400 mm/min. When printing electrospun fibers, we use the same material in same extruder, however, the temperature is much higher and feed rates are much slower. In general, we electrospin PLA at a temperature of 290°C with a movement feed rate 1300 mm/min, an extrusion feed rate of 10 mm/min with objects processed at a 20% infill density. These parameters can be adjusted to achieve different effects. We describe these parameters and associated tests that we performed to determine them in the next section. G-code files generated for our 3D

printer are post-processed with a Python script to ensure the proper feed rates for electrospinning are set before printing.

We represent the two different types of printing (electrospinning vs. normal) as separate configurations that may be combined in "dual" extrusion prints. Because electrospun fibers are spun at high temperatures and propelled down quickly, they readily bond once in contact with previously printed plastic. To ensure a stronger bond, one can print rigid plastic directly on top of desired regions of the fibers.

The material types may be printed in any order with two constraints: (1) the maximum height of rigid plastic that can be printed below regions that will have fibers spun on top is 0.6 mm; (2) the maximum height of electrospun fibers is constrained to at most 1.2 mm. We explain these constraints further in [Section 6.7](#).

Note that our printer can print these two material types using the same PLA filament on a single extruder without human-intervention during the printing process. Our firmware handles enabling high voltage and offsetting the extruder when necessary. The high voltage is set to 7kV and the extruder's Z position offset for electrospinning is set to 1.5 cm by default.

6.4 ELECTROSPINNING PROCESS PARAMETERS

In this section, we report the results of tests performed to determine optimal electrospinning parameters for our 3D printer ([Figure 6.6](#)). In agreement with prior work [[118](#), [342](#)], our results demonstrate temperature and extrusion rate are crucial factors for optimal electrospinning. We also describe how infill density⁹, a slicing parameter that controls material density, affects the size of an object when electrospun. Lastly, we discuss mitigating size discrepancies by applying a scale factor to the input geometry before generating a printable tool-path. All the tests were performed using a 30x30mm square swatch with the same printing parameters except for the parameter being manipulated. The default parameters are an extrusion rate of 10 mm/min, a temperature of 290°C, and a 20% infill density.

⁹<https://ultimaker.com/en/resources/52670-infill>

6.4.1 *Extrusion Rate*

Extrusion rate refers to the speed (and thereby amount) of material that is advanced during the printing process. For typical 3D printing, the feed rate (or movement speed for the X, Y, and Z axes

in mm/min) along with hot-end nozzle diameter, extrusion width, and layer height are used by the slicing engine to determine how much material should be advanced given a particular tool-path operation. For electrospinning, we found it is necessary to keep a slow, constant extrusion rate that is independent of the movement feed rate and these other parameters. As seen in [Figure 6.6A-E](#), a fast extrusion rate (A) produces material that is more rigid and similar to typical 3D printed PLA. While a much slower extrusion rate (E) allows electrostatic force to pull out thin fibers creating a soft textile. To prevent inconsistent production of fibers and globs of material from forming at the nozzle, the extrusion rate must be held constant during the printing process.

6.4.2 *Temperature*

In agreement with prior research [[118](#), [342](#)], we found temperature affects the diameter of the produced electrospun fibers ([Figure 6.6F-J](#)). A low temperature of 260°C (though high compared to normal rigid plastic printing) causes fibers to be stringy and more plastic-like in appearance (F). As the temperature increases, the diameter of produced fibers decreases. Anecdotally, we note that the fibers have diameters smaller than a typical human hair at 300°C(J). However, at this temperature and above, we found electrospinning became inconsistent—extrusion halted temporarily and plastic subsequently was extruded in the form of small beads.

6.4.3 *Infill Density*

We examined infill density, a common 3D printing slicing parameter, as a way to control material density in a tool-path for electrospinning. In our tests, we used a rectilinear infill pattern with the various fill densities listed in [Figure 6.6K-O](#). We found infill density was positively correlated with the size of a produced electrospun object. In all cases, the infill density test tool-paths produced objects with dimensions larger than the expected 30x30mm square swatch. [Figure 6.7A](#) shows the relationship between infill density percentage and the ratio of the produced object's size to its expected size. To account for the size impact of a particular infill density on the produced electrospun object's size, we calculate a geometry scale factor as the inverse of this ratio as seen in [Figure 6.7B](#). The geometry scale factor is applied to the size of 3D modeled objects prior to slicing.

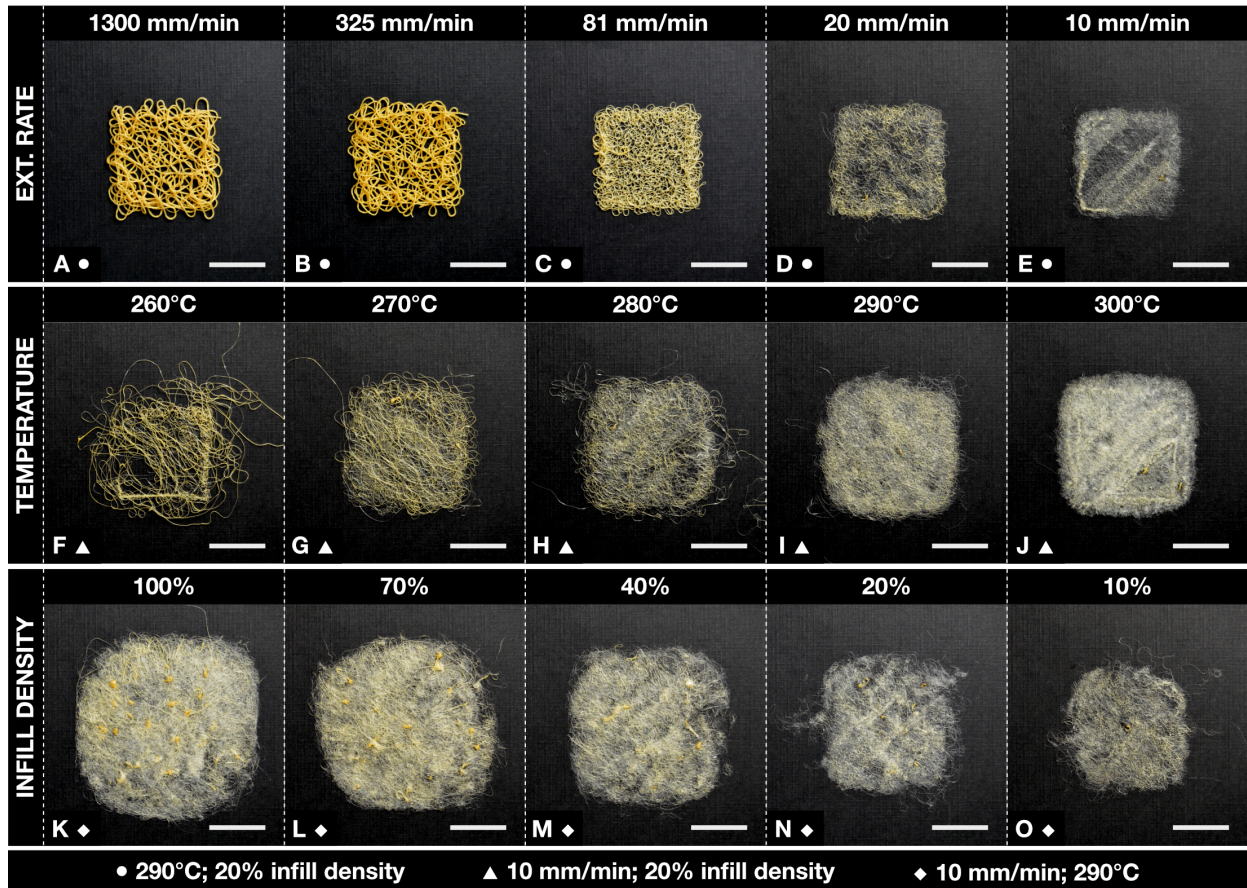


FIGURE 6.6: A series of tests we performed on extrusion rate (A-E), temperature (F-J), and infill density (K-O) to determine melt electrospinning process parameters for our 3D printer. Tool-paths were generated from the geometry of a 30x30mm square swatch using a 3D printer slicer engine. Scale bar: 20mm.

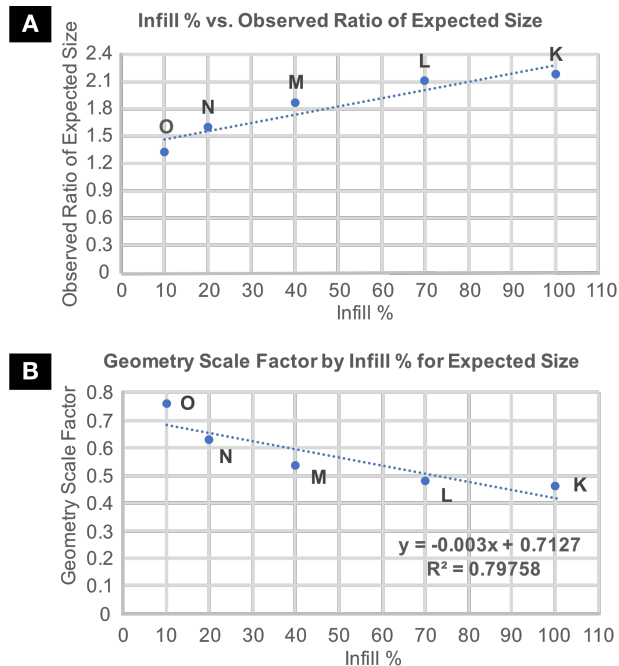


FIGURE 6.7: Infill density is positively correlated with the size of fabricated electrospun objects (A). The inverse of this relationship determines a geometry scale factor that when applied to objects prior to slicing will result in an electrospun object of desired size.

We evaluated the geometry scale factor by printing 4 square electrospun swatches (30x30mm) at 20% infill with the scale factor of 0.65 (obtained using the fitted function in Figure 6.7B). We measured their width and height once fabricated. The average dimension across the swatches was 30.09 mm (SD=0.49). In general, the geometry scale factor based on the infill density percentage is used to control the output shapes of our electrospun objects; however, because we are fabricating textiles, we can also post-process any deviations in size using similar textile-working techniques as [232].

6.5 SOFT SENSOR FABRICATION

Combining melt electrospinning with 3D printing affords new opportunities for creating soft sensors. In this section, we describe how we use electrospinning to facilitate sensing based on capacitance, piezoresistivity, and liquid absorption.

6.5.1 Capacitive Sensing

An electrospun textile is not conductive on its own. However, when combined with a conductor (e.g., copper foil), the textile can be used to create capacitive sensors that offer soft touch affordances. We control the placement of fibers to pattern custom-shaped sheets such as the star in [Figure 6.8A](#) onto a conductive material.

We embed copper foil during the printing process after a layer of fibers is printed and the high voltage is disabled. We then continue printing with rigid plastic to create a binding enclosure for the copper foil and electrospun textile. The electrospun textile creates custom-shaped, soft affordances for the capacitive sensor while serving as a compliant material that mediates changes in capacitance [Figure 6.8B](#).

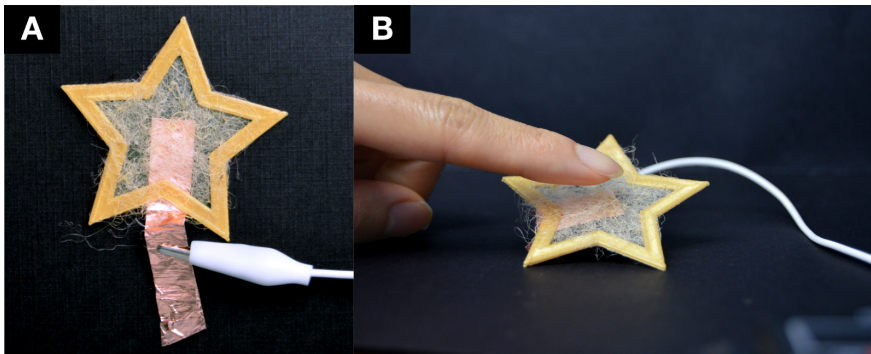


FIGURE 6.8: Electrospun fibers can be patterned onto conductive materials then bound together with rigid plastic to create custom-shaped capacitive sensors (A). The electrospun textile offers soft touch affordances and compliance to a capacitive sensor (B).

6.5.2 Piezoresistive Sensing

Electrospun swatches or collections of fibers can be made piezoresistive by coating them in a mixture of conductive paint ([Figure 6.9A](#)). We mix a 1:2 ratio of conductive paint¹⁰ to water by volume and coat areas of the electrospun textile using a paint brush. The sensors are left to dry overnight. After attaching test leads to the ends of the sensing region, manipulation of the textile produces changes in electrical resistivity ([Figure 6.9B](#)).

¹⁰Bare Conductive Paint: <https://www.bareconductive.com/shop/electric-paint-50ml/>

6.5.3 Liquid Absorption Sensing

Fibers produced via melt electrospinning can be used to absorb liquids. We use this property to create an absorption sensor that

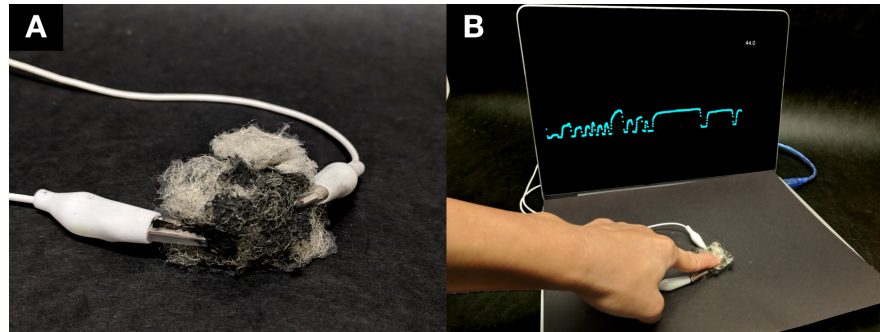


FIGURE 6.9: Electrospun fibers coated in conductive paint become a piezoresistive sensor (A), changing electrical resistance based on applied pressure (B).

changes electrical resistance based on how much liquid is absorbed. We tested the feasibility of this sensor by attaching test leads to copper electrodes at opposite ends of a folded electrospun swatch (fabricated as a 30x30mm square).

Initially there is no electrical connection formed as there is no fluid to carry charge across the fibers. We place the swatch in tap water to establish an initial connection and then squeeze the swatch to remove as much water as possible. The swatch is placed in the test setup seen in [Figure 6.10A](#). We then use a liquid dropper (1 ml) to add individual drops of water to the center of the electrospun fibers.

After each additional water drop, we wait approximately 15 seconds for the voltage reading to stabilize then record the value. The chart in [Figure 6.10B](#) shows that increasing the amount of water in the fibers causes an increase in the sensed voltage (or decrease in electrical resistance) between the two electrodes fixed at the ends of the fibers. The 13th drop of water results in the fibers becoming overly saturated and expelling some water. This loss of water leads to a lower sensed voltage.

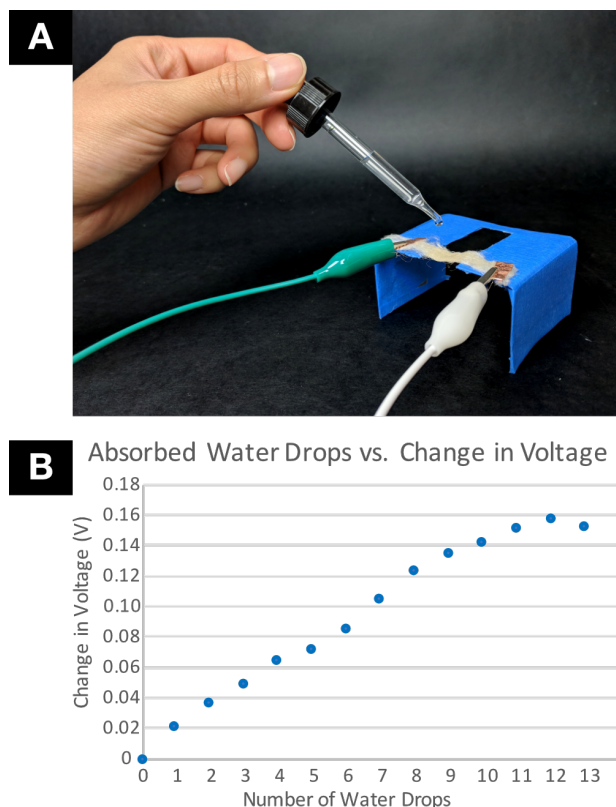


FIGURE 6.10: Experimental setup (A) and results (B) for evaluating electrospun fibers as a liquid absorption sensor. Each additional drop of water added to the fibers causes an increase in the sensed voltage between the two electrodes fixed at opposite ends of the fibers.

6.6 APPLICATIONS

We created a set of examples to demonstrate various looks, feels and interactions (e.g., water absorption sensing) enabled with our printer. For each example, we describe the electrospinning process parameters and their intended effects.

6.6.1 *Water Me: Actuated Flower Reminder*

We fabricated a flower with soft electrospun petals and rigid plastic channels that enable tendon actuation with gel-spun polyethylene fishing line. The flower is electrospun with a mid-infill density, high temperature, and low extrusion rate (40%; 290°C; 11 mm/min), creating a soft, dense surface for supporting the rigid plastic channels. In addition, we electrospun a sensor that changes electrical resistance based on the amount of moisture absorbed in its fibers.

These objects are placed together in a flower pot alongside a

living plant to provide visual and physical feedback of the soil's moisture level. When the sensor detects the soil is dry, the flower's petals close using a servo motor (Figure 6.11A). Once water is added to the soil, the servo releases and the flower's petals open, indicating sufficient water is available for the nearby living plants (Figure 6.11B).



FIGURE 6.11: A custom-shaped flower made of electrospun textile and rigid plastic that actuates based on the soil's water level sensed using an electrospun liquid absorption sensor. When the soil is dry, the flower closes its petals (A). When the soil is moist, the flower actuates open.

6.6.2 Interactive Woolly the Sheep Comic

We created a touch-sensitive comic of a sheep named “Woolly” using paper, copper foil traces and a custom-shaped electrospun textile. We fabricated the comic by inkjet printing the comic onto paper, adding a copper foil trace for wiring connections, applying light adhesive using a glue stick and then electrospinning directly onto the comic. The body of the sheep is electrospun with a high infill density, a mid-temperature, and a mid-extrusion rate (50%; 280°C; 18 mm/min) to achieve a fluffy and spongy tactile experience. Capacitive sensors are embedded under the sheep's electrospun fibers: one sensor is present on the sheep's back (visible in Figure 6.12A for the purposes of showing the sensor); the other is placed on the sheep's head behind the comic paper. When the sheep's back is petted, a “Baaah” sound characteristic of a sheep is produced. When the sheep's head is touched, a light-hearted giggle is produced to indicate the sheep's enjoyment. This example demonstrates the possibility of using existing objects (i.e., paper and copper foil) alongside electrospun fibers to create soft, custom-shaped interactive experiences.

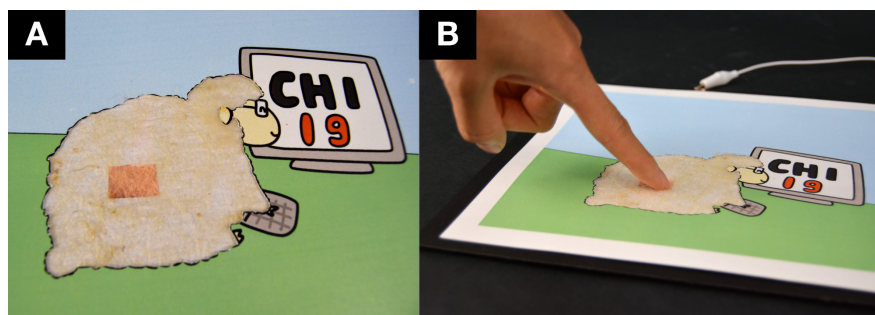


FIGURE 6.12: An interactive comic featuring a cartoon sheep whose body is made of a custom-shaped electrospun textile for soft capacitive sensing and tactile experience (A). Touching the sheep in various regions of its body produces different sound effects from a “Baaaah” to a giggle (B).

6.6.3 Foldaway Phone Stand

We printed a flexible, foldable stand that can be affixed to a mobile phone to offer a preferred viewing angle for watching videos (Figure 6.13A). The stand features a custom-shaped electrospun textile fabricated with a low infill density, high temperature, and low extrusion rate (20%; 298°C; 10 mm/min) to create a smooth and soft surface for hinging. Rigid plastic patterned on the textile enables bending into a configuration that can support the weight of the accompanying phone (Figure 6.13B). When not in use, the stand can be flattened to minimize its size. Anecdotally, the stand was used approximately 30 times to watch videos before the folded regions began to wear down and separate. We believe this issue could be mitigated by adding more layers of electrospun textile beyond the four used to fabricate the object.

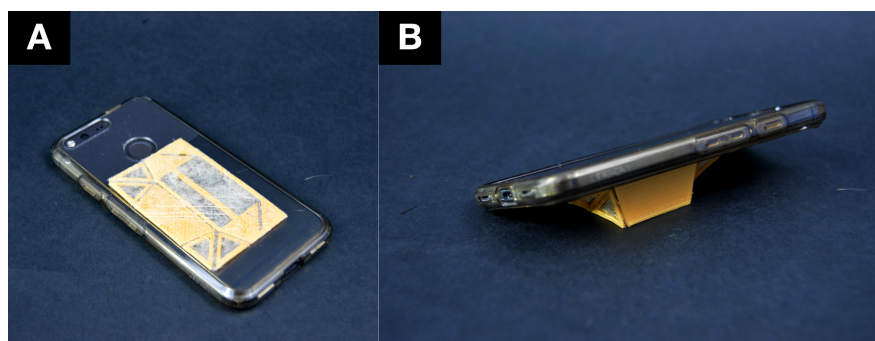


FIGURE 6.13: A foldaway phone stand fabricated using rigid plastic and electrospun textile. The phone stand is affixed to a phone case (A) and can be deployed when needed to obtain a preferred view angle for watching videos.

6.6.4 Textile Origami Lamp and Controls

We fabricated an origami-style lamp that is printed flat using rigid plastic and electrospun textile (Figure 6.14A). The lamp's electrospun areas have a low infill density, high temperature, and low extrusion rate (10%; 290°C; 10 mm/min) to create a surface that diffuses the lamp's light. The lamp takes on a 3D form when folded and placed into its accompanying 3D printed holder. In addition, we printed a capsule that holds electrospun piezoresistive fibers (Figure 6.14B) and use this sensor to control the lamp's brightness (Figure 6.1B). Lastly, the lamp can be switched on and off using a soft, star-shaped capacitive toggle switch.

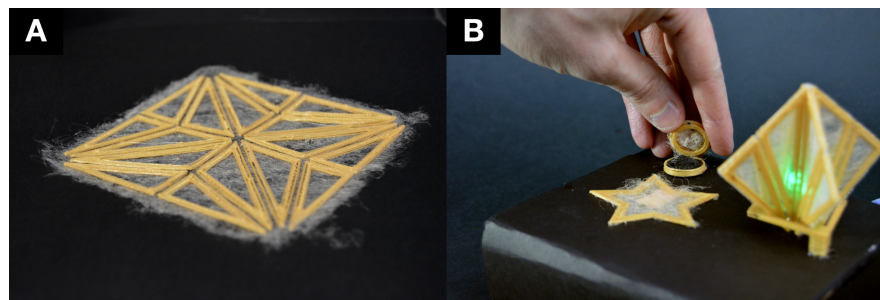


FIGURE 6.14: A custom-shaped origami-style lamp printed using rigid plastic and electrospun textile (A). Once folded into its final form, the lamp is paired with a soft, star-shaped capacitive toggle switch, and an electrospun piezoresistive capsule sensor to control the lamp's brightness (B).

6.7 DISCUSSION AND LIMITATIONS

There are a few limitations of our approach to fabricating combined rigid plastic and electrospun textile-based objects. First, the height of electrospun textiles produced on the printer is constrained by the strength of the electric field between the hot-end nozzle and the printer surface. As more non-conductive material is printed or placed between the two charged surfaces, the electric field strength decreases, reducing the ability to electrospin. In line with existing work on melt electrospinning, we are only able to electrospin textiles that have heights of at most 1.2 mm. This perhaps can be increased by using conductive materials (e.g., conductive paint, and conductive PLA) during the printing process, but further exploration is needed.

Similarly, when printing large plastic objects (e.g., a tower), because the height of the extruder used for electrospinning must

be raised to prevent collisions, the ability to electrospin is also reduced. This is a result of the electric field strength being inversely proportional to the squared distance between the two charged surfaces (the hot-end nozzle and the build plate). On our printer, we found the minimum distance for electrospinning at 7kV without electrical arcing is 15mm while the maximum distance before the electric field strength becomes too weak to electrospin is 50 mm. This could potentially be increased by adjusting the applied high voltage dynamically as a function of the current printing height or by using a positionable charged probe for targeted electrospinning similar to collector probe arrays in [169].

6.8 CONCLUSION

In this chapter, we presented a technique to fabricate objects made of both rigid plastic and textiles using a new 3D printer that supports melt electrospinning. This printer is equipped with low-cost and open-source modifications to make the technique amenable to other consumer-grade 3D printers. With this techniques, properties of textiles such as softness, flexibility and absorbency can be tuned using simple printing parameters. We demonstrated a series of proof-of-concept objects including an interactive tactile comic, a foldable phone stand, and a flower that actuates based on sensed water levels. As a whole, this technique opens up new opportunities to create objects with mixed rigidity, flexibility, texture and absorbency for personal fabrication.

7

3D Printing with a Novel Biodegradable Material

7.1 INTRODUCTION

Many functional materials exist around us as a part of nature. Cellulose—the most abundant natural polymer in the world [234]—forms the fibers of plants and trees along with hemi-cellulose and lignin. In this chapter, we investigate these natural materials for 3D printing. Unlike thermoplastics that are commonly used in 3D printing, these materials are both renewable and biodegradable. These characteristics are ideal for no-waste prototyping, and more broadly personal fabrication. To this end, this chapter introduces a new material technique for 3D printing with these natural materials via spent coffee grounds. It examines how the material can be recycled during prototyping sessions and explores it can enable the design of objects that readily biodegrade during/after their intended use (Figure 7.1).

7.2 BACKGROUND

Nations around the world are grappling with global environmental challenges including climate change, pollution, and waste production. Within the HCI community, there has been growing interest in addressing these sustainability issues as creators and enablers of technology [35, 63, 183, 187, 233]. Researchers have examined the effects of digital technology use on energy consumption [82, 326] as well as strategies to mitigate over-use [223, 327]. Others have investigated reducing waste output by reusing objects such as electronics [112, 141] and textiles [335].



FIGURE 7.1: Examples of biodegradable objects fabricated using our new 3D printing material: an ornament necklace, two custom-shaped planter pots, and two espresso cups coated in beeswax.

Recently, a five-year review of physical prototyping within the HCI community has foregrounded the environmental impacts of different types of materials and machines being used [306]. In an effort to encourage more sustainable approaches, researchers have proposed using bio-based materials such as mycelium [156, 157] and examining their life-cycle [158]. However, there has been limited exploration in how we might mitigate environmental challenges associated with personal fabrication, and particularly 3D printing [145].

As previously discussed in Chapter 2, expiring patents coupled with open-source movements (i.e., Fab@Home [181] and RepRap [132]) pushed 3D printers into the consumer domain. With some kits now costing less than \$170¹, 3D printers are rapidly finding their way into the homes of consumers and small businesses. At least 2 million printers have been purchased for consumer use as of 2019 [242]. Though, this is an underestimate as it only accounts for sales reported by large companies and excludes sales of low-cost kits [242]. Notably, adoption of these machines stands to exacerbate environmental challenges by increasing use of plastic materials (which have been shown to have detrimental ecological effects [43, 71]); waste output (e.g., through discarded prototypes and failed prints [275]); and energy consumption [2, 75].

In terms of materials, the most commonly printed on FDM/FFF 3D printers are the thermoplastic polymers acrylonitrile butadiene

¹2021 Best Cheap/Budget 3D Printers in 2021: <https://all3dp.com/1/best-cheap-budget-3d-printer-affordable-under-500-1000/>

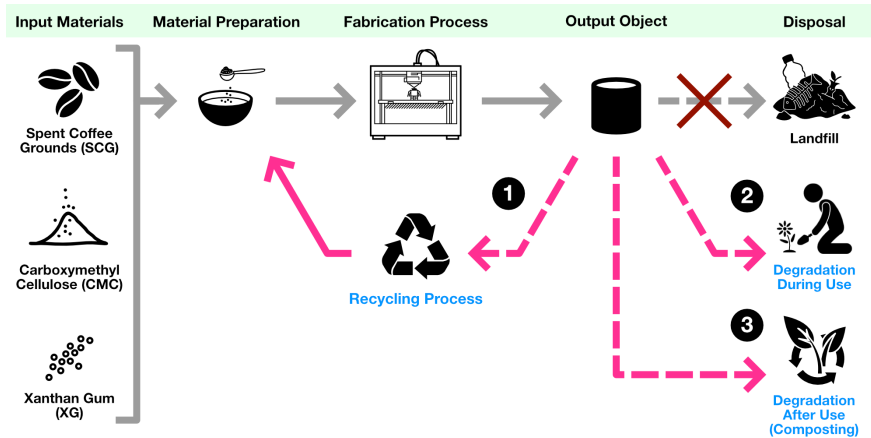


FIGURE 7.2: Overview of the personal fabrication workflows enabled with our spent coffee ground material: (1) Previously printed objects can be easily recycled at home to form new printing material; (2) Objects made with our material can readily biodegrade during their use such as a flower planter pot once placed into soil; (3) Objects and printing material that have completed their usage-cycle can be composted at home to create a fertilizer for gardening. These workflows minimize waste output and avoid disposal in landfills.

styrene (ABS) and polylactic acid (PLA). ABS is not biodegradable and is produced from petroleum, a non-renewable resource [212]. PLA, on the other hand, is produced from plant starch and generally viewed as being biodegradable. However, its biodegradability has some caveats. The material will decompose into carbon dioxide and water within 90 days, if processed in a controlled composting facility that contains a specific microbiome while consistently being heated at a high temperature (60 °C) [237]. Owing to these requirements, very few facilities accept PLA for composting so the material almost exclusively ends up in landfills [264]. Within landfills, PLA can take at least 100 years to degrade [146].

Processing of PLA through traditional recycling streams is also problematic as it often contaminates other commonly recycled plastics such as polyethylene terephthalate (PET, e.g., soda bottles) [152]. Recently, some companies (e.g., Filabot²) have explored recycling printed PLA objects back into a printable filament. Objects are ground, melted, and mixed with fresh plastic pellets before being extruded into a filament. Though promising, this approach requires expensive machinery and is generally not accessible to consumers.

With in the HCI community, researchers have sought to print less plastic material [196, 197] and/or substitute it with plastic

²Filabot Machines: <https://www.filabot.com/collections/filabot-core>

bottles [147, 148] or reusable Lego-style blocks [197]; however, these efforts have focused primarily on addressing challenges with fabrication speed [196, 197], object size [147, 148], and the lack of interactivity [147] associated with objects made using current 3D printing processes. Others have developed ways to reduce plastic consumption by reusing scrap materials as infill for printed objects [313] and re-printing on top of previously printed objects during prototyping iterations [287]. More broadly, researchers have examined the use of biomass resources (e.g., bamboo fiber [323], lignin [151], and spent coffee grounds [44]) as filler materials in thermoplastic filaments. These fillers are used in low percentages (typically $\leq 30\%$) and usually combined with PLA [28]. Taken as a whole, these approaches still require substantial use of plastic materials.

In general, reducing the use of plastics (and especially thermoplastics) in 3D printing is ecologically-beneficial. While researchers have shown that the ecological impacts of 3D printing are primarily driven by electricity use [75], material choice can greatly influence the amount of electricity used during a 3D printing process [76]. With thermoplastic 3D printing, significant energy is used to heat the material for extrusion as well as maintain an appropriate build plate/volume temperature during printing [76]. Thus, materials that can be printed without heating (i.e., bond chemically as opposed to thermally) can greatly reduce the environmental impacts of 3D printing [74, 76]. These impacts can further be reduced if the material is non-toxic, abundant, renewable and compostable [74].

The work presented in this chapter is directly motivated by a need for low environmental impact materials for 3D printing and personal fabrication. Guided by principles of Sustainable Interaction Design [35], we introduce a new biodegradable material for 3D printing that consists primarily ($\sim 85\%$) of plant-derived cellulose, hemi-cellulose, and lignin supplied by spent coffee grounds—a commonly wasted natural material. In contrast to typical plastic filaments, the demonstrated printing material is renewable, does not require heating during printing, and can be made with kitchen-friendly ingredients. Likewise, objects made with it can easily be recycled back into printing material during prototyping sessions and be composted at home. These aspects of our material open new possibilities for creating objects that are designed to biodegrade during and after their intended use (Figure 7.1). In the following sections, we describe the design of our material, its use with a 3D printer, the fabrication workflows that it enables, and

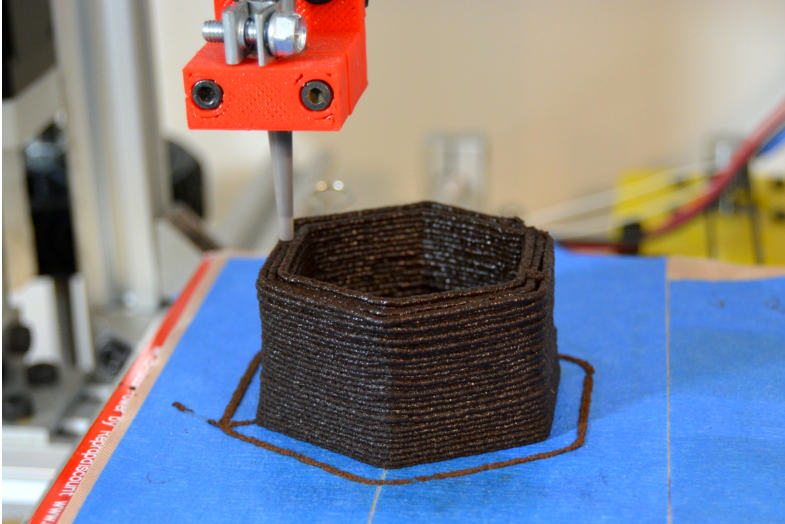


FIGURE 7.3: A biodegradable planter pot being printed using our spent coffee ground material.

a characterization of its properties. We conclude with a discussion of our material and how life-cycle considerations can foster new opportunities for collaborations and sustainability in personal fabrication.

7.3 MATERIAL DESIGN

The design of our material was guided by principles of Sustainable Interaction Design (SID) [35] and prior work highlighting strategies to reduce the environmental impacts of 3D printing [74, 75, 76]. In this section, we describe these motivations and the components of our material.

Sustainable Interaction Design establishes principles that the design of an object should consider from the perspective of sustainability, whether with physical or digital materials [35]. It calls on the design of objects to link invention and disposal, and promote renewal and reuse. The former principle dictates that the invention of an object must include a detailed account of how it and materials resulting from its use will be discarded. The latter principle requires the design of an object to consider possibilities for the renewal and reuse of existing objects or systems [35].

In the design of our material, we linked invention and disposal by prioritizing the use of components that are renewable, biodegradable, and compostable. These considerations minimize

TABLE 7.1: Proportions of the different components that are used to prepare our material for 3D printing.

| Name | Mass Proportion (g) |
|-------------------------------|---------------------|
| Spent Coffee Grounds (SCG) | 50 |
| Carboxymethyl Cellulose (CMC) | 8 |
| Xanthan Gum (XG) | 1.2 |
| Water | 100 |

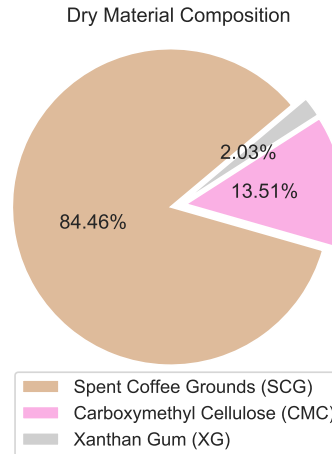


FIGURE 7.4: After drying, objects made with our material are primarily composed of spent coffee grounds (84.46%). The remaining composition is of carboxymethyl cellulose (13.51%) and xanthan gum (2.03%).

waste output and support a circular material life-cycle. The design of our material promotes renewal and reuse by recycling a commonly wasted natural material—spent coffee grounds—as its primary component. Objects made with our material can also be recycled back into printing material during prototyping iterations and be composted at home to create a soil fertilizer (Figure 7.2).

As previously discussed in the [Background](#) Section, prior work has demonstrated that avoiding the use of thermal energy to print materials can greatly reduce the environmental impacts of 3D printing [74, 76]. Moreover, materials that are non-toxic, abundant, renewable, and compostable can further reduce these impacts [74]. In support of low environmental impact, we designed our material to be printed without thermal energy, and in alignment with our SID goals, all of our materials are non-toxic, abundant, renewable and compostable.

Our material consists of four components: spent coffee grounds,

carboxymethyl cellulose, xanthan gum, and water as seen in [Table 7.1](#). We now provide a description of each of these components and their purpose.

7.3.1 *Spent Coffee Grounds*

Coffee is one of the most consumed beverages in the world. At least 9.6 billion kg of coffee have been consumed every year since 2016 [[210](#)]. During brewing, typically only 18-22% of coffee mass is extracted as solubles into a beverage [[34](#), [172](#), [266](#)]. The remaining amount (78-82%) is referred to as spent coffee grounds (SCG). SCG are the primary by-product of coffee production in both consumer settings (e.g., at home, coffee shops) and industrial processes (e.g., instant coffee production) [[6](#)]. The majority of SCG are disposed of in landfills [[129](#), [240](#)], making them an ideal candidate for being recycled as a printing material. Additionally, SCG are a natural material primarily composed of cellulose, hemi-cellulose and lignin [[16](#)]*—*components that make up the cell walls of plants and trees [[234](#)]. Thus, they are renewable and biodegradable. SCG can also be composted and used as a soil fertilizer [[42](#), [54](#), [235](#)]. In collaboration with a local coffee shop, We recycle SCG for use as the main component of our printing material.

7.3.2 *Carboxymethyl Cellulose*

Carboxymethyl cellulose (CMC) is a biodegradable water-soluble polymer derived from cellulose [[20](#)]. It is commonly used as a binding, thickening and stabilizing agent in food (e.g., ice cream, cheese) and cosmetic products (e.g., lotions, toothpaste) [[23](#), [87](#), [107](#)]. CMC is compostable and has been shown to beneficially increase the retention of water in soil [[193](#)]. In our material, CMC primarily serves as a binding agent for the spent coffee grounds. It also increases the viscosity of the material for printing.

7.3.3 *Xanthan Gum*

Xanthan gum (XG) is natural polysaccharide produced by the fermentation of carbohydrates (e.g., glucose) by the bacteria *Xanthomonas campestris* [[84](#), [137](#)]. It is completely biodegradable within two days [[137](#)]. XG is water-soluble and often used as a stabilizer and thickener in food products (e.g., salad dressing) and cosmetics (e.g., toothpaste) [[137](#)]. In our material, XG prevents the spent coffee grounds from separating out of the mixture and

increases both the mixture's viscosity and its degree of shear thinning. Without XG's inclusion, we found that our material would not readily flow during printing. In some early tests without XG, we found the pressure applied during extrusion would cause a channel to form in the solution that would separate out the SCG from the CMC and water mixture.

7.3.4 *Water*

The primary purpose of water in our material is to combine the SCG, CMC, and XG components for printing. As hydrocolloids, both CMC and XG dissolve in water and form gel networks around the granules of the SCG. After printing, the water evaporates and the gel network dries bonding the SCG together. Once dry, our material is primarily composed of SCG (84.46%) as seen in [Figure 7.4](#).

7.4 FABRICATION TECHNIQUE

This section describes our preparation procedure for our spent coffee ground material (SCG material), our 3D printer set-up, and strategies for successful printing.

7.4.1 *Material Preparation*

Our SCG material for printing consists of spent coffee grounds (SCG), carboxymethyl cellulose (CMC)³, xanthan gum (XG)⁴ and water mixed together in a ratio of 50:8:1.2:100 by mass measured in grams ([Table 7.1](#)).

We partnered with a local coffee shop⁵ to receive their spent coffee grounds that were previously used to make espresso-based drinks (e.g., lattes, cappuccinos). The grounds were obtained finely ground to approximately 200 μm in diameter (visually similar in size to table salt) and were initially wet. We dried the grounds before creating the printing material. The grounds can either be dried in an oven at 93 °C for 30 minutes with occasional stirring, or in direct sunlight for a few days. The latter approach can be used to reduce energy consumption. Once fully dried, we sifted the grounds using a basic kitchen strainer⁶ to remove any large clumps.

After measuring their proper proportions as seen in [Table 7.1](#), all of the dry powders (SCG, XG, CMC) are combined together in a single jar. The powders are then shaken together for approximately 1 min to ensure a uniform mixture. This combination is then slowly

³Modernist Pantry Carboxyl-methyl Cellulose: <https://www.amazon.com/dp/B07YLZ136F/>

⁴Modernist Pantry Xanthan Gum: <https://www.amazon.com/dp/B00C3HL7B4/>

⁵Arriviste Coffee Bar: <https://arriviste.coffee>

⁶OXO 8-inch Strainer: <https://www.amazon.com/dp/B00133DRIK/>

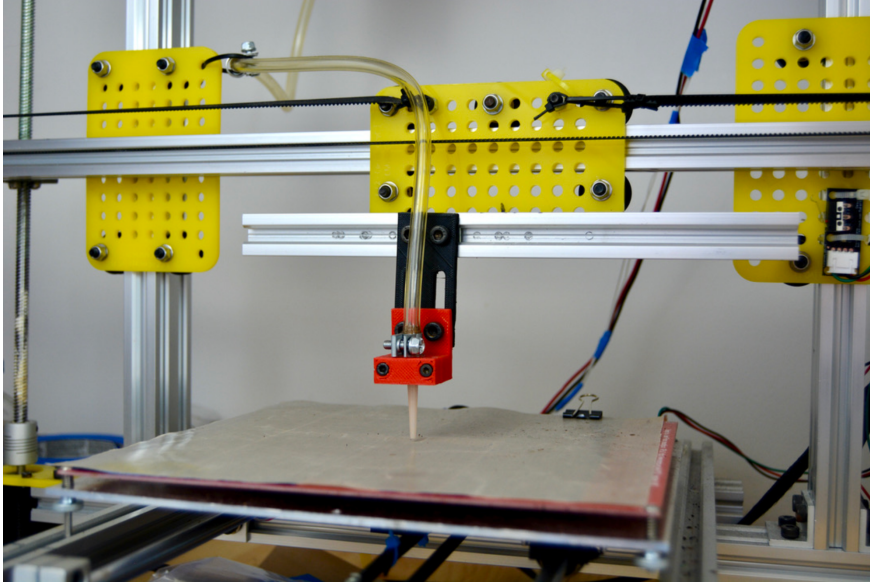


FIGURE 7.5: The extrusion set-up used to print our spent coffee ground material on a modified FDM/FFF 3D printer.

mixed into another jar containing the appropriate amount of water. Once the mixture is homogeneous, the SCG material is ready for 3D printing. Notably, this entire procedure can be accomplished in a kitchen at home with food-safe ingredients.

7.4.2 3D Printer Set-Up

We modified a consumer-grade FDM/FFF 3D printer similar in design to a Prusa I3⁷ to support printing the SCG material (Figure 7.3). After preparation, the material is loaded into a 60 mL syringe⁸ and extruded using an open-source, large volume syringe pump [228]. The slip-end of the syringe is inserted into one end of PVC plastic tubing (5/32" inner diameter)⁹. The other end of the tubing is connected to a barbed luer lock coupling¹⁰. Both the syringe tip and the coupling are secured to the hose using bolt clamps¹¹. Finally, the luer lock coupling is fitted with a 14 gauge (1.6 mm inner diameter) dispensing needle tip¹². We experimented using needle tips with have smaller inner diameters (e.g., 16 and 20 gauge) but found these were more prone to clogging. The luer lock coupling and needle are mounted onto the X-axis of the printer using a 3D printed adapter (Figure 7.5). We have open-sourced the designs of the adapter¹³.

Within our slicing software for 3D printing, the nozzle diameter

⁷Prusa I3: https://reprap.org/wiki/Prusa_i3

⁸60 mL Syringe: <https://www.amazon.com/gp/product/B01M1R392V/>

⁹Tygon PVC Soft Plastic Tubing (5/32" ID, 9/32" OD): <https://www.mcmaster.com/6516t16>

¹⁰Plastic Quick-Turn Tube Coupling (5/32" ID Barbed Tube): <https://www.mcmaster.com/51525k274>

¹¹Bolt Clamps for Soft Hose (9/32" to 21/64" ID): <https://www.mcmaster.com/53175K81/>

¹²Dispensing Tip with Luer Lock Connection (14 Gauge Gauge): <https://www.mcmaster.com/6699A1/>

¹³<https://github.com/mriveralee/coffee-grounds-printing>

is set to 1.6 mm to match the diameter of the dispensing needle. The layer height is generally set to 1.0 mm. The SCG material is printed at a speed (i.e., feed rate) of 300 mm min⁻¹. We generally slice 3D models with a solid infill (100%) and print with retraction disabled to maintain a consistent flow of material during printing.

7.5 WORKFLOWS AND EXAMPLES

This section presents a series of ways that our SCG material can be used for prototyping and personal fabrication. We describe three workflows (summarized in [Figure 7.2](#)) and include examples of objects 3D printed with our material.

7.5.1 *Material Recycling for No-Waste Prototyping*

Prototyping with 3D printing creates physical waste in the form of stale designs and failed prints. This can amount to over 30% of the plastic material used in a workshop [275]. Our SCG material enables objects to be recycled back into printing material during prototyping sessions ([Figure 7.6](#)). Printed objects and failed prints, once broken into pieces, can be ground up into fine granules using a coffee grinder¹⁴ at home. The resulting powder is a dry mixture containing SCG, CMC and XG. Once weighed, this powder can be mixed into a proportional amount of water—100 g of water per 59.2 g of dry powder as seen in [Table 7.1](#)—to re-form the SCG material for printing.

As an example of this workflow, we prototyped a biodegradable ornament necklace that went through 3 iterations. In the first iteration, we explored the shape and logo of the ornament, producing a hexagonal object with the letters "MR" in the center. In the second iteration, we reused the material from the first prototype and other objects ([Figure 7.6A](#)) to re-make the ornament with a circular shape, an infinity symbol in the center, and a hoop region for tying the necklace. However, due to a printing error (circled in the bottom left of [Figure 7.6E](#)), the hoop of the second prototype was not printed fully closed. We re-printed the final prototype as seen in [Figure 7.7](#).

7.5.2 *Degradation During Use*

The notions of "un-making" [272] and printing with perishable materials [60] have opened up design opportunities for enabling objects to change and decay over time. Objects made with biodegrad-

¹⁴Krups Adjustable Burr Grinder (GX500050): <https://www.krupsusa.com/BREAKFAST-APPLIANCES/COFFEE-GRINDERS/Adjustable-Burr-Grinder-GX500050/p/8000035582>

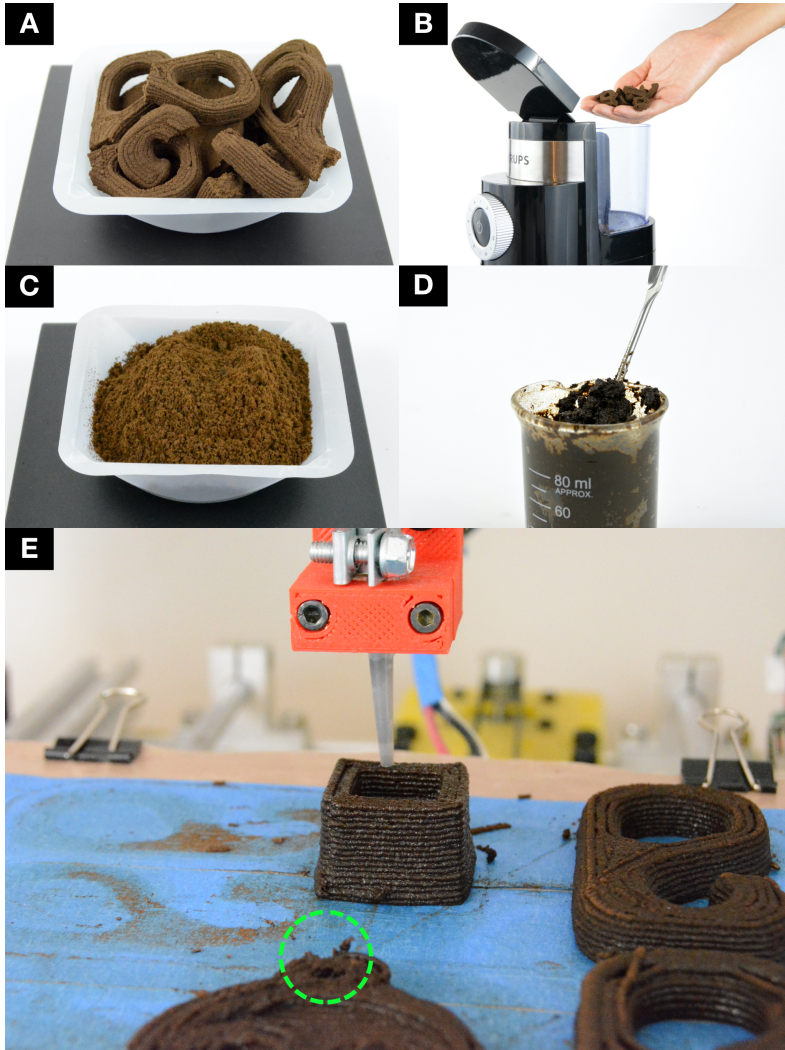


FIGURE 7.6: Material Recycling Workflow. Objects printed with our SCG material such as prototypes and failed prints (A) can be ground up using a basic coffee grinder at home (B). The resulting granules (C), once weighed, can then be mixed with a proportional amount of water (D) to produce our SCG material again for printing (E). This recycling approach is useful in minimizing waste when printing errors occur as highlighted in the green circle.

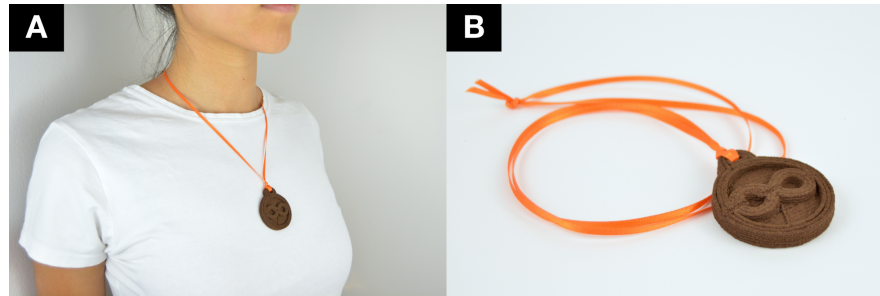


FIGURE 7.7: A biodegradable ornament necklace that was prototyped and printed with our SCG material (A). The ornament has a printed hoop for attaching a necklace and features the infinity symbol at its center (B).

able materials can encapsulate their decomposition as a part of their intended use. The components of our SCG material are all biodegradable and have been shown to have positive effects in soil including increasing water retention [8, 26, 193] and promoting plant growth [42, 54, 91, 193, 235]. With these considerations, our SCG material enables the creation of objects that are designed to beneficially decompose in soil over time. We created two custom-shaped planter pots to demonstrate this workflow as seen in Figure 7.8. These pots can serve as an initial home for small plants. Once the plants have sufficiently matured, they can be buried with their pots in a larger bed of soil to continue supporting their growth.

7.5.3 Degradation After Use

Objects made with typical 3D printing materials are almost exclusively disposed of in landfills after their intended use. Many of these materials (e.g., ABS) will never biodegrade, while others like PLA will take hundreds of years to decompose. In contrast, objects made with our SCG material readily biodegrade and can be composted at home (Figure 7.9), avoiding disposal in landfills entirely. The resulting compost can then be used as a soil fertilizer.

The ability to compost our SCG material opens up opportunities to create custom objects that readily biodegrade after their intended use. We designed and fabricated two custom-shaped disposable espresso cups with our SCG material (Figure 7.10). Inspired by Cradle-to-Cradle design [186], the grounds of previously created espresso drinks serve as vessels for subsequent drinks. We coated the inside of these cups with beeswax¹⁵—another biodegradable material—to waterproof the cups during use. Once a cup serves it

¹⁵Organic White Beeswax Pellets (1lb): <https://www.amazon.com/gp/product/B01LYMZK4V/>



FIGURE 7.8: Biodegradable planter pots printed with our SCG material and their flowering plants (A). The first pot has a hexagonal-shape (B). The second pot is cylindrical with a ribbed pattern (C).

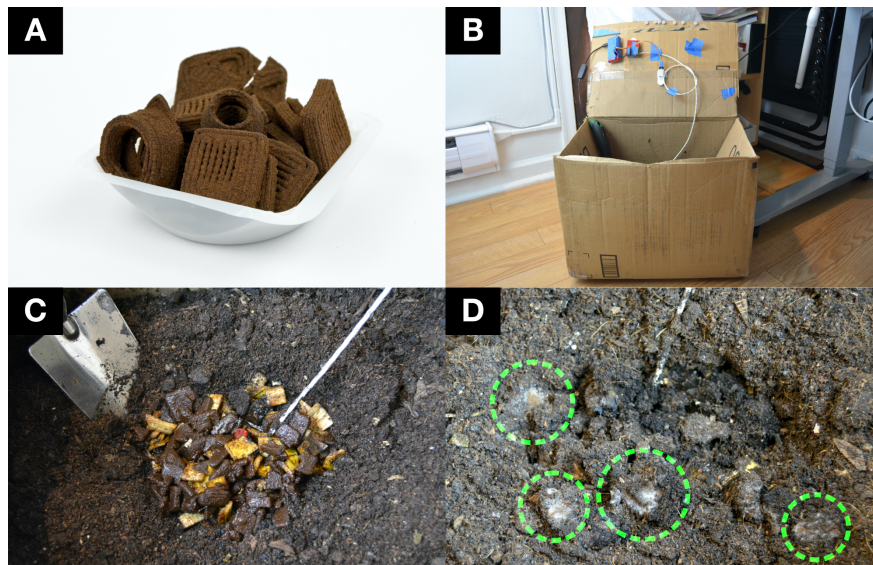


FIGURE 7.9: Composting Workflow. Objects made with our SCG material such as prototypes and failed prints (A) can be inserted into a compost box at home (B) with other food scraps (C). Within a few days, microorganisms like mold will grow and begin breaking the material down into compost (D).



FIGURE 7.10: Biodegradable espresso cups made with our SCG material (A). The cups hold liquid once beeswax is applied either on the inside of the cup (B, left) or around the cup entirely (B, right).

purpose, it can be disposed of in a compost bin.

7.6 MATERIAL CHARACTERIZATION

This section provides a characterization of different aspects of our SCG material. We describe and provide empirical results of the SCG material's shrinkage, tensile strength, and surface texture. For both tensile strength and surface texture, we compare newly made SCG material to recycled SCG material. Finally, we provide the results of a composting study that demonstrates the ability of our SCG material to be composted at home.

7.6.1 *Shrinkage Characterization and Mitigation*

In our preliminary printing tests, we discovered that the SCG material was prone to shrinking as an object dried. This behavior is due to the evaporation of water from the xanthan gum and carboxymethyl cellulose. These two materials are hydrocolloids—they swell and form gels when dispersed in water. During printing, these materials are in a swelled state. Thus as they dry, they shrink. We characterized the shrinkage behavior of the SCG material after printing to determine a mitigation strategy.

We printed five rectangular samples (30 mm x 30 mm x 5.6 mm) with a solid (100%) infill. The samples were left to air dry for three days. We then recorded the length, width and height of each sample. These measurements were averaged across all five samples and an error percentage was computed for each dimension and their average as seen in [Figure 7.11](#). The error in length, width, and height are -14.61% (SD=2.64); -14.69% (SD=1.71); and -14.29%

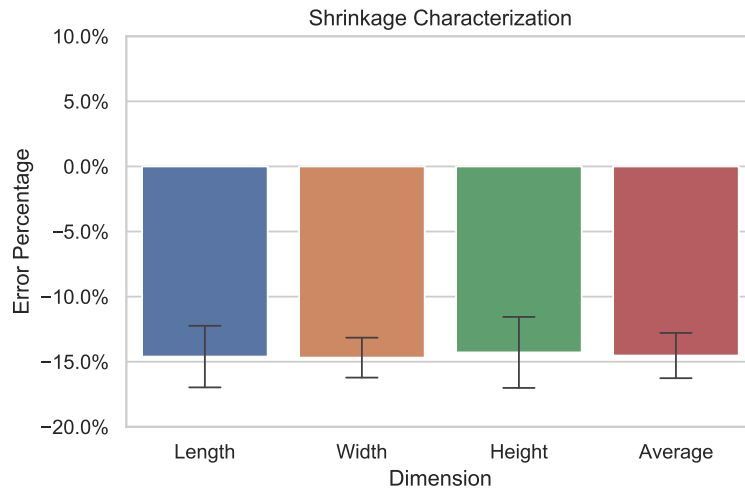


FIGURE 7.11: Shrinkage characterization. The average error in dimensional accuracy for five printed samples (30 mm x 30 mm x 5.6 mm) once dried is -14.53% (SD=1.94).

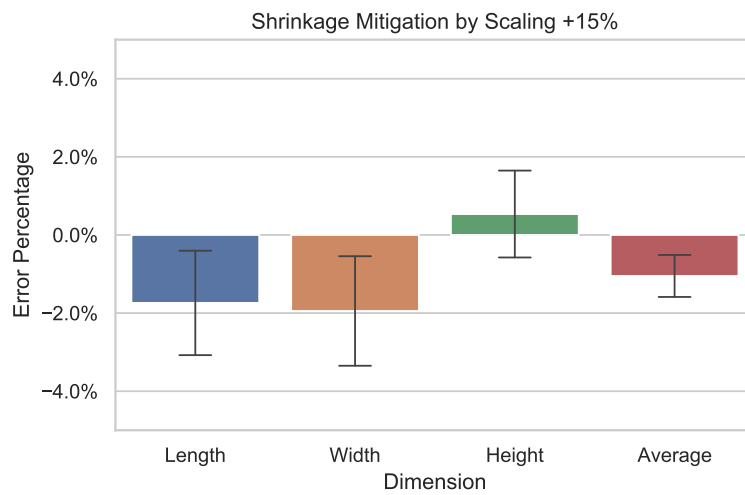


FIGURE 7.12: After uniformly scaling the geometry of samples by 15.0% before printing, the average error in dimensional accuracy caused by shrinkage for five printed samples reduced to -1.05% (SD=0.60).

(SD=3.05), respectively. The average across all of these dimensions is -14.53% (SD=1.94).

As a shrinkage mitigation strategy, we examined applying a uniform scale factor (15%) to object geometry prior to slicing for printing. We scaled the rectangular geometry that was used for the shrinkage characterization and printed five samples (34.5 mm x 34.5 mm x 6.4 mm) with solid infill. The samples were left to completely dry for three days. We then measured the dimensions of the samples and computed the percent error based on their expected values (30 mm x 30 mm x 5.6 mm) as seen in [Figure 7.12](#). The error in length, width, and height are -1.74% (SD=1.49); -1.95% (SD=1.57); and 0.54% (SD=1.24), respectively. The average error across all of these dimensions was reduced to -1.05% (SD=0.60). These results indicate a uniform scaling can greatly increase the dimensional accuracy of solid objects when printed with our SCG material. We use this strategy to mitigate shrinkage in objects printed throughout the rest of this work.

7.6.2 Strength Characterization

We performed a preliminary characterization of our SCG material's tensile strength using a hanging load test as seen in [Figure 7.13A](#). We printed a series of open-source tensile test hooks¹⁶. Each hook was printed with a solid (100%) infill and 3 perimeters. During the test, a hook was suspended on the test rig and masses¹⁷ were incrementally suspended on the hook. We waited 30 seconds after each mass was added to ensure it was securely held. Once the printed hook broke ([Figure 7.13B](#)), we recorded both the load at failure and the maximum load that was stably held.

The results of the tensile test are shown in [Figure 7.14](#). We examined two sets of printed hooks. In the first set (N=4), hooks were printed with newly made SCG material. These hooks had a mean maximum stable load of 1.43 kg (SD=0.15) and a mean failure load of 1.58 kg (SD=0.10). In the second set (N=2), we tested hooks that were made with recycled SCG material. The hooks made with recycled SCG material had a mean maximum stable load of 1.00 kg (SD=0.28) and a mean failure load of 1.15 kg (SD=0.21). While the newly made SCG material performed better than the recycled SCG material (on average, 0.43 kg more mass was supported), the results across both tests indicate that the SCG material is strong enough to withstand handling (e.g., during prototyping iterations) and to enable some functional use cases (e.g.,

¹⁶Open-Pull Hooks: <https://github.com/CNCKitchen/Open-Pull/blob/master/CAD/Specimens/testHook.stl>

¹⁷Hook Weight Set: <https://www.amazon.com/gp/product/B00EPQMEWC/>

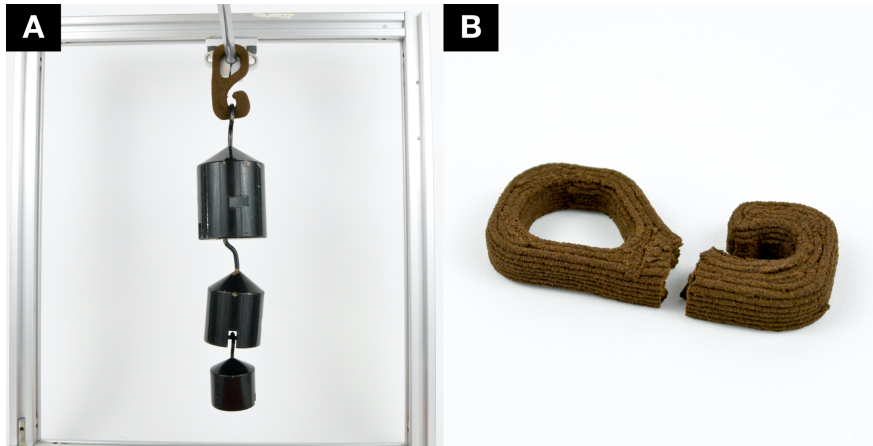


FIGURE 7.13: The tensile strength test set-up showing a hook printed with the SCG material holding 1.7 kg of mass (A) before breaking into two separate parts (B).

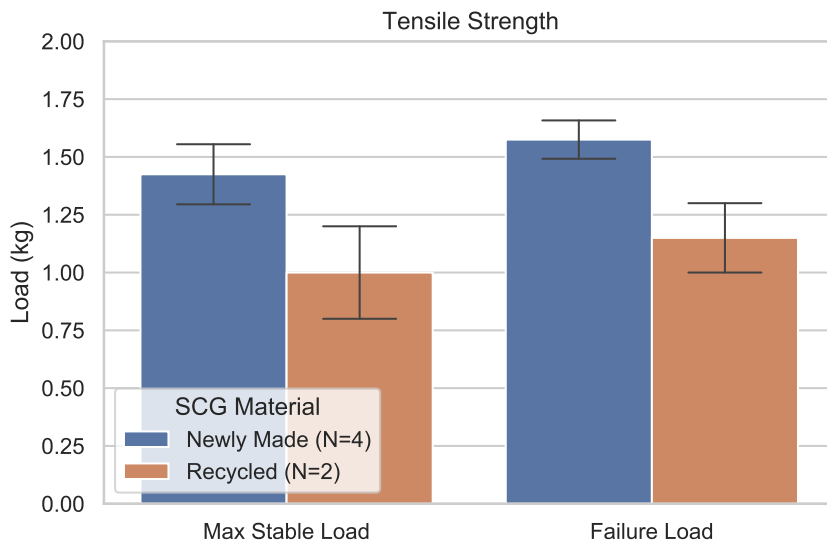


FIGURE 7.14: Results of the tensile strength test. On average, hooks printed with newly made SCG material had a higher maximum stable mass (1.43 kg) and failure mass (1.58 kg) than hooks printed with recycled SCG material with a difference of (0.43 kg).

supporting the weight of another object, acting as a enclosure, etc.).

7.6.3 *Surface Texture Characterization*

To understand how our material recycling workflow affects the surface characteristics of objects, we examined the layer lines of two box-shaped test specimens (30 mm x 30 mm x 30 mm). The first specimen was printed with newly made SCG material while the second specimen was printed with once recycled material using our recycling workflow as shown in [Figure 7.6](#). Images of the surface texture were captured of both samples under the same lighting conditions. These images are placed side-by-side in [Figure 7.15](#).

The test specimen printed with the newly made SCG material has a smoother surface texture than the specimen printed with the recycled material as evidenced by shallower valleys between layer lines. This distinction in the recycled material's surface texture (and potentially its decreased tensile strength as described in the [Strength Characterization](#) Section) may be the result of granules having a non-uniform size distribution in our once recycled SCG material. We used a low-cost coffee burr grinder to grind up previously printed objects. This may have affected the consistency of the granules. In contrast, the size of granules in the raw materials used for the newly made SCG material is much more consistent. Both the XG and CMC powders are very finely ground (visually similar to flour). The spent coffee grounds also have high consistency which is likely the result of being ground on high-end equipment at the specialty coffee shop. The size difference between recycled granules may have affected the ability of layers to securely bond to one another, reducing overall strength. However, neither the surface texture nor the tensile strength of the recycled material affected our ability to use the material for prototyping and application development.

7.6.4 *Composting Study*

Composting is the controlled decomposition of organic matter [[51](#), [62](#), [295](#)]. This decomposition is achieved by providing a rich environment for microorganisms to thrive. Both the growth of microorganisms and increased soil temperature relative to ambient temperature serve as indicators of the biodegradation of materials [[51](#), [62](#), [295](#)]. We examined the ability of our SCG material to decompose through an indoor home composting study. We opted for a home composting study (as opposed to industrial composting)

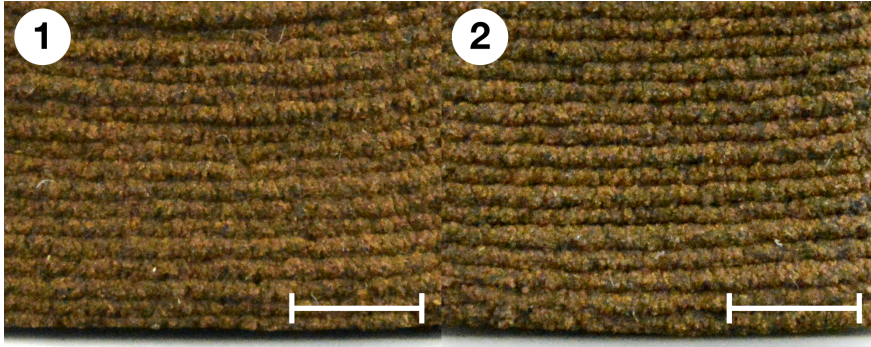


FIGURE 7.15: Comparison of layer lines on test specimens printed with (1) newly made SCG material and (2) material that been recycled from previously printed objects. The surface texture of the recycled material appears less smooth than that of the freshly made material. Scale bar: 5 mm.

to demonstrate that our material can be readily composted at home in contrast to thermoplastics commonly used in 3D printing.

We use a simple aerobic home composting approach [283, 284]. This approach can process approximately 500 g of organic waste material (e.g., food scraps) per day that would otherwise be disposed of in landfills. We mixed coco coir¹⁸ and horticultural ash¹⁹ (biochar) in a 2:1 ratio into a cardboard box (29 cm x 29 cm x 43 cm) until the box was approximately two-thirds full. When inserting material, we dug a hole in the center of the box, placed the material, and covered it up. The box lid was then closed, covered with a thin towel and placed on top of wooden blocks to increase aeration. We also turned, or mixed, the contents of the box every other day with a garden trowel²⁰ to increase aeration. The box was stored with an indoor temperature between 20 °C to 30 °C and away from excessive moisture (i.e., rain).

We set up a Raspberry Pi Zero²¹ as a microcontroller with an ambient temperature-humidity sensor²² and a waterproof temperature sensor²³ to capture data from our compost box during the study. The ambient temperature-humidity sensor was mounted onto the lid inside of the compost box to provide baseline ambient temperature and humidity readings (Figure 7.9B). We used the humidity readings to ensure that our compost materials had optimal moisture content (40-60%) for promoting microbial growth [62]. The waterproof temperature sensor was placed into soil at the depth of the most recently inserted material (as seen in Figure 7.9C) to capture any increase in temperature resulting from microorganisms breaking the material down. The sensor readings for soil temper-

¹⁸Burpee Natural & Organic GardenCoir: <https://www.amazon.com/gp/product/B078GQPRX4/>

¹⁹Wakefield Biochar Soil Conditioner: <https://www.amazon.com/gp/product/B0775WSPC4/>

²⁰Edward Tools Bend-Proof Garden Trowel: <https://www.amazon.com/gp/product/B01N297HU0/>

²¹Raspberry Pi Zero: <https://www.adafruit.com/product/3708>

²²DHT22 Temperature-Humidity Sensor: <https://www.adafruit.com/product/385>

²³High Temp Waterproof DS18B20 Digital Temperature Sensor: <https://www.adafruit.com/product/642>

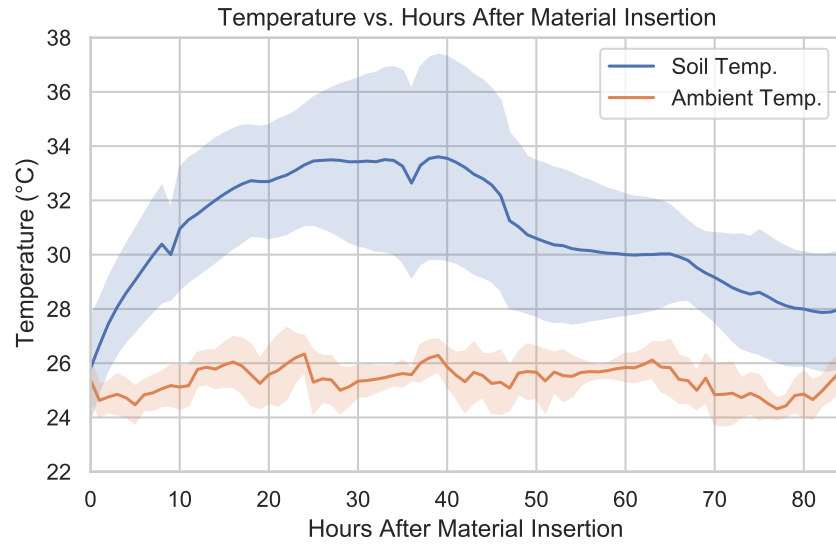


FIGURE 7.16: Compost Study Results. Material inserted into our home compost box consistently resulted in increased soil temperature relative to ambient temperature, indicating the material's decomposition by microorganisms. This trend of increased temperature continued for more than 80 hours after the material's insertion. The mean ambient and soil temperatures for five occurrences of material insertion are depicted in the bold orange and blue solid lines, respectively. The standard deviation is depicted as shaded regions around the each line.



FIGURE 7.17: A few small pieces of SCG material recovered after 3 weeks of composting, distinguishable by the color of the coffee grounds highlighted in the pink rectangular outline above. The recovered pieces were brittle and showed significant mold growth (highlighted in green circles) indicating their decomposition.

ature, ambient temperature, and humidity were recorded at an interval of one minute throughout the duration of the study.

Across a three week period, we performed five material insertions with a mean insertion mass of 227.40 g (SD=37.48) containing a mean SCG material mass of 62.98 g (SD=20.50) per insertion. The resulting change in temperature after material insertion is shown in [Figure 7.16](#). Soil temperature consistently rose after each material insertion. In some cases, the soil temperature rose approximately 10 °C higher than ambient temperature. The overall trend of increased temperature continued for more than 80 hours after a given material insertion.

A few days after our initial material insertion, mold began growing as shown in [Figure 7.9D](#). After three weeks of the study, we recovered a few small pieces of SCG material (approximately 10 mm to 15 mm in length). In contrast to our SCG material before composting, the pieces were brittle and showed significant mold growth as seen in [Figure 7.17](#). Both the growth of microorganisms and increased soil temperature relative to ambient temperature throughout our compost study indicate that our SCG material can be composted at home.

7.7 DISCUSSION AND LIMITATIONS

In this section we discuss challenges, limitations, and opportunities for future work with our SCG material. More broadly, we explore how consideration of the life-cycle of materials in personal fabrication can open new opportunities for collaborations with environmental scientists.

7.7.1 *Strength and Resolution of Printed Objects*

This work offers basic modifications to a consumer-grade 3D printer that enables our SCG material to be printed. We rely on an open-source large-volume motor-driven pump [228] for extrusion. The motor used as part of this pump is adapted from the 3D printer's existing drive mechanism for filament-based extrusion. While this motor has more than enough torque to drive plastic filaments, we had to tune the viscosity of our material with xanthan gum, and choose a relatively large diameter dispensing needle tip to promote printability. In our initial explorations, we noticed that the apparent strength of our material when cast decreased with the addition of xanthan gum. Future work should examine other biodegradable



FIGURE 7.18: A single layer square printed flat with our SCG material morphed into a saddle shape as a result of shrinkage during drying.

viscosity modifiers such as guar gum to increase material strength. Likewise, using a dispensing needle tip directly on the syringe instead of connected through plastic tubing may enable printing with smaller diameter tips. This would allow for a finer printing resolution (e.g., smaller layer heights, thinner extrusion widths) than demonstrated in this work.

7.7.2 *Material Shrinkage and Drying*

The shrinkage exhibited by objects printed with our SCG material is the result of using CMC as a binder and XG as a stabilizer. Both CMC and XG are hydrocolloids—they form gels when dissolved in water. These gels shrink as water evaporates during the drying process. While we provide some empirical characterization of this shrinkage, many factors can contribute to the shrinkage of a printed object including its shape, its interior density (i.e., infill), and its method of drying (e.g., using a fan). Thus, shrinkage compensation may need to be adjusted depending on these contributing factors.

Shrinkage is generally not ideal for most applications. However, previous work [7, 95, 230, 285, 316] has leveraged this behavior to create shape-changing interfaces. In some early explorations, we observed that objects printed with our material would morph out-of-plane into different structures after drying (Figure 7.18). Biodegradable shape-changing objects are an interesting opportunity for future work.

7.7.3 *Material Biodegradability and Compostability*

The growth of microorganisms and increased soil temperature are indicators of the biodegradation of materials in compost settings [62, 295]. In our compost study, we use these indicators as proxies for the decomposition of our SCG material. However, this approach does not provide insight into the quality of the compost produced with the SCG material. We rely on the results of prior studies which have demonstrated that the components of our SCG material are biodegradable [137, 163, 235] and provide benefits in soil [42, 54, 91, 193, 235]. As researchers in HCI continue to tackle environmental sustainability challenges with personal fabrication, future work should examine the development of accessible material evaluation approaches for biodegradability, compostability, and overall environmental impact—an opportunity for collaborations with environmental scientists.

7.7.4 *Life-Cycle Assessment, Prototyping, and Beyond*

Every material has a life-cycle that includes the sourcing of its components from Earth, their transport and processing into the material, how the material is used and eventually disposed. Life-Cycle Assessment (LCA) is a common method that is used to assess environmental impacts throughout the life-cycle of different materials and/or products [50, 185].

As discussed in the **Background** Section, works have examined the environmental impacts of 3D printers and different materials using LCA [75, 76]. The results of these prior efforts were used to help motivate the material developed in this work. Heating the hot-end and build plate in typical FDM/FFF 3D printers has been identified as a key contributor to the energy consumption, and thereby the environmental impacts, of FDM/FFF 3D printers [76]. In the current work, we explicitly developed a biodegradable material that is printed without the use of a hot-end and heated build plate to minimize energy consumption. Following principles of Sustainable Interaction Design [35], our material is made by reusing spent coffee grounds and can be recycled back into a printing material during prototyping iterations. Though, we have not performed a formal LCA of our material and prototyping process.

LCA is difficult to perform as data for many materials and processes may be not available. In the absence of data, an LCA's validity relies on the assessor to estimate environmental impacts using similar processes and materials (if they exist) with the caveat that the

results of any analysis will have an associated level of uncertainty. While there are on-going efforts to increase awareness of life-cycle thinking [77, 276] and broaden access to LCA data and methods [1, 190, 276, 288], some material components and procedures used in this work have no associated data. For example, xanthan gum, despite being a common food additive [84], has no available information in LCA databases [289]. We were also unable to find data for reusing/recycling of spent coffee grounds and for at-home composting.

More broadly, the democratization of personal fabrication technology has continued to foster new material and process developments that are difficult for their creators to examine using LCA. Evaluating the sustainability of these techniques with LCA will require increasing the approachability of LCA and broadening access to LCA data through collaborations with environmental sustainability researchers and LCA practitioners. Within the HCI community, these collaborations may also serve as a springboard to design systems that support environmentally-conscious behaviors beyond personal fabrication.

7.8 CONCLUSION

This chapter has presented a technique for 3D printing objects with a new biodegradable material primarily made of plant-derived cellulose, hemi-cellulose, and lignin from spent coffee grounds—a commonly wasted natural material. Unlike typical plastic filaments used in 3D printing, this material is printed without heat to minimize energy consumption. In addition, it can be recycled back into printing material during prototyping iterations and afterwards be composted at home to reduce waste output. As a whole, this material opens up new opportunities for fabricating objects that readily biodegrade as part of or after their intended use.

8

Conclusion

8.1 SUMMARY

This dissertation has examined materials that surround us everyday as a means of broadening what can be made with 3D printing for personal fabrication. When we consider everyday materials as inputs and outputs for fabrication techniques, we open up opportunities to produce objects with capabilities that extend what is possible with and beyond typical rigid plastic printing, and create new ways of interacting with these objects.

In [Chapter 4](#), textiles (the most common material with which we interact) embedded during an rigid plastic 3D printing process enabled objects to become soft, flexible, and input devices. In [Chapter 5](#), exchanging rigid plastic for food-grade hydrogel in a 3D printing process allowed textiles to become moisture-responsive interface that change shape in response to water. [Chapter 6](#) introduced a method to directly fabricate textiles alongside rigid plastic using a 3D printer. This process opened up the ability to tune properties of these textiles like texture based on a particular application. Finally, [Chapter 7](#) investigated natural material (e.g., cellulose) as a biodegradable material for 3D printing. Objects made with this material are capable of being recycled back into printable material during prototyping sessions, and can be designed to beneficially degrade during/after their use (e.g., through at-home composting).

Across all of this work, the presented techniques have sought to be accessible to end-users and amenable to existing 3D printer setups. These techniques have relied on the most common materials (e.g., textiles, cellulose). Material formulations have been purposefully designed for use at home. Printer modifications, where possible, are 3D printable. Finally, all electronics designs and soft-

*“But at the laste, every thing hath
ende”*

—Geoffrey Chaucer

ware are open-source. Bridging across these elements has enabled everyday materials to become an extension of 3D printing.

8.2 FUTURE DIRECTIONS

3D printing is an incredibly versatile tool. As demonstrated throughout this dissertation, it can give us a lot of power to control and create with the materials that are all around us everyday. This section lays out future directions that can broaden the use of digital fabrication technologies with everyday materials and advance personal fabrication.

8.2.1 *Designing Behaviors Around Everyday Materials*

For every material, consideration must be given to how we design with and around its functionality. Often we design around real-world objects by using physical measurements or 3D scanning to create a digital representation for use within a computer-aided design (CAD) tool. These methods can only capture static geometric representations. Moreover, CAD tools are generally material-agnostic which makes it difficult to explore mixing materials in objects and creating interactive behaviors.

In some instances, we can get away with simplified representations. In [Chapter 4](#), for the most part we were able represent textiles with simplified geometry (e.g., rectangular prisms). However, when the behavior of a textile became critical (e.g., during stretching), we relied on experimentation (e.g., adhesion testing) and trial-and-error to understand the behavior of a given textile and its accompanying rigid plastic when stretched.

Uncovering the effect of different designs through iterative prototyping can be laborious. It can also be difficult to leverage knowledge about material behavior to other designs and/or materials that might behave in similar ways. Building material models of an object (as we saw in [Chapter 5](#)) can be used to alleviate trial-and-error, support iterative prototyping through simulation, and enable designing complex behaviors. However, building such a models can, by its very nature, require experimentation in printing different test specimens to try and understand how a material behaves.

Capturing dynamic material behavior (such as shape-change due to shrinkage) and converting this is to usable material model is not currently possible. Recent works have examined capturing

physical changes (e.g., cuts, bends, folds) to a real object as a way to create and/or update its digital representation [96, 324]. These approaches show promise for streamlining how we design with complex material behaviors. One could capture a few photos of a material's behavior, and an intelligent system could automatically generate an appropriate geometric representation and material model for simulation. Such a system reduce modeling challenges and up new possibilities for designing with everyday materials.

8.2.2 *Modular Machines for Digital Fabrication*

Despite its versatility, one persistent challenge for 3D printing has been that different materials can often require the use of entirely different extrusion hardware. This makes combining materials of different types (e.g., thermoplastics and hydrogels) difficult. In some instances, current hardware can be adapted to support new functionality as Chapter 6 demonstrated by integrating electrospinning into a typical FDM/FFF 3D printer. However, liquid materials such as the hydrogel in Chapter 5 and the biodegradable material in Chapter 7 required syringe-based extrusion set-ups (instead of filament-based hot-ends). The majority of 3D printers and other digital fabrication machines have very similar electromechanical set-ups (e.g., a 3-axis linear motion platform). And yet, there has been little work on making these machines modular (with notable exceptions being [307, 317]). In the commercial setting, control electronics for these machines are heavily optimized for a specific function (such as having only the necessary electrical components for a single hot-end), usually to reduce costs. Modular machine designs such as tool-changers (as in [307]) show promise for enabling new types of materials to be readily combined and controlled.

8.2.3 *Sustainable Personal Fabrication*

Research in personal fabrication has largely been concerned with technological innovations around use: creating new prototyping possibilities (e.g., fabrication of objects that have interactive capabilities); developing software tools that lower the barrier to entry for users to design complex objects; reducing fabrication time; and exploring new applications (e.g., personalized objects, assistive technology, etc.). Many of these elements have appeared throughout this dissertation. We have seen ways to print faster, larger, and softer objects with textiles; create input devices, sensors, and actuators; and even leverage a design and simulation

tool to create water-responsive interfaces. However, given existing global environmental challenges (e.g., climate change, pollution, waste output), sustainability is perhaps the most important and yet under-explored area within personal fabrication.

Few works in this space have examined ways to remedy sustainability challenges resulting from the increased use of digital fabrication technologies. Chapter 7 approached environmental sustainability from a material perspective, printing with natural materials to consume less energy during printing and to create objects that readily biodegrade. Developing materials that are both sustainable and functional will be increasingly more important as personal fabrication continues to grow. Materials like chitosan produced from the shells of crustaceans [78]; mycelium produced from fungi [156, 157]; and keratin, a protein found in human hair, offer promising alternatives to commonly used plastics. Upcycling of commonly used everyday objects, which has shown promise for Internet-of-Things systems [329, 330], could also serve as another way to address waste-related sustainability issues in personal fabrication.

Beyond materials, there are opportunities to explore how we can nudge users to be conscious of sustainability throughout the design and fabrication workflow. At design time, 3D modeling software could proactively suggest changes to an object's geometry that would reduce the use of support material if the object were to be 3D printed. At fabrication time (e.g., in control software), a plugin could help a user choose a material based on an object's intended purpose and life-span. If an object is intended to be a prototype that tests the fit of a component (i.e., has a short life-span), then a material that can readily biodegrade like cellulose and/or that doesn't require heating a build chamber could be recommended to reduce physical waste and energy consumption, respectively.

8.3 FINAL REMARKS

Combining materials that are familiar and accessible to us with digital fabrication opens up new possibilities to create objects that are personalized, can be interactive, and have capabilities beyond bulk engineering materials. As access to digital fabrication technologies continues to grow, everyday materials can offer more opportunities to use and extend these tools for personal use.

References

- [1] United States Department of Agriculture. *Welcome to the Federal LCA Commons*. Apr. 2021. URL: <https://www.lcacommons.gov/> (cit. on p. 114).
- [2] Jerry Ajay, Aditya Singh Rathore, Chen Song, Chi Zhou, and Wenyao Xu. “Don’t Forget Your Electricity Bills! An Empirical Study of Characterizing Energy Consumption of 3D Printers”. In: *Proceedings of the 7th ACM SIGOPS Asia-Pacific Workshop on Systems*. APSys ’16. Hong Kong, Hong Kong: Association for Computing Machinery, 2016. DOI: [10.1145/2967360.2967377](https://doi.org/10.1145/2967360.2967377) (cit. on p. 92).
- [3] Lea Albaugh, Scott Hudson, and Lining Yao. “Digital Fabrication of Soft Actuated Objects by Machine Knitting”. In: *Proceedings of the 2019 CHI Conference on Human Factors in Computing Systems*. CHI ’19. Glasgow, Scotland Uk: ACM, 2019, 184:1–184:13. DOI: [10.1145/3290605.3300414](https://doi.org/10.1145/3290605.3300414) (cit. on pp. 28, 57).
- [4] Thomas Alderighi, Luigi Malomo, Daniela Giorgi, Bernd Bickel, Paolo Cignoni, and Nico Pietroni. “Volume-Aware Design of Composite Molds”. In: *ACM Trans. Graph.* 38.4 (July 2019). ISSN: 0730-0301. DOI: [10.1145/3306346.3322981](https://doi.org/10.1145/3306346.3322981) (cit. on p. 23).
- [5] All3DP. *27 great 3D printer filament types (a guide)*. 2016. URL: <https://all3dp.com/best-3d-printer-filament-types-pla-abs-pet-exotic-wood-metal/> (visited on 07/07/2016) (cit. on p. 37).
- [6] Rita C. Alves, Francisca Rodrigues, Maria Antónia Nunes, Ana F. Vinha, and M. Beatriz P.P. Oliveira. “State of the art in coffee processing by-products”. In: *Handbook of Coffee Processing By-Products: Sustainable Applications* (Jan. 2017), pp. 1–26. DOI: [10.1016/B978-0-12-811290-8.00001-3](https://doi.org/10.1016/B978-0-12-811290-8.00001-3) (cit. on p. 97).
- [7] Byoungkwon An, Ye Tao, Jianzhe Gu, Tingyu Cheng, Xiang’Anthony’ Chen, Xiaoxiao Zhang, Wei Zhao, Youngwook Do, Shigeo Takahashi, Hsiang-Yun Wu, et al. “Thermorph: Democratizing 4D printing of self-folding materials and interfaces”. In: *Proceedings of the 2018 CHI Conference on Human Factors in Computing Systems*. ACM. 2018, p. 260 (cit. on pp. 20, 60, 69, 112).
- [8] H. Andry, T. Yamamoto, T. Irie, S. Moritani, M. Inoue, and H. Fujiyama. “Water retention, hydraulic conductivity of hydrophilic polymers in sandy soil as affected by temperature and water quality”. In: *Journal of Hydrology* 373 (1-2 June 2009), pp. 177–183. ISSN: 0022-1694. DOI: [10.1016/J.JHYDROL.2009.04.020](https://doi.org/10.1016/J.JHYDROL.2009.04.020) (cit. on p. 102).
- [9] Michael F Ashby and David Rayner Hunkin Jones. *Engineering materials 1: an introduction to properties, applications and design*. Vol. 1. Elsevier, 2012 (cit. on p. 2).
- [10] Badreddine Assouar, Bin Liang, Ying Wu, Yong Li, Jian-Chun Cheng, and Yun Jing. “Acoustic metasurfaces”. In: *Nature Reviews Materials* 3.12 (2018), pp. 460–472 (cit. on p. 19).
- [11] Vahid Babaei, Kiril Vidimče, Michael Foshey, Alexandre Kaspar, Piotr Didyk, and Wojciech Matusik. “Color Contoning for 3D Printing”. In: *ACM Trans. Graph.* 36.4 (July 2017). ISSN: 0730-0301. DOI: [10.1145/3072959.3073605](https://doi.org/10.1145/3072959.3073605) (cit. on p. 18).
- [12] Moritz Bächer, Bernd Bickel, Doug L James, and Hanspeter Pfister. “Fabricating articulated characters from skinned meshes”. In: *ACM Transactions on Graphics (TOG)* 31.4 (2012), pp. 1–9 (cit. on p. 16).
- [13] Moritz Bächer, Stelian Coros, and Bernhard Thomaszewski. “LinkEdit: interactive linkage editing using symbolic kinematics”. In: *ACM Transactions on Graphics (TOG)* 34.4 (2015), pp. 1–8 (cit. on p. 15).
- [14] Moritz Bächer, Benjamin Hepp, Fabrizio Pece, Paul G. Kry, Bernd Bickel, Bernhard Thomaszewski, and Otmar Hilliges. “DefSense: Computational Design of Customized Deformable Input Devices”. In: *Proceedings of the 2016 CHI Conference on Human Factors in Computing Systems*. CHI ’16. San Jose, California, USA: ACM, 2016, pp. 3806–3816. DOI: [10.1145/2858036.2858354](https://doi.org/10.1145/2858036.2858354) (cit. on pp. 21, 28, 71).

- [15] Moritz Bächer, Emily Whiting, Bernd Bickel, and Olga Sorkine-Hornung. “Spin-it: optimizing moment of inertia for spinnable objects”. In: *ACM Transactions on Graphics (TOG)* 33.4 (2014), pp. 1–10 (cit. on p. 15).
- [16] Lina F. Ballesteros, José A. Teixeira, and Solange I. Mussatto. “Chemical, Functional, and Structural Properties of Spent Coffee Grounds and Coffee Silverskin”. In: *Food and Bioprocess Technology* 7 (12 Dec. 2014), pp. 3493–3503. DOI: [10.1007/S11947-014-1349-Z](https://doi.org/10.1007/S11947-014-1349-Z) (cit. on p. 97).
- [17] David Baraff. “Fast contact force computation for nonpenetrating rigid bodies”. In: *Proceedings of the 21st annual conference on Computer graphics and interactive techniques*. 1994, pp. 23–34 (cit. on p. 14).
- [18] David Baraff and Andrew Witkin. “Large steps in cloth simulation”. In: *Proceedings of the 25th annual conference on Computer graphics and interactive techniques - SIGGRAPH '98*. New York, New York, USA: ACM Press, July 1998, pp. 43–54. DOI: [10.1145/280814.280821](https://doi.org/10.1145/280814.280821) (cit. on p. 14).
- [19] E.J.W. Barber. *Prehistoric textiles: The development of cloth in the neolithic and bronze ages with special reference to the aegean*. Princeton paperbacks. Princeton University Press, 1991. ISBN: 9780691002248. URL: <https://books.google.com/books?id=HnSlynSfeEIC> (cit. on p. 33).
- [20] J. G. Batelaan, C. G. van Ginkel, and F. Balk. “Carboxymethylcellulose (CMC)”. In: *Handbook of Environmental Chemistry* 3 (1992), pp. 329–336. DOI: [10.1007/978-3-540-47108-0_11](https://doi.org/10.1007/978-3-540-47108-0_11) (cit. on p. 97).
- [21] Patrick Baudisch, Stefanie Mueller, et al. “Personal fabrication”. In: *Foundations and Trends® in Human-Computer Interaction* 10.3–4 (2017), pp. 165–293 (cit. on pp. 1, 13, 14).
- [22] Fiona Bell, Alice Hong, Andreea Danielescu, Aditi Maheshwari, Ben Greenspan, Hiroshi Ishii, Laura Devendorf, and Mirela Alistar. “Self-DeStaining Textiles: Designing Interactive Systems with Fabric, Stains and Light”. In: *Proceedings of the 2021 CHI Conference on Human Factors in Computing Systems*. New York, NY, USA: Association for Computing Machinery, 2021 (cit. on p. 28).
- [23] Adel Benchabane and Karim Bekkour. “Rheological properties of carboxymethyl cellulose (CMC) solutions”. In: *Colloid and Polymer Science* 286:10 286 (10 May 2008), pp. 1173–1180. ISSN: 1435-1536. DOI: [10.1007/S00396-008-1882-2](https://doi.org/10.1007/S00396-008-1882-2) (cit. on p. 97).
- [24] Amit H Bermano, Thomas Funkhouser, and Szymon Rusinkiewicz. “State of the art in methods and representations for fabrication-aware design”. In: *Computer Graphics Forum*. Vol. 36. 2. Wiley Online Library. 2017, pp. 509–535 (cit. on p. 15).
- [25] James M Bern, Kai-Hung Chang, and Stelian Coros. “Interactive design of animated plushies”. In: *ACM Transactions on Graphics (TOG)* 36.4 (2017), pp. 1–11 (cit. on p. 15).
- [26] Teresa Berninger, Natalie Dietz, and Óscar González López. “Water-soluble polymers in agriculture: xanthan gum as eco-friendly alternative to synthetics”. In: *Microbial Biotechnology* (2021). ISSN: 1751-7915. DOI: [10.1111/1751-7915.13867](https://doi.org/10.1111/1751-7915.13867). URL: <https://sfamjournals.onlinelibrary.wiley.com/doi/full/10.1111/1751-7915.13867> (cit. on p. 102).
- [27] Katia Bertoldi, Vincenzo Vitelli, Johan Christensen, and Martin van Hecke. “Flexible mechanical metamaterials”. In: *Nature Reviews Materials* 2.11 (2017), pp. 1–11 (cit. on p. 17).
- [28] Samarthya Bhagia, Kamlesh Bornani, Ruchi Agarwal, Alok Satlewal, Jaroslav Ďurkovič, Rastislav Lagaňa, Meher Bhagia, Chang Geun Yoo, Xianhui Zhao, Vlastimil Kunc, Yunqiao Pu, Soydan Ozcan, and Arthur J. Ragauskas. “Critical review of FDM 3D printing of PLA biocomposites filled with biomass resources, characterization, biodegradability, upcycling and opportunities for biorefineries”. In: *Applied Materials Today* 24 (Sept. 2021), p. 101078. ISSN: 2352-9407. DOI: [10.1016/J.APMT.2021.101078](https://doi.org/10.1016/J.APMT.2021.101078) (cit. on p. 94).
- [29] Gaurav Bharaj, David I. W. Levin, James Tompkin, Yun Fei, Hanspeter Pfister, Wojciech Matusik, and Changxi Zheng. “Computational Design of Metallophone Contact Sounds”. In: *ACM Trans. Graph.* 34.6 (Oct. 2015). ISSN: 0730-0301. DOI: [10.1145/2816795.2818108](https://doi.org/10.1145/2816795.2818108) (cit. on p. 19).
- [30] Nandana Bhardwaj and Subhas C Kundu. “Electrospinning: a fascinating fiber fabrication technique”. In: *Biotechnology advances* 28.3 (2010), pp. 325–347 (cit. on pp. 73, 74).

- [31] Bharat Bhushan and Matt Caspers. “An overview of additive manufacturing (3D printing) for microfabrication”. In: *Microsystem Technologies* 23.4 (2017), pp. 1117–1124 (cit. on p. 7).
- [32] Bernd Bickel, Moritz Bächer, Miguel A Otaduy, Wojciech Matusik, Hanspeter Pfister, and Markus Gross. “Capture and modeling of non-linear heterogeneous soft tissue”. In: *ACM Transactions on Graphics (TOG)* 28.3 (2009), pp. 1–9 (cit. on p. 14).
- [33] Bernd Bickel, Moritz Bächer, Miguel A. Otaduy, Hyunho Richard Lee, Hanspeter Pfister, Markus Gross, and Wojciech Matusik. “Design and Fabrication of Materials with Desired Deformation Behavior”. In: *ACM SIGGRAPH 2010 Papers. SIGGRAPH '10*. Los Angeles, California: ACM, 2010, 63:1–63:10. DOI: [10.1145/1833349.1778800](https://doi.org/10.1145/1833349.1778800) (cit. on pp. 16, 29, 71).
- [34] Emma Bladyka. “Coffee brewing: Wetting, hydrolysis & extraction revisited”. In: *Specialty Coffee Association of America* (2015) (cit. on p. 97).
- [35] Eli Blevis. “Sustainable Interaction Design: Invention & Disposal, Renewal & Reuse”. In: *Proceedings of the SIGCHI Conference on Human Factors in Computing Systems*. New York, NY, USA: Association for Computing Machinery, 2007, pp. 503–512. ISBN: 9781595935939 (cit. on pp. 91, 94, 95, 113).
- [36] Dave Bourell, Brent Stucker, Yong Chen, Chi Zhou, and Jingyuan Lao. “A layerless additive manufacturing process based on CNC accumulation”. In: *Rapid Prototyping Journal* (2011) (cit. on p. 7).
- [37] Benjamin Bridgens and Matthew Birchall. “Form and function: The significance of material properties in the design of tensile fabric structures”. In: *Engineering structures* 44 (2012), pp. 1–12 (cit. on p. 33).
- [38] Robert Bridson, Ronald Fedkiw, and John Anderson. “Robust treatment of collisions, contact and friction for cloth animation”. In: *Proceedings of the 29th annual conference on Computer graphics and interactive techniques - SIGGRAPH '02*. Vol. 21. 3. New York, New York, USA: ACM Press, July 2002, p. 594. DOI: [10.1145/566570.566623](https://doi.org/10.1145/566570.566623) (cit. on p. 14).
- [39] Toby D Brown, Paul D Dalton, and Dietmar W Hutmacher. “Direct writing by way of melt electrospinning”. In: *Advanced Materials* 23.47 (2011), pp. 5651–5657 (cit. on p. 73).
- [40] Alan Brunton, Can Ates Arikan, and Philipp Urban. “Pushing the Limits of 3D Color Printing: Error Diffusion with Translucent Materials”. In: *ACM Trans. Graph.* 35.1 (Dec. 2016). ISSN: 0730-0301. DOI: [10.1145/2832905](https://doi.org/10.1145/2832905) (cit. on p. 18).
- [41] Jacques Cali, Dan A Calian, Cristina Amati, Rebecca Kleinberger, Anthony Steed, Jan Kautz, and Tim Weyrich. “3D-printing of non-assembly, articulated models”. In: *ACM Transactions on Graphics (TOG)* 31.6 (2012), pp. 1–8 (cit. on p. 16).
- [42] Ana Cervera-Mata, Silvia Pastoriza, José Ángel Rufián-Henares, Jesús Párraga, Juan Manuel Martín-García, and Gabriel Delgado. “Impact of spent coffee grounds as organic amendment on soil fertility and lettuce growth in two Mediterranean agricultural soils”. In: <https://doi.org/10.1080/03650340.2017.1387651> 64 (6 May 2017), pp. 790–804. DOI: [10.1080/03650340.2017.1387651](https://doi.org/10.1080/03650340.2017.1387651). URL: <https://www.tandfonline.com/doi/abs/10.1080/03650340.2017.1387651> (cit. on pp. 97, 102, 113).
- [43] Yooeun Chae and Youn-Joo An. “Current research trends on plastic pollution and ecological impacts on the soil ecosystem: A review”. In: *Environmental pollution* 240 (2018), pp. 387–395 (cit. on p. 92).
- [44] Yu-Chung Chang, Yao Chen, Jialong Ning, Cheng Hao, Mitch Rock, Maher Amer, Shuo Feng, Mojtaba Falahati, Li-Ju Wang, Roland K. Chen, Jinwen Zhang, Jow-Lian Ding, and Lei Li. “No Such Thing as Trash: A 3D-Printable Polymer Composite Composed of Oil-Extracted Spent Coffee Grounds and Polylactic Acid with Enhanced Impact Toughness”. In: *ACS Sustainable Chemistry & Engineering* 7 (18 Sept. 2019), pp. 15304–15310. DOI: [10.1021/ACSSUSCHEMENG.9B02527](https://doi.org/10.1021/ACSSUSCHEMENG.9B02527). URL: <https://pubs.acs.org/doi/abs/10.1021/acssuschemeng.9b02527> (cit. on p. 94).
- [45] Xiang Chen, Changxi Zheng, Weiwei Xu, and Kun Zhou. “An asymptotic numerical method for inverse elastic shape design”. In: *ACM Transactions on Graphics (TOG)* 33.4 (2014), pp. 1–11 (cit. on p. 23).

- [46] Xiang “Anthony” Chen, Stelian Coros, and Scott E. Hudson. “Medley: A Library of Embeddables to Explore Rich Material Properties for 3D Printed Objects”. In: *Proceedings of the 2018 CHI Conference on Human Factors in Computing Systems*. CHI ’18. Montreal QC, Canada: Association for Computing Machinery, 2018. DOI: [10.1145/3173574.3173736](https://doi.org/10.1145/3173574.3173736) (cit. on pp. 23, 24).
- [47] Xiang “Anthony” Chen, Stelian Coros, Jennifer Mankoff, and Scott E. Hudson. “Encore: 3D Printed Augmentation of Everyday Objects with Printed-Over, Affixed and Interlocked Attachments”. In: *Proceedings of the 28th Annual ACM Symposium on User Interface Software & Technology*. UIST ’15. Charlotte, NC, USA: Association for Computing Machinery, 2015, pp. 73–82. DOI: [10.1145/2807442.2807498](https://doi.org/10.1145/2807442.2807498) (cit. on p. 23).
- [48] Xiang “Anthony” Chen, Jeeun Kim, Jennifer Mankoff, Tovi Grossman, Stelian Coros, and Scott E. Hudson. “Reprise: A Design Tool for Specifying, Generating, and Customizing 3D Printable Adaptations on Everyday Objects”. In: *Proceedings of the 29th Annual Symposium on User Interface Software and Technology*. UIST ’16. Tokyo, Japan: Association for Computing Machinery, 2016, pp. 29–39. DOI: [10.1145/2984511.2984512](https://doi.org/10.1145/2984511.2984512) (cit. on pp. 16, 23).
- [49] Xiang “Anthony” Chen, Ye Tao, Guanyun Wang, Runchang Kang, Tovi Grossman, Stelian Coros, and Scott E. Hudson. “Forte: User-Driven Generative Design”. In: *Proceedings of the 2018 CHI Conference on Human Factors in Computing Systems*. CHI ’18. Montreal QC, Canada: Association for Computing Machinery, 2018, pp. 1–12. DOI: [10.1145/3173574.3174070](https://doi.org/10.1145/3173574.3174070) (cit. on p. 14).
- [50] David F Ciambrone. *Environmental life cycle analysis*. CRC Press, 2018 (cit. on p. 113).
- [51] Leslie Cooperband. “The art and science of composting”. In: *Center for Integrated agricultural systems* (2002). URL: <https://www.iowadnr.gov/Portals/idnr/uploads/waste/artandscienceofcomposting.pdf> (cit. on p. 108).
- [52] Stelian Coros, Bernhard Thomaszewski, Gioacchino Noris, Shinjiro Sueda, Moira Forberg, Robert W. Sumner, Wojciech Matusik, and Bernd Bickel. “Computational Design of Mechanical Characters”. In: vol. 32. 4. New York, NY, USA: ACM, July 2013, 83:1–83:12. DOI: [10.1145/2461912.2461953](https://doi.org/10.1145/2461912.2461953) (cit. on p. 15).
- [53] S Scott Crump. *Apparatus and method for creating three-dimensional objects*. US Patent 5,121,329. June 1992 (cit. on p. 11).
- [54] Rebeca Cruz, Eulália Mendes, Álvaro Torrinha, Simone Morais, José Alberto Pereira, Paula Baptista, and Susana Casal. “Revalorization of spent coffee residues by a direct agronomic approach”. In: *Food Research International* 73 (July 2015), pp. 190–196. ISSN: 0963-9969. DOI: [10.1016/J.FOODRES.2014.11.018](https://doi.org/10.1016/J.FOODRES.2014.11.018) (cit. on pp. 97, 102, 113).
- [55] Scott Curran, Paul Chambon, Randall Lind, Lonnie Love, Robert Wagner, Steven Whitted, David Smith, Brian Post, Ronald Graves, Craig Blue, et al. *Big area additive manufacturing and hardware-in-the-loop for rapid vehicle powertrain prototyping: A case study on the development of a 3-D-printed Shelby Cobra*. Tech. rep. SAE Technical Paper, 2016 (cit. on p. 26).
- [56] Wataru Date and Yasuaki Kakehi. “Paperprinting: a machine for prototyping paper and its applications for graphic design”. In: *ACM SIGGRAPH 2018 Studio*. 2018, pp. 1–2 (cit. on p. 27).
- [57] Claudia Daudén Roquet, Jeeun Kim, and Tom Yeh. “3D Folded PrintGami: Transforming Passive 3D Printed Objects to Interactive by Inserted Paper Origami Circuits”. In: *Proceedings of the 2016 ACM Conference on Designing Interactive Systems*. DIS ’16. Brisbane, QLD, Australia: Association for Computing Machinery, 2016, pp. 187–191. DOI: [10.1145/2901790.2901891](https://doi.org/10.1145/2901790.2901891) (cit. on p. 24).
- [58] Mathieu Desbrun, Peter Schröder, and Alan Barr. “Interactive animation of structured deformable objects”. In: *Graphics Interface*. Vol. 99. 5. 1999, p. 10 (cit. on p. 14).
- [59] Laura Devendorf, Joanne Lo, Noura Howell, Jung Lin Lee, Nan-Wei Gong, M Emre Karagozler, Shihō Fukuhara, Ivan Poupyrev, Eric Paulos, and Kimiko Ryokai. “I don’t want to wear a screen: probing perceptions of and possibilities for dynamic displays on clothing”. In: *Proceedings of the 2016 CHI Conference on Human Factors in Computing Systems*. ACM. 2016, pp. 6028–6039 (cit. on pp. 28, 57).

- [60] Kristin N. Dew, Samantha Shorey, and Daniela Rosner. “Making within limits: Towards salvage fabrication”. In: *ACM International Conference Proceeding Series* (May 2018). DOI: [10.1145/3232617.3232626](https://doi.org/10.1145/3232617.3232626) (cit. on p. 100).
- [61] I. Diañez, C. Gallegos, E. Brito-de la Fuente, I. Martínez, C. Valencia, M.C. Sánchez, M.J. Diaz, and J.M. Franco. “3D printing in situ gelification of κ -carrageenan solutions: Effect of printing variables on the rheological response”. In: *Food Hydrocolloids* 87 (2019), pp. 321–330. ISSN: 0268-005X. DOI: [10.1016/j.foodhyd.2018.08.010](https://doi.org/10.1016/j.foodhyd.2018.08.010) (cit. on pp. 58, 59).
- [62] Nancy Dickson, Thomas Richard, and Robert Kozlowski. *Composting to reduce the waste stream-A guide to small scale food and yard waste composting*. Northeast regional agricultural engineering service, 1991. URL: <https://ecommons.cornell.edu/handle/1813/44736> (cit. on pp. 108, 109, 113).
- [63] Carl DiSalvo, Phoebe Sengers, and Hrönn Brynjarsdóttir. “Mapping the Landscape of Sustainable HCI”. In: *Proceedings of the SIGCHI Conference on Human Factors in Computing Systems*. CHI ’10. Atlanta, Georgia, USA: Association for Computing Machinery, 2010, pp. 1975–1984. DOI: [10.1145/1753326.1753625](https://doi.org/10.1145/1753326.1753625) (cit. on p. 91).
- [64] Mustafa Doga Dogan, Faraz Faruqi, Andrew Day Churchill, Kenneth Friedman, Leon Cheng, Sriram Subramanian, and Stefanie Mueller. “G-ID: identifying 3D Prints using slicing parameters”. In: *Proceedings of the 2020 CHI Conference on Human Factors in Computing Systems (CHI 2020)*. ACM, 2020, pp. 1–13 (cit. on p. 19).
- [65] Yue Dong, Jiaping Wang, Fabio Pellacini, Xin Tong, and Baining Guo. “Fabricating spatially-varying subsurface scattering”. In: *ACM SIGGRAPH 2010 papers*. 2010, pp. 1–10 (cit. on p. 18).
- [66] Jiachun Du, Panos Markopoulos, Qi Wang, Marina Toeters, and Ting Gong. “ShapeTex: Implementing Shape-Changing Structures in Fabric for Wearable Actuation”. In: *Proceedings of the Twelfth International Conference on Tangible, Embedded, and Embodied Interaction*. TEI ’18. Stockholm, Sweden: ACM, 2018, pp. 166–176. DOI: [10.1145/3173225.3173245](https://doi.org/10.1145/3173225.3173245) (cit. on pp. 28, 57).
- [67] Chad E Duty, Vlastimil Kunc, Brett Compton, Brian Post, Donald Erdman, Rachel Smith, Randall Lind, Peter Lloyd, and Lonnie Love. “Structure and mechanical behavior of Big Area Additive Manufacturing (BAAM) materials”. In: *Rapid Prototyping Journal* (2017) (cit. on p. 27).
- [68] Lynn Egli, Ching-yao Hsu, Beat D Bruederlin, and Gershon Elber. “Inferring 3D models from freehand sketches and constraints”. In: *Computer-Aided Design* 29.2 (1997), pp. 101–112 (cit. on p. 14).
- [69] Stephen Eichhorn, John W.S. Hearle, Mike Jaffe, and Takeshi Kikutani. *Handbook of textile fibre structure: Natural, regenerated, inorganic and specialist fibres*. Vol. 2. Elsevier, 2009 (cit. on p. 34).
- [70] Ahmed Elkholly and Roger Kempers. “Investigation into the Influence of Fused Deposition Modeling (FDM) Process Parameters on the Thermal Properties of 3D-Printed Parts”. In: (2018) (cit. on p. 20).
- [71] Marcus Eriksen, Laurent CM Lebreton, Henry S Carson, Martin Thiel, Charles J Moore, Jose C Borerro, Francois Galgani, Peter G Ryan, and Julia Reisser. “Plastic pollution in the world’s oceans: more than 5 trillion plastic pieces weighing over 250,000 tons afloat at sea”. In: *PloS one* 9.12 (2014), e111913 (cit. on p. 92).
- [72] Hussein Esfahlani, Herve Lissek, and Juan R. Mosig. “Generation of acoustic helical wavefronts using metasurfaces”. In: *Phys. Rev. B* 95 (2 Jan. 2017), p. 024312. DOI: [10.1103/PhysRevB.95.024312](https://doi.org/10.1103/PhysRevB.95.024312) (cit. on p. 19).
- [73] David Espalin, Danny W Muse, Eric MacDonald, and Ryan B Wicker. “3D Printing multifunctionality: structures with electronics”. In: *The International Journal of Advanced Manufacturing Technology* 72.5-8 (2014), pp. 963–978 (cit. on p. 24).
- [74] Jeremy Faludi, Natasha Cline-Thomas, and Shardul Agrawala. “3D printing and its environmental implications”. In: *The Next Production Revolution. Implications for Governments and Businesses* (2017) (cit. on pp. 94–96).

- [75] Jeremy Faludi, Zhongyin Hu, Shahd Alrashed, Christopher Braunholz, Suneesh Kaul, and Leulekal Kassaye. “Does material choice drive sustainability of 3D printing?” In: *International Journal of Mechanical, Aerospace, Industrial and Mechatronics Engineering* (2015) (cit. on pp. 92, 94, 95, 113).
- [76] Jeremy Faludi, Corrie M. Van Sice, Yuan Shi, Justin Bower, and Owen M.K. Brooks. “Novel materials can radically improve whole-system environmental impacts of additive manufacturing”. In: *Journal of Cleaner Production* 212 (2019), pp. 1580–1590. ISSN: 0959-6526 (cit. on pp. 94–96, 113).
- [77] James A Fava. “Life cycle initiative: a joint UNEP/SETAC partnership to advance the life-cycle economy”. In: *The International Journal of Life Cycle Assessment* 7.4 (2002), pp. 196–198 (cit. on p. 114).
- [78] Javier G. Fernandez and Donald E. Ingber. “Manufacturing of Large-Scale Functional Objects Using Biodegradable Chitosan Bioplastic”. In: *Macromolecular Materials and Engineering* 299 (8 Aug. 2014), pp. 932–938. ISSN: 1439-2054. DOI: [10.1002/MAME.201300426](https://doi.org/10.1002/MAME.201300426) (cit. on p. 118).
- [79] Michael Feygin. *Apparatus and method for forming an integral object from laminations*. US Patent 4,752,352. June 1988 (cit. on p. 10).
- [80] Michael Feygin, Alexandr Shkolnik, Michael N Diamond, and Emmanuil Dvorskiy. *Laminated object manufacturing system*. US Patent 5,730,817. Mar. 1998 (cit. on p. 10).
- [81] Jack Forman, Taylor Tabb, Youngwook Do, Meng-Han Yeh, Adrian Galvin, and Lining Yao. “ModiFiber: Two-Way Morphing Soft Thread Actuators for Tangible Interaction”. In: *Proceedings of the 2019 CHI Conference on Human Factors in Computing Systems*. CHI ’19. Glasgow, Scotland Uk: ACM, 2019, 660:1–660:11. DOI: [10.1145/3290605.3300890](https://doi.org/10.1145/3290605.3300890) (cit. on pp. 28, 57).
- [82] Charlotte Freitag, Mike Berners-Lee, Kelly Widdicks, Bran Knowles, Gordon Blair, and Adrian Friday. “The climate impact of ICT: A review of estimates, trends and regulations”. In: *arXiv preprint arXiv:2102.02622* (2021) (cit. on p. 91).
- [83] Wei Gao, Yunbo Zhang, Diogo C. Nazzetta, Karthik Ramani, and Raymond J. Cipra. “RevoMaker: Enabling Multi-Directional and Functionally-Embedded 3D Printing Using a Rotational Cuboidal Platform”. In: *Proceedings of the 28th Annual ACM Symposium on User Interface Software & Technology*. UIST ’15. Charlotte, NC, USA: Association for Computing Machinery, 2015, pp. 437–446. DOI: [10.1145/2807442.2807476](https://doi.org/10.1145/2807442.2807476) (cit. on p. 23).
- [84] F Garcia-Ochoa, VE Santos, JA Casas, and E Gómez. “Xanthan gum: production, recovery, and properties”. In: *Biotechnology advances* 18.7 (2000), pp. 549–579 (cit. on pp. 97, 114).
- [85] Damien Gauge, Stelian Coros, Sandro Mani, and Bernhard Thomaszewski. “Interactive design of modular tensegrity characters”. In: *Proceedings of the ACM SIGGRAPH/Eurographics Symposium on Computer Animation*. Citeseer. 2014, pp. 131–138 (cit. on p. 15).
- [86] Neil A Gershenfeld. *Fab: the coming revolution on your desktop—from personal computers to personal fabrication*. Basic Books (AZ), 2005 (cit. on pp. 1, 13).
- [87] Mamdouh T Ghannam and M Nabil Esmail. “Rheological Properties of Carboxymethyl Cellulose”. In: *J Appl Polym Sci* 64 (1997), pp. 289–301. DOI: [10.1002/\(SICI\)1097-4628\(19970411\)64:2](https://doi.org/10.1002/(SICI)1097-4628(19970411)64:2) (cit. on p. 97).
- [88] Ian Gibson, David Rosen, and Brent Stucker. “Sheet Lamination Processes”. In: *Additive Manufacturing Technologies: 3D Printing, Rapid Prototyping, and Direct Digital Manufacturing*. New York, NY: Springer New York, 2015, pp. 219–244. DOI: [10.1007/978-1-4939-2113-3_9](https://doi.org/10.1007/978-1-4939-2113-3_9) (cit. on p. 10).
- [89] PW Gibson, HL Schreuder-Gibson, and D Rivin. “Electrospun fiber mats: transport properties”. In: *AIChE journal* 45.1 (1999), pp. 190–195 (cit. on p. 73).
- [90] Michael Gleicher and Andrew Witkin. “Drawing with constraints”. In: *The Visual Computer* 11.1 (1994), pp. 39–51 (cit. on p. 14).

- [91] Teresa Gomes, J.A. Pereira, Elsa Ramalhosa, Susana Casal, and Paula Baptista. “Effect of fresh and composted spent coffee grounds on lettuce growth, photosynthetic pigments and mineral composition”. In: *VII Congreso Ibérico de Agroingeniería y Ciencias Hortícolas* (2014), pp. 1–5. URL: <https://bibliotecadigital.ipb.pt/handle/10198/8719%20https://bibliotecadigital.ipb.pt/handle/10198/8719?mode=full> (cit. on pp. 102, 113).
- [92] Eitan Grinspun, Anil N. Hirani, Mathieu Desbrun, and Peter Schröder. “Discrete Shells”. In: *Proceedings of the 2003 ACM SIGGRAPH/Eurographics Symposium on Computer Animation*. SCA '03. San Diego, California: Eurographics Association, 2003, pp. 62–67 (cit. on p. 65).
- [93] Daniel Groeger, Elena Chong Loo, and Jürgen Steimle. “HotFlex: Post-Print Customization of 3D Prints Using Embedded State Change”. In: *Proceedings of the 2016 CHI Conference on Human Factors in Computing Systems*. CHI '16. San Jose, California, USA: Association for Computing Machinery, 2016, pp. 420–432. DOI: [10.1145/2858036.2858191](https://doi.org/10.1145/2858036.2858191) (cit. on p. 24).
- [94] Daniel Groeger, Martin Feick, Anusha Withana, and Jürgen Steimle. “Tactlets: Adding Tactile Feedback to 3D Objects Using Custom Printed Controls”. In: *Proceedings of the 32nd Annual ACM Symposium on User Interface Software and Technology*. UIST '19. New Orleans, LA, USA: Association for Computing Machinery, 2019, pp. 923–936. DOI: [10.1145/3332165.3347937](https://doi.org/10.1145/3332165.3347937) (cit. on p. 21).
- [95] Jianzhe Gu, David E Breen, Jenny Hu, Lifeng Zhu, Ye Tao, Tyson Van de Zande, Guanyun Wang, Yongjie Jessica Zhang, and Lining Yao. “Geodesy: Self-rising 2.5 D Tiles by Printing along 2D Geodesic Closed Path”. In: *Proceedings of the 2019 CHI Conference on Human Factors in Computing Systems*. 2019, pp. 1–10 (cit. on pp. 20, 112).
- [96] Emrecan Gulay, Toni Kotnik, and Andrés Lucero. “Exploring a Feedback-Oriented Design Process Through Curved Folding”. In: *Proceedings of the 2021 CHI Conference on Human Factors in Computing Systems*. New York, NY, USA: Association for Computing Machinery, 2021. DOI: [10.1145/3411764.3445639](https://doi.org/10.1145/3411764.3445639) (cit. on p. 117).
- [97] Anhong Guo, Jeeun Kim, Xiang “Anthony” Chen, Tom Yeh, Scott E. Hudson, Jennifer Mankoff, and Jeffrey P. Bigham. “Facade: Auto-Generating Tactile Interfaces to Appliances”. In: *Proceedings of the 2017 CHI Conference on Human Factors in Computing Systems*. CHI '17. Denver, Colorado, USA: Association for Computing Machinery, 2017, pp. 5826–5838. DOI: [10.1145/3025453.3025845](https://doi.org/10.1145/3025453.3025845) (cit. on p. 21).
- [98] James K Hahn. “Realistic animation of rigid bodies”. In: *Acm Siggraph Computer Graphics* 22.4 (1988), pp. 299–308 (cit. on p. 14).
- [99] Kathleen Hajash, Bjorn Sparrman, Christophe Guberan, Jared Laucks, and Skylar Tibbits. “Large-Scale Rapid Liquid Printing”. In: *3D Printing and Additive Manufacturing* 4.3 (2017), pp. 123–132 (cit. on p. 27).
- [100] Ollie Hanton, Michael Wessely, Stefanie Mueller, Mike Fraser, and Anne Roudaut. “ProtoSpray: Combining 3D Printing and Spraying to Create Interactive Displays with Arbitrary Shapes”. In: *Proceedings of the 2020 CHI Conference on Human Factors in Computing Systems*. CHI '20. Honolulu, HI, USA: Association for Computing Machinery, 2020, pp. 1–13. DOI: [10.1145/3313831.3376543](https://doi.org/10.1145/3313831.3376543) (cit. on p. 25).
- [101] Miloš Hašan, Martin Fuchs, Wojciech Matusik, Hanspeter Pfister, and Szymon Rusinkiewicz. “Physical Reproduction of Materials with Specified Subsurface Scattering”. In: *ACM SIGGRAPH 2010 Papers*. SIGGRAPH '10. Los Angeles, California: Association for Computing Machinery, 2010. DOI: [10.1145/1833349.1778798](https://doi.org/10.1145/1833349.1778798) (cit. on p. 18).
- [102] Liang He, Huaishu Peng, Michelle Lin, Ravikanth Konjeti, François Guimbretière, and Jon E Froehlich. “Ondulé: Designing and Controlling 3D Printable Springs”. In: *Proceedings of the 32nd Annual ACM Symposium on User Interface Software and Technology*. 2019, pp. 739–750 (cit. on p. 17).
- [103] John WS Hearle. “The structural mechanics of fibers”. In: *Journal of Polymer Science: Polymer Symposia*. Vol. 20. 1. Wiley Online Library. 1967, pp. 215–251 (cit. on p. 34).

- [104] John WS Hearle, Percy Grosberg, and Stanley Backer. “Structural mechanics of fibers, yarns, and fabrics”. In: (1969) (cit. on p. 34).
- [105] John WS Hearle and William Ernest Morton. *Physical properties of textile fibres*. Elsevier, 2008 (cit. on p. 34).
- [106] Thomas J Hinton, Quentin Jallerat, Rachele N Palchesko, Joon Hyung Park, Martin S Grodzicki, Hao-Jan Shue, Mohamed H Ramadan, Andrew R Hudson, and Adam W Feinberg. “Three-dimensional printing of complex biological structures by freeform reversible embedding of suspended hydrogels”. In: *Science advances* 1.9 (2015), e1500758 (cit. on p. 7).
- [107] C. B. Hollabaugh, Leland H. Burt, and Anna Peterson Walsh. “Carboxymethylcellulose. Uses and Applications”. In: *Industrial & Engineering Chemistry* 37 (10 Oct. 1945), pp. 943–947. DOI: [10.1021/IE50430A015](https://doi.org/10.1021/IE50430A015) (cit. on p. 97).
- [108] Douglas P Holmes. “Elasticity and Stability of Shape Changing Structures”. In: *Current opinion in colloid & interface science* (2019) (cit. on p. 60).
- [109] Chris Holshouser, Clint Newell, Sid Palas, Lonnie J Love, Vlastimil Kunc, Randall F Lind, Peter D Lloyd, John C Rowe, Craig A Blue, Chad E Duty, et al. “Out of bounds additive manufacturing”. In: *Advanced Materials and Processes* 171.3 (2013) (cit. on pp. 26, 29).
- [110] Larry L Howell. “Compliant mechanisms”. In: *21st Century Kinematics*. Springer, 2013, pp. 189–216 (cit. on p. 16).
- [111] Larry L Howell, Spencer P Magleby, and Brian M Olsen. *Handbook of compliant mechanisms*. John Wiley & Sons, 2013 (cit. on p. 16).
- [112] Elaine M. Huang and Khai N. Truong. “Breaking the Disposable Technology Paradigm: Opportunities for Sustainable Interaction Design for Mobile Phones”. In: CHI ’08. Florence, Italy: Association for Computing Machinery, 2008. DOI: [10.1145/1357054.1357110](https://doi.org/10.1145/1357054.1357110) (cit. on p. 91).
- [113] Zheng-Ming Huang, Y-Z Zhang, M Kotaki, and S Ramakrishna. “A review on polymer nanofibers by electrospinning and their applications in nanocomposites”. In: *Composites science and technology* 63.15 (2003), pp. 2223–2253 (cit. on pp. 73, 74).
- [114] Nathaniel Hudson, Celena Alcock, and Parmit K. Chilana. “Understanding Newcomers to 3D Printing: Motivations, Workflows, and Barriers of Casual Makers”. In: *Proceedings of the 2016 CHI Conference on Human Factors in Computing Systems*. CHI ’16. San Jose, California, USA: Association for Computing Machinery, 2016, pp. 384–396. DOI: [10.1145/2858036.2858266](https://doi.org/10.1145/2858036.2858266) (cit. on p. 2).
- [115] Scott E. Hudson. “Printing Teddy Bears: A Technique for 3D Printing of Soft Interactive Objects”. In: *Proceedings of the SIGCHI Conference on Human Factors in Computing Systems*. CHI ’14. Toronto, Ontario, Canada: ACM, 2014, pp. 459–468. DOI: [10.1145/2556288.2557338](https://doi.org/10.1145/2556288.2557338) (cit. on pp. 28, 29, 35).
- [116] Charles W Hull. “Apparatus for production of three-dimensional objects by stereolithography”. In: *United States Patent, Appl., No. 638905, Filed* (1984) (cit. on p. 8).
- [117] Matthew T Hunley, Afia S Karikari, Matthew G McKee, Brian D Mather, John M Layman, Ann R Fornof, and Timothy E Long. “Taking advantage of tailored electrostatics and complementary hydrogen bonding in the design of nanostructures for biomedical applications”. In: *Macromolecular symposia*. Vol. 270. 1. Wiley Online Library, 2008, pp. 1–7 (cit. on p. 76).
- [118] Dietmar W Hutmacher and Paul D Dalton. “Melt electrospinning”. In: *Chemistry—An Asian Journal* 6.1 (2011), pp. 44–56 (cit. on pp. 73, 74, 76, 79, 80).
- [119] Takeo Igarashi and John F Hughes. “A suggestive interface for 3D drawing”. In: *ACM SIGGRAPH 2007 courses*. 2007, 20–es (cit. on p. 14).
- [120] Takeo Igarashi, Satoshi Matsuoka, and Hidehiko Tanaka. “Teddy: a sketching interface for 3D freeform design”. In: *ACM SIGGRAPH 2006 Courses*. 2006, 11–es (cit. on p. 14).

- [121] Instructables. *How to 3D print onto fabric*. 2016. URL: <http://www.instructables.com/id/How-to-3D-Print-Onto-Fabric/> (visited on 07/10/2016) (cit. on p. 41).
- [122] Alexandra Ion, Johannes Frohnhofen, Ludwig Wall, Robert Kovacs, Mirela Alistar, Jack Lindsay, Pedro Lopes, Hsiang-Ting Chen, and Patrick Baudisch. “Metamaterial Mechanisms”. In: *Proceedings of the 29th Annual Symposium on User Interface Software and Technology*. UIST ’16. Tokyo, Japan: ACM, 2016, pp. 529–539. DOI: [10.1145/2984511.2984540](https://doi.org/10.1145/2984511.2984540) (cit. on p. 17).
- [123] Alexandra Ion, Robert Kovacs, Oliver S Schneider, Pedro Lopes, and Patrick Baudisch. “Metamaterial textures”. In: *Proceedings of the 2018 CHI Conference on Human Factors in Computing Systems*. 2018, pp. 1–12 (cit. on pp. 17, 21).
- [124] Alexandra Ion, David Lindlbauer, Philipp Herholz, Marc Alexa, and Patrick Baudisch. “Understanding metamaterial mechanisms”. In: *Proceedings of the 2019 CHI Conference on Human Factors in Computing Systems*. 2019, pp. 1–14 (cit. on p. 17).
- [125] Alexandra Ion, Ludwig Wall, Robert Kovacs, and Patrick Baudisch. “Digital mechanical metamaterials”. In: *Proceedings of the 2017 CHI Conference on Human Factors in Computing Systems*. 2017, pp. 977–988 (cit. on p. 17).
- [126] Yoshio Ishiguro and Ivan Poupyrev. “3D Printed Interactive Speakers”. In: *Proceedings of the SIGCHI Conference on Human Factors in Computing Systems*. CHI ’14. Toronto, Ontario, Canada: Association for Computing Machinery, 2014, pp. 1733–1742. DOI: [10.1145/2556288.2557046](https://doi.org/10.1145/2556288.2557046) (cit. on p. 25).
- [127] Vikram Iyer, Justin Chan, Ian Culhane, Jennifer Mankoff, and Shyamnath Gollakota. “Wireless Analytics for 3D Printed Objects”. In: *Proceedings of the 31st Annual ACM Symposium on User Interface Software and Technology*. UIST ’18. Berlin, Germany: Association for Computing Machinery, 2018, pp. 141–152. DOI: [10.1145/3242587.3242639](https://doi.org/10.1145/3242587.3242639) (cit. on p. 21).
- [128] Vikram Iyer, Justin Chan, and Shyamnath Gollakota. “3D Printing Wireless Connected Objects”. In: *ACM Trans. Graph.* 36.6 (Nov. 2017). ISSN: 0730-0301. DOI: [10.1145/3130800.3130822](https://doi.org/10.1145/3130800.3130822) (cit. on p. 21).
- [129] Ana Jiménez-Zamora, Silvia Pastoriza, and José A. Rufián-Henares. “Revalorization of coffee by-products. Prebiotic, antimicrobial and antioxidant properties”. In: *LWT - Food Science and Technology* 61 (1 Apr. 2015), pp. 12–18. ISSN: 0023-6438. DOI: [10.1016/j.lwt.2014.11.031](https://doi.org/10.1016/j.lwt.2014.11.031) (cit. on p. 97).
- [130] Yuhua Jin, Isabel Qamar, Michael Wessely, Aradhana Adhikari, Katarina Bulovic, Parinya Punpongsanon, and Stefanie Mueller. “Photo-Chromeleon: Re-Programmable Multi-Color Textures Using Photochromic Dyes”. In: *Proceedings of the 32nd Annual ACM Symposium on User Interface Software and Technology*. UIST ’19. New Orleans, LA, USA: Association for Computing Machinery, 2019, pp. 701–712. DOI: [10.1145/3332165.3347905](https://doi.org/10.1145/3332165.3347905) (cit. on p. 25).
- [131] Hendrik John. *Apparatus for manufacturing a three-dimensional object*. US Patent 7,052,263. May 2006 (cit. on p. 8).
- [132] Rhys Jones, Patrick Haufe, Edward Sells, Pejman Iravani, Vik Olliver, Chris Palmer, and Adrian Bowyer. “RepRap—the replicating rapid prototyper”. In: *Robotica* 29.1 (2011), pp. 177–191 (cit. on pp. 1, 11, 92).
- [133] Michael L Jost, Olaf Knabenbauer, Jin Cheng, and Hans-Peter Harjes. “Fault plane solutions of microearthquakes and small events in the Hellenic arc”. In: *Tectonophysics* 356.1-3 (2002), pp. 87–114 (cit. on p. 14).
- [134] Hsin-Liu (Cindy) Kao, Miren Bamforth, David Kim, and Chris Schmandt. “Skinmorph: Texture-tunable On-skin Interface Through Thin, Programmable Gel”. In: *Proceedings of the 2018 ACM International Symposium on Wearable Computers*. ISWC ’18. Singapore, Singapore: ACM, 2018, pp. 196–203. DOI: [10.1145/3267242.3267262](https://doi.org/10.1145/3267242.3267262) (cit. on p. 58).
- [135] Alexandre Kaspar, Liane Makatura, and Wojciech Matusik. “Knitting Skeletons: A Computer-Aided Design Tool for Shaping and Patterning of Knitted Garments”. In: *Proceedings of the 32nd Annual ACM Symposium on User Interface Software and Technology*. 2019, pp. 53–65 (cit. on p. 15).

- [136] Shohei Katakura, Yuto Kuroki, and Keita Watanabe. “A 3D Printer Head as a Robotic Manipulator”. In: *Proceedings of the 32nd Annual ACM Symposium on User Interface Software and Technology*. UIST '19. New Orleans, LA, USA: Association for Computing Machinery, 2019, pp. 535–548. DOI: [10.1145/3332165.3347885](https://doi.org/10.1145/3332165.3347885) (cit. on p. 27).
- [137] Barbara Katzbauer. “Properties and applications of xanthan gum”. In: *Polymer Degradation and Stability* 59 (1-3 Jan. 1998), pp. 81–84. ISSN: 0141-3910. DOI: [10.1016/S0141-3910\(97\)00180-8](https://doi.org/10.1016/S0141-3910(97)00180-8) (cit. on pp. 97, 113).
- [138] Brett E Kelly, Indrasen Bhattacharya, Hossein Heidari, Maxim Shusteff, Christopher M Spadaccini, and Hayden K Taylor. “Volumetric additive manufacturing via tomographic reconstruction”. In: *Science* 363.6431 (2019), pp. 1075–1079 (cit. on pp. 7–9, 26, 29).
- [139] Jeeun Kim, Anhong Guo, Tom Yeh, Scott E. Hudson, and Jennifer Mankoff. “Understanding Uncertainty in Measurement and Accommodating Its Impact in 3D Modeling and Printing”. In: *Proceedings of the 2017 Conference on Designing Interactive Systems*. DIS '17. Edinburgh, United Kingdom: Association for Computing Machinery, 2017, pp. 1067–1078. DOI: [10.1145/3064663.3064690](https://doi.org/10.1145/3064663.3064690) (cit. on p. 17).
- [140] Sangbae Kim, Cecilia Laschi, and Barry Trimmer. “Soft robotics: a bioinspired evolution in robotics”. In: *Trends in Biotechnology* 31.5 (2013), pp. 287–294. ISSN: 0167-7799. DOI: <https://doi.org/10.1016/j.tibtech.2013.03.002> (cit. on p. 27).
- [141] Sunyoung Kim and Eric Paulos. “Practices in the Creative Reuse of E-Waste”. In: *Proceedings of the SIGCHI Conference on Human Factors in Computing Systems*. CHI '11. Vancouver, BC, Canada: Association for Computing Machinery, 2011, pp. 2395–2404. DOI: [10.1145/1978942.1979292](https://doi.org/10.1145/1978942.1979292) (cit. on p. 91).
- [142] Yoonho Kim, Hyunwoo Yuk, Ruike Zhao, Shawn A Chester, and Xuanhe Zhao. “Printing ferromagnetic domains for untethered fast-transforming soft materials”. In: *Nature* 558.7709 (2018), pp. 274–279 (cit. on pp. 27, 29).
- [143] Josephine Klefeker and Laura Devendorf. “String Figuring: A Story of Reflection, Material Inquiry, and a Novel Sensor”. In: *Extended Abstracts of the 2018 CHI Conference on Human Factors in Computing Systems*. CHI EA '18. Montreal QC, Canada: ACM, 2018, LBW086:1–LBW086:6. DOI: [10.1145/3170427.3188570](https://doi.org/10.1145/3170427.3188570) (cit. on pp. 28, 57).
- [144] Hideo Kodama. “Automatic method for fabricating a three-dimensional plastic model with photo-hardening polymer”. In: *Review of scientific instruments* 52.11 (1981), pp. 1770–1773 (cit. on pp. 7, 8).
- [145] Cindy Kohtala and Sampsa Hyysalo. “Anticipated environmental sustainability of personal fabrication”. In: *Journal of Cleaner Production* 99 (2015), pp. 333–344 (cit. on p. 92).
- [146] Jeffrey J Kolstad, Erwin TH Vink, Bruno De Wilde, and Lies Debeer. “Assessment of anaerobic degradation of Ingeo™ polylactides under accelerated landfill conditions”. In: *Polymer Degradation and Stability* 97.7 (2012), pp. 1131–1141 (cit. on p. 93).
- [147] Robert Kovacs, Alexandra Ion, Pedro Lopes, Tim Oesterreich, Johannes Filter, Philipp Otto, Tobias Arndt, Nico Ring, Melvin Witte, Anton Synytsia, and Patrick Baudisch. “TrussFormer: 3D Printing Large Kinetic Structures”. In: *Proceedings of the 31st Annual ACM Symposium on User Interface Software and Technology*. UIST '18. Berlin, Germany: Association for Computing Machinery, 2018, pp. 113–125. DOI: [10.1145/3242587.3242607](https://doi.org/10.1145/3242587.3242607) (cit. on pp. 24, 94).
- [148] Robert Kovacs, Anna Seufert, Ludwig Wall, Hsiang-Ting Chen, Florian Meinel, Willi Müller, Sijing You, Maximilian Brehm, Jonathan Striebel, Yannis Kommana, Alexander Popiak, Thomas Bläslius, and Patrick Baudisch. “TrussFab: Fabricating Sturdy Large-Scale Structures on Desktop 3D Printers”. In: *Proceedings of the 2017 CHI Conference on Human Factors in Computing Systems*. CHI '17. Denver, Colorado, USA: Association for Computing Machinery, 2017, pp. 2606–2616. DOI: [10.1145/3025453.3026016](https://doi.org/10.1145/3025453.3026016) (cit. on pp. 24, 94).

- [149] Yuki Koyama, Shinjiro Sueda, Emma Steinhardt, Takeo Igarashi, Ariel Shamir, and Wojciech Matusik. “AutoConnect: computational design of 3D-printable connectors”. In: *ACM Transactions on Graphics (TOG)* 34.6 (2015), pp. 1–11 (cit. on p. 16).
- [150] Yuki Kubo, Kana Eguchi, and Ryosuke Aoki. “3D-Printed Object Identification Method Using Inner Structure Patterns Configured by Slicer Software”. In: *Extended Abstracts of the 2020 CHI Conference on Human Factors in Computing Systems Extended Abstracts*. CHI ’20. Honolulu, HI, USA: Association for Computing Machinery, 2020, pp. 1–7. DOI: [10.1145/3334480.3382847](https://doi.org/10.1145/3334480.3382847) (cit. on p. 19).
- [151] Ashish Kumar, Venkatappa Rao Tumu, Subhendu Ray Chowdhury, and Ramana Reddy Ramana. “A green physical approach to compatibilize a bio-based poly (lactic acid)/lignin blend for better mechanical, thermal and degradation properties”. In: *International Journal of Biological Macromolecules* 121 (Jan. 2019), pp. 588–600. ISSN: 0141-8130. DOI: [10.1016/j.ijbiomac.2018.10.057](https://doi.org/10.1016/j.ijbiomac.2018.10.057) (cit. on p. 94).
- [152] FP La Mantia, L Botta, M Morreale, and R Scaffaro. “Effect of small amounts of poly (lactic acid) on the recycling of poly (ethylene terephthalate) bottles”. In: *Polymer Degradation and Stability* 97.1 (2012), pp. 21–24 (cit. on p. 93).
- [153] Nikolas Lamb, Sean Banerjee, and Natasha Kholgade Banerjee. “Automated Reconstruction of Smoothly Joining 3D Printed Restorations to Fix Broken Objects”. In: *Proceedings of the ACM Symposium on Computational Fabrication*. SCF ’19. Pittsburgh, Pennsylvania: Association for Computing Machinery, 2019. DOI: [10.1145/3328939.3329005](https://doi.org/10.1145/3328939.3329005) (cit. on p. 23).
- [154] Gierad Laput, Eric Brockmeyer, Moshe Mahler, Scott E. Hudson, and Chris Harrison. “Acoustruments: Passive, Acoustically-Driven, Interactive Controls for Handheld Devices”. In: *ACM SIGGRAPH 2015 Emerging Technologies*. SIGGRAPH ’15. Los Angeles, California: Association for Computing Machinery, 2015. DOI: [10.1145/2782782.2792490](https://doi.org/10.1145/2782782.2792490) (cit. on p. 19).
- [155] Gierad Laput, Xiang ’Anthony’ Chen, and Chris Harrison. “3D Printed Hair: Fused Deposition Modeling of Soft Strands, Fibers, and Bristles”. In: *Proceedings of the 28th Annual ACM Symposium on User Interface Software & Technology*. UIST ’15. Charlotte, NC, USA: ACM, 2015, pp. 593–597. DOI: [10.1145/2807442.2807484](https://doi.org/10.1145/2807442.2807484) (cit. on p. 21).
- [156] Eldy S. Lazaro Vasquez and Katia Vega. “From plastic to biomaterials: Prototyping DIY electronics with mycelium”. In: *UbiComp/ISWC 2019- Adjunct Proceedings of the 2019 ACM International Joint Conference on Pervasive and Ubiquitous Computing and Proceedings of the 2019 ACM International Symposium on Wearable Computers*. New York, NY, USA: Association for Computing Machinery, Inc, Sept. 2019, pp. 308–311. DOI: [10.1145/3341162.3343808](https://doi.org/10.1145/3341162.3343808) (cit. on pp. 92, 118).
- [157] Eldy S. Lazaro Vasquez and Katia Vega. “Myco-accessories: Sustainable wearables with biodegradable materials”. In: *Proceedings - International Symposium on Wearable Computers, ISWC*. New York, NY, USA: Association for Computing Machinery, Sept. 2019, pp. 306–311. DOI: [10.1145/3341163.3346938](https://doi.org/10.1145/3341163.3346938) (cit. on pp. 92, 118).
- [158] Eldy S. Lazaro Vasquez, Hao-Chuan Wang, and Katia Vega. “Introducing the Sustainable Prototyping Life Cycle for Digital Fabrication to Designers”. In: *Proceedings of the 2020 ACM Designing Interactive Systems Conference*. New York, NY, USA: Association for Computing Machinery, 2020, pp. 1301–1312 (cit. on p. 92).
- [159] Seungsin Lee and S Kay Obendorf. “Developing protective textile materials as barriers to liquid penetration using melt-electrospinning”. In: *Journal of Applied Polymer Science* 102.4 (2006), pp. 3430–3437 (cit. on p. 73).
- [160] Yujin Lee, Jee Bin Yim, Daye Kang, HyeonBeom Yi, and Daniel Saakes. “Designing Internal Structure of Chocolate and Its Effect on Food Texture”. In: *Companion Publication of the 2019 on Designing Interactive Systems Conference 2019 Companion*. DIS ’19 Companion. San Diego, CA, USA: Association for Computing Machinery, 2019, pp. 231–235. DOI: [10.1145/3301019.3323896](https://doi.org/10.1145/3301019.3323896) (cit. on p. 22).

- [161] Simon J Leigh, Robert J Bradley, Christopher P Purssell, Duncan R Billson, and David A Hutchins. “A simple, low-cost conductive composite material for 3D printing of electronic sensors”. In: *PloS one* 7.11 (2012) (cit. on p. 20).
- [162] Joanne Leong, Patrick Parzer, Florian Perteneder, Teo Babic, Christian Rendl, Anita Vogl, Hubert Egger, Alex Olwal, and Michael Haller. “proCover: Sensory Augmentation of Prosthetic Limbs Using Smart Textile Covers”. In: *Proceedings of the 29th Annual Symposium on User Interface Software and Technology, UIST 2016, Tokyo, Japan, October 16-19, 2016*. 2016, pp. 335–346. DOI: [10.1145/2984511.2984572](https://doi.org/10.1145/2984511.2984572) (cit. on pp. 28, 71).
- [163] Ilona Leppänen, Minna Vikman, Ali Harlin, and Hannes Orelma. “Enzymatic Degradation and Pilot-Scale Composting of Cellulose-Based Films with Different Chemical Structures”. In: *Journal of Polymers and the Environment* 28:2 28 (2 Nov. 2019), pp. 458–470. ISSN: 1572-8919. DOI: [10.1007/S10924-019-01621-W](https://doi.org/10.1007/S10924-019-01621-W). URL: <https://link.springer.com/article/10.1007/s10924-019-01621-w> (cit. on p. 113).
- [164] Dingzeyu Li, David I. W. Levin, Wojciech Matusik, and Changxi Zheng. “Acoustic Voxels: Computational Optimization of Modular Acoustic Filters”. In: *ACM Trans. Graph.* 35.4 (July 2016). ISSN: 0730-0301. DOI: [10.1145/2897824.2925960](https://doi.org/10.1145/2897824.2925960) (cit. on p. 19).
- [165] Jiahao Li, Jeeun Kim, and Xiang “Anthony” Chen. “Robiot: A Design Tool for Actuating Everyday Objects with Automatically Generated 3D Printable Mechanisms”. In: *Proceedings of the 32nd Annual ACM Symposium on User Interface Software and Technology. UIST ’19*. New Orleans, LA, USA: Association for Computing Machinery, 2019, pp. 673–685. DOI: [10.1145/3332165.3347894](https://doi.org/10.1145/3332165.3347894) (cit. on p. 24).
- [166] Lei Li, Johannes M Scheiger, and Pavel A Levkin. “Design and Applications of Photoresponsive Hydrogels”. In: *Advanced Materials* 31.26 (2019), p. 1807333 (cit. on p. 58).
- [167] Ying-Ju Lin, Parinya Punpongsonon, Xin Wen, Daisuke Iwai, Kosuke Sato, Marianna Obrist, and Stefanie Mueller. “FoodFab: creating food perception illusions using food 3D printing”. In: *Proceedings of the 2020 CHI Conference on Human Factors in Computing Systems (CHI 2020)*. ACM. 2020 (cit. on p. 22).
- [168] Ke Liu, Jiangtao Wu, Glaucio H Paulino, and H Jerry Qi. “Programmable deployment of tensegrity structures by stimulus-responsive polymers”. In: *Scientific reports* 7.1 (2017), pp. 1–8 (cit. on p. 20).
- [169] Yifang Liu, Ruimin Liu, Xiang Wang, Jiabin Jiang, Wenwang Li, Juan Liu, Shumin Guo, and Gaofeng Zheng. “Electrospun Three-Dimensional Nanofibrous Structure via Probe Arrays Inducing”. In: *Micromachines* 9.9 (Aug. 2018), p. 427. ISSN: 2072-666X. DOI: [10.3390/mi9090427](https://doi.org/10.3390/mi9090427) (cit. on p. 89).
- [170] Zhenbin Liu, Bhesh Bhandari, Sangeeta Prakash, and Min Zhang. “Creation of internal structure of mashed potato construct by 3D printing and its textural properties”. In: *Food Research International* 111 (2018), pp. 534–543 (cit. on p. 21).
- [171] Zhengqing Liu, Jiaying Zhan, Mohammad Fard, and John Laurence Davy. “Acoustic properties of multilayer sound absorbers with a 3D printed micro-perforated panel”. In: *Applied Acoustics* 121 (2017), pp. 25–32 (cit. on p. 19).
- [172] Ernerst E. Lockhart. *The soluble solids in beverage coffee as an index to cup quality*. 1969 (cit. on p. 97).
- [173] Lin Lu, Andrei Sharf, Haisen Zhao, Yuan Wei, Qingnan Fan, Xuelin Chen, Yann Savoye, Changhe Tu, Daniel Cohen-Or, and Baoquan Chen. “Build-to-last: strength to weight 3D printed objects”. In: *ACM Transactions on Graphics (TOG)* 33.4 (2014), pp. 1–10 (cit. on p. 15).
- [174] Linjie Luo, Ilya Baran, Szymon Rusinkiewicz, and Wojciech Matusik. “Chopper: partitioning models into 3D-printable parts”. In: *ACM Transactions on Graphics (TOG)* 31.6 (2012), pp. 1–9 (cit. on p. 16).
- [175] Jason Lyons, Christopher Li, and Frank Ko. “Melt-electrospinning part I: processing parameters and geometric properties”. In: *Polymer* 45.22 (2004), pp. 7597–7603 (cit. on p. 76).
- [176] Li-Ke Ma, Yizhong Zhang, Yang Liu, Kun Zhou, and Xin Tong. “Computational Design and Fabrication of Soft Pneumatic Objects with Desired Deformations”. In: *ACM Trans. Graph.* 36.6 (Nov. 2017). ISSN: 0730-0301. DOI: [10.1145/3130800.3130850](https://doi.org/10.1145/3130800.3130850) (cit. on p. 16).

- [177] Robert MacCurdy, Robert Katzschmann, Youbin Kim, and Daniela Rus. “Printable hydraulics: A method for fabricating robots by 3D co-printing solids and liquids”. In: *2016 IEEE International Conference on Robotics and Automation (ICRA)*. IEEE. 2016, pp. 3878–3885 (cit. on p. 27).
- [178] Shiran Magrisso, Moran Mizrahi, and Amit Zoran. “Digital Joinery For Hybrid Carpentry”. In: *Proceedings of the 2018 CHI Conference on Human Factors in Computing Systems*. CHI ’18. Montreal QC, Canada: Association for Computing Machinery, 2018. DOI: [10.1145/3173574.3173741](https://doi.org/10.1145/3173574.3173741) (cit. on p. 24).
- [179] Henrique Teles Maia, Dingzeyu Li, Yuan Yang, and Changxi Zheng. “LayerCode: optical barcodes for 3D printed shapes”. In: *ACM Transactions on Graphics (TOG)* 38.4 (2019), pp. 1–14 (cit. on p. 18).
- [180] Luigi Malomo, Nico Pietroni, Bernd Bickel, and Paolo Cignoni. “FlexMolds: Automatic Design of Flexible Shells for Molding”. In: *ACM Trans. Graph.* 35.6 (Nov. 2016). ISSN: 0730-0301. DOI: [10.1145/2980179.2982397](https://doi.org/10.1145/2980179.2982397) (cit. on p. 23).
- [181] Evan Malone and Hod Lipson. “Fab@ Home: the personal desktop fabricator kit”. In: *Rapid Prototyping Journal* (2007) (cit. on pp. 1, 11, 92).
- [182] Teunis van Manen, Shahram Janbaz, and Amir A Zadpoor. “Programming 2D/3D shape-shifting with hobbyist 3D printers”. In: *Materials horizons* 4.6 (2017), pp. 1064–1069 (cit. on p. 20).
- [183] Jennifer C. Mankoff, Eli Blevis, Alan Borning, Batya Friedman, Susan R. Fussell, Jay Hasbrouck, Allison Woodruff, and Phoebe Sengers. “Environmental Sustainability and Interaction”. In: *CHI ’07 Extended Abstracts on Human Factors in Computing Systems*. CHI EA ’07. San Jose, CA, USA: Association for Computing Machinery, 2007, pp. 2121–2124. DOI: [10.1145/1240866.1240963](https://doi.org/10.1145/1240866.1240963) (cit. on p. 91).
- [184] Jonàs Martínez, Jérémie Dumas, and Sylvain Lefebvre. “Procedural Voronoi Foams for Additive Manufacturing”. In: *ACM Trans. Graph.* 35.4 (July 2016), 44:1–44:12. ISSN: 0730-0301. DOI: [10.1145/2897824.2925922](https://doi.org/10.1145/2897824.2925922) (cit. on pp. 16, 71).
- [185] H Scott Matthews, Chris T Hendrickson, and Deanna H Matthews. “Life cycle assessment: Quantitative approaches for decisions that matter”. In: *Retrieved June 1* (2015), p. 2016. URL: <https://www.lcatextbook.com/> (cit. on p. 113).
- [186] William McDonough and Michael Braungart. *Cradle to cradle: Remaking the way we make things*. North point press, 2010 (cit. on p. 102).
- [187] Yogesh Kumar Meena, Xing-Dong Yang, Markus Löchtefeld, Matt Carnie, Niels Henze, Steve Hodges, Matt Jones, Nivedita Arora, and Gregory D. Abowd. “SelfSustainableCHI: Self-Powered Sustainable Interfaces and Interactions”. In: *Extended Abstracts of the 2020 CHI Conference on Human Factors in Computing Systems*. CHI EA ’20. Honolulu, HI, USA: Association for Computing Machinery, 2020, pp. 1–7. DOI: [10.1145/3334480.3375167](https://doi.org/10.1145/3334480.3375167) (cit. on p. 91).
- [188] Vittorio Megaro, Jonas Zehnder, Moritz Bächer, Stelian Coros, Markus Gross, and Bernhard Thomaszewski. “A Computational Design Tool for Compliant Mechanisms”. In: *ACM Trans. Graph.* 36.4 (July 2017), 82:1–82:12. ISSN: 0730-0301. DOI: [10.1145/3072959.3073636](https://doi.org/10.1145/3072959.3073636) (cit. on pp. 17, 71).
- [189] Jussi Mikkonen, Reetta Myllymäki, Sari Kivioja, Santeri Vanhakartano, and Helena Suonsilta. “Printed material and fabric”. In: *Nordes* 1.5 (2013) (cit. on p. 35).
- [190] Llorenç Milà i Canals. *Global LCA Data Access network*. 2021. URL: <https://www.globallcadataaccess.org/> (cit. on p. 114).
- [191] Viktor Miruchna, Robert Walter, David Lindlbauer, Maren Lehmann, Regine von Klitzing, and Jörg Müller. “GelTouch: Localized Tactile Feedback Through Thin, Programmable Gel”. In: *Proceedings of the 28th Annual ACM Symposium on User Interface Software & Technology*. UIST ’15. Charlotte, NC, USA: ACM, 2015, pp. 3–10. DOI: [10.1145/2807442.2807487](https://doi.org/10.1145/2807442.2807487) (cit. on p. 58).
- [192] Moran Mizrahi, Amos Golan, Ariel Bezaleli Mizrahi, Rotem Gruber, Alexander Zoonder Lachnise, and Amit Zoran. “Digital Gastronomy: Methods & Recipes for Hybrid Cooking”. In: *Proceedings of the 29th Annual Symposium on User Interface Software and Technology*. UIST ’16. Tokyo, Japan: Association for Computing Machinery, 2016, pp. 541–552. DOI: [10.1145/2984511.2984528](https://doi.org/10.1145/2984511.2984528) (cit. on p. 21).

- [193] Francesco F. Montesano, Angelo Parente, Pietro Santamaria, Alessandro Sannino, and Francesco Serio. “Biodegradable Superabsorbent Hydrogel Increases Water Retention Properties of Growing Media and Plant Growth”. In: *Agriculture and Agricultural Science Procedia* 4 (Jan. 2015), pp. 451–458. ISSN: 2210-7843. DOI: [10.1016/J.AASPRO.2015.03.052](https://doi.org/10.1016/J.AASPRO.2015.03.052) (cit. on pp. 97, 102, 113).
- [194] Yuki Mori and Takeo Igarashi. “Plushie: an interactive design system for plush toys”. In: *ACM SIGGRAPH 2007 papers*. 2007, 45–es (cit. on p. 15).
- [195] Catarina Mota. “The Rise of Personal Fabrication”. In: *Proceedings of the 8th ACM Conference on Creativity and Cognition*. C&C ’11. Atlanta, Georgia, USA: Association for Computing Machinery, 2011, pp. 279–288. DOI: [10.1145/2069618.2069665](https://doi.org/10.1145/2069618.2069665) (cit. on pp. 1, 2, 13).
- [196] Stefanie Mueller, Sangha Im, Serafima Gurevich, Alexander Teibrich, Lisa Pfisterer, François Guimbretière, and Patrick Baudisch. “WirePrint: 3D printed previews for fast prototyping”. In: *Proceedings of the 27th annual ACM Symposium on User Interface Software & Technology*. UIST ’14. ACM. 2014, pp. 273–280 (cit. on pp. 15, 93, 94).
- [197] Stefanie Mueller, Tobias Mohr, Kerstin Guenther, Johannes Frohnhofen, and Patrick Baudisch. “FaB-rikkation: Fast 3D Printing of Functional Objects by Integrating Construction Kit Building Blocks”. In: *Proceedings of the SIGCHI Conference on Human Factors in Computing Systems*. CHI ’14. Toronto, Ontario, Canada: Association for Computing Machinery, 2014, pp. 3827–3834. DOI: [10.1145/2556288.2557005](https://doi.org/10.1145/2556288.2557005) (cit. on pp. 23, 93, 94).
- [198] Matthias Müller, David Charypar, and Markus Gross. “Particle-based fluid simulation for interactive applications”. In: *Proceedings of the 2003 ACM SIGGRAPH/Eurographics symposium on Computer animation*. Eurographics Association. 2003, pp. 154–159 (cit. on p. 14).
- [199] Joseph T Muth, Daniel M Vogt, Ryan L Truby, Yiğit Mengüç, David B Kolesky, Robert J Wood, and Jennifer A Lewis. “Embedded 3D printing of strain sensors within highly stretchable elastomers”. In: *Advanced Materials* 26.36 (2014), pp. 6307–6312 (cit. on p. 27).
- [200] Sara Nabil, Jan Kučera, Nikoletta Karastathi, David S. Kirk, and Peter Wright. “Seamless Seams: Crafting Techniques for Embedding Fabrics with Interactive Actuation”. In: *Proceedings of the 2019 on Designing Interactive Systems Conference*. DIS ’19. San Diego, CA, USA: ACM, 2019, pp. 987–999. DOI: [10.1145/3322276.3322369](https://doi.org/10.1145/3322276.3322369) (cit. on pp. 28, 57).
- [201] Satoshi Nakamaru, Ryosuke Nakayama, Ryuma Niiyama, and Yasuaki Kakehi. “FoamSense: Design of Three Dimensional Soft Sensors with Porous Materials”. In: *Proceedings of the 30th Annual ACM Symposium on User Interface Software and Technology, UIST 2017, Quebec City, QC, Canada, October 22 - 25, 2017*. 2017, pp. 437–447. DOI: [10.1145/3126594.3126666](https://doi.org/10.1145/3126594.3126666) (cit. on pp. 27, 71).
- [202] Ryosuke Nakayama, Ryo Suzuki, Satoshi Nakamaru, Ryuma Niiyama, Yoshihiro Kawahara, and Yasuaki Kakehi. “MorphIO: Entirely Soft Sensing and Actuation Modules for Programming Shape Changes through Tangible Interaction”. In: *Proceedings of the 2019 on Designing Interactive Systems Conference*. DIS ’19. San Diego, CA, USA: Association for Computing Machinery, 2019, pp. 975–986. DOI: [10.1145/3322276.3322337](https://doi.org/10.1145/3322276.3322337) (cit. on p. 25).
- [203] Vidya Narayanan, Lea Albaugh, Jessica Hodgins, Stelian Coros, and James McCann. “Automatic machine knitting of 3D meshes”. In: *ACM Transactions on Graphics (TOG)* 37.3 (2018), pp. 1–15 (cit. on p. 15).
- [204] Tuan D Ngo, Alireza Kashani, Gabriele Imbalzano, Kate TQ Nguyen, and David Hui. “Additive manufacturing (3D printing): A review of materials, methods, applications and challenges”. In: *Composites Part B: Engineering* 143 (2018), pp. 172–196 (cit. on pp. 7, 9, 10).
- [205] Amirali Nojoomi, Hakan Arslan, Kwan Lee, and Kyungsuk Yum. “Bioinspired 3D structures with programmable morphologies and motions”. In: *Nature communications* 9.1 (2018), p. 3705 (cit. on p. 58).
- [206] Lora Oehlberg, Wesley Willett, and Wendy E. Mackay. “Patterns of Physical Design Remixing in Online Maker Communities”. In: *Proceedings of the 33rd Annual ACM Conference on Human Factors in Computing Systems*. CHI ’15. Seoul, Republic of Korea: Association for Computing Machinery, 2015, pp. 639–648. DOI: [10.1145/2702123.2702175](https://doi.org/10.1145/2702123.2702175) (cit. on p. 2).

- [207] Masa Ogata and Yuki Koyama. “A Computational Approach to Magnetic Force Feedback Design”. In: *Proceedings of the 2021 CHI Conference on Human Factors in Computing Systems*. New York, NY, USA: Association for Computing Machinery, 2021 (cit. on pp. 21, 25, 29).
- [208] Hyunjoo Oh, Tung D. Ta, Ryo Suzuki, Mark D. Gross, Yoshihiro Kawahara, and Lining Yao. “PEP (3D Printed Electronic Papercrafts): An Integrated Approach for 3D Sculpting Paper-Based Electronic Devices”. In: *Proceedings of the 2018 CHI Conference on Human Factors in Computing Systems*. CHI ’18. Montreal QC, Canada: Association for Computing Machinery, 2018, pp. 1–12. DOI: [10.1145/3173574.3174015](https://doi.org/10.1145/3173574.3174015) (cit. on p. 10).
- [209] Alex Olwal, Jon Moeller, Greg Priest-Dorman, Thad Starner, and Ben Carroll. “I/O Braid: Scalable Touch-Sensitive Lighted Cords Using Spiraling, Repeating Sensing Textiles and Fiber Optics”. In: *Proceedings of the 31st Annual ACM Symposium on User Interface Software and Technology*. UIST ’18. Berlin, Germany: ACM, 2018, pp. 485–497. DOI: [10.1145/3242587.3242638](https://doi.org/10.1145/3242587.3242638) (cit. on pp. 28, 57).
- [210] International Coffee Organization. *Coffee Market Report (July 2021)*. 2021. URL: <https://www.ico.org/documents/cy2020-21/cmr-0721-e.pdf> (cit. on p. 97).
- [211] Jifei Ou, Gershon Dublon, Chin-Yi Cheng, Felix Heibeck, Karl Willis, and Hiroshi Ishii. “Cillia: 3D Printed Micro-Pillar Structures for Surface Texture, Actuation and Sensing”. In: *Proceedings of the 2016 CHI Conference on Human Factors in Computing Systems*. CHI ’16. San Jose, California, USA: ACM, 2016, pp. 5753–5764. DOI: [10.1145/2858036.2858257](https://doi.org/10.1145/2858036.2858257) (cit. on p. 21).
- [212] Jukka Pakkanen, Diego Manfredi, Paolo Minetola, and Luca Iuliano. “About the use of recycled or biodegradable filaments for sustainability of 3D printing”. In: *International Conference on Sustainable Design and Manufacturing*. Springer. 2017, pp. 776–785 (cit. on p. 93).
- [213] Julian Panetta, Qingnan Zhou, Luigi Malomo, Nico Pietroni, Paolo Cignoni, and Denis Zorin. “Elastic textures for additive fabrication”. In: *ACM Transactions on Graphics (TOG)* 34.4 (2015), pp. 1–12 (cit. on pp. 16, 29).
- [214] Fabrizio Pece, Juan Jose Zarate, Velko Vechev, Nadine Besse, Olexandr Gudozhnik, Herbert Shea, and Otmar Hilliges. “MagTics: Flexible and Thin Form Factor Magnetic Actuators for Dynamic and Wearable Haptic Feedback”. In: *Proceedings of the 30th Annual ACM Symposium on User Interface Software and Technology*. UIST ’17. Québec City, QC, Canada: Association for Computing Machinery, 2017, pp. 143–154. DOI: [10.1145/3126594.3126609](https://doi.org/10.1145/3126594.3126609) (cit. on p. 25).
- [215] Eujin Pei, Jinsong Shen, and Jennifer Watling. “Direct 3D printing of polymers onto textiles: experimental studies and applications”. In: *Rapid Prototyping Journal* 21.5 (2015), pp. 556–571 (cit. on pp. 35, 38).
- [216] Huaishu Peng, François Guimbretière, James McCann, and Scott Hudson. “A 3D Printer for Interactive Electromagnetic Devices”. In: *Proceedings of the 29th Annual Symposium on User Interface Software and Technology*. UIST ’16. Tokyo, Japan: Association for Computing Machinery, 2016, pp. 553–562. DOI: [10.1145/2984511.2984523](https://doi.org/10.1145/2984511.2984523) (cit. on pp. 27, 29).
- [217] Huaishu Peng, Jennifer Mankoff, Scott E. Hudson, and James McCann. “A Layered Fabric 3D Printer for Soft Interactive Objects”. In: *Proceedings of the 33rd Annual ACM Conference on Human Factors in Computing Systems*. CHI ’15. Seoul, Republic of Korea: ACM, 2015, pp. 1789–1798. DOI: [10.1145/2702123.2702327](https://doi.org/10.1145/2702123.2702327) (cit. on pp. 10, 28, 29, 35).
- [218] Huaishu Peng, Rundong Wu, Steve Marschner, and François Guimbretière. “On-The-Fly Print: Incremental Printing While Modelling”. In: *Proceedings of the 2016 CHI Conference on Human Factors in Computing Systems*. CHI ’16. San Jose, California, USA: Association for Computing Machinery, 2016, pp. 887–896. DOI: [10.1145/2858036.2858106](https://doi.org/10.1145/2858036.2858106) (cit. on p. 27).
- [219] Thiago Pereira, Szymon Rusinkiewicz, and Wojciech Matusik. “Computational Light Routing: 3D Printed Optical Fibers for Sensing and Display”. In: *ACM Trans. Graph.* 33.3 (June 2014). ISSN: 0730-0301. DOI: [10.1145/2602140](https://doi.org/10.1145/2602140) (cit. on p. 18).

- [220] Jesús Pérez, Miguel A. Otaduy, and Bernhard Thomaszewski. “Computational Design and Automated Fabrication of Kirchhoff-plateau Surfaces”. In: *ACM Trans. Graph.* 36.4 (July 2017), 62:1–62:12. ISSN: 0730-0301. DOI: [10.1145/3072959.3073695](https://doi.org/10.1145/3072959.3073695) (cit. on pp. 16, 71).
- [221] Jesús Pérez, Bernhard Thomaszewski, Stelian Coros, Bernd Bickel, José A Canabal, Robert Sumner, and Miguel A Otaduy. “Design and fabrication of flexible rod meshes”. In: *ACM Transactions on Graphics (TOG)* 34.4 (2015), pp. 1–12 (cit. on p. 16).
- [222] Daniel Periard, Evan Malone, and Hod Lipson. “Printing embedded circuits”. In: *Proceedings of the 18th Solid Freeform Fabrication Symposium*. Citeseer. 2007, pp. 503–512 (cit. on p. 24).
- [223] James Pierce, Diane J. Schiano, and Eric Paulos. “Home, Habits, and Energy: Examining Domestic Interactions and Energy Consumption”. In: *Proceedings of the SIGCHI Conference on Human Factors in Computing Systems*. New York, NY, USA: Association for Computing Machinery, 2010, pp. 1985–1994. ISBN: 9781605589299 (cit. on p. 91).
- [224] Ivan Poupyrev, Nan-Wei Gong, Shiho Fukuhara, Mustafa Emre Karagozler, Carsten Schwesig, and Karen E. Robinson. “Project Jacquard: Interactive Digital Textiles at Scale”. In: *Proceedings of the 2016 CHI Conference on Human Factors in Computing Systems, San Jose, CA, USA, May 7-12, 2016*. 2016, pp. 4216–4227. DOI: [10.1145/2858036.2858176](https://doi.org/10.1145/2858036.2858176) (cit. on pp. 28, 57, 72).
- [225] Hardikkumar Prajapati, Darshan Ravoory, Robert L Woods, and Ankur Jain. “Measurement of anisotropic thermal conductivity and inter-layer thermal contact resistance in polymer fused deposition modeling (FDM)”. In: *Additive Manufacturing* 21 (2018), pp. 84–90 (cit. on p. 20).
- [226] Romain Prévost, Emily Whiting, Sylvain Lefebvre, and Olga Sorkine-Hornung. “Make it stand: balancing shapes for 3D fabrication”. In: *ACM Transactions on Graphics (TOG)* 32.4 (2013), pp. 1–10 (cit. on p. 15).
- [227] Parinya Punpongsanon, Xin Wen, David S. Kim, and Stefanie Mueller. “ColorMod: Recoloring 3D Printed Objects Using Photochromic Inks”. In: *Proceedings of the 2018 CHI Conference on Human Factors in Computing Systems*. CHI ’18. Montreal QC, Canada: Association for Computing Machinery, 2018. DOI: [10.1145/3173574.3173787](https://doi.org/10.1145/3173574.3173787) (cit. on pp. 27, 29).
- [228] Kira Pusch, Thomas J. Hinton, and Adam W. Feinberg. “Large volume syringe pump extruder for desktop 3D printers”. In: *HardwareX* 3 (2018), pp. 49–61. ISSN: 2468-0672. DOI: [10.1016/j.ohx.2018.02.001](https://doi.org/10.1016/j.ohx.2018.02.001) (cit. on pp. 59, 99, 111).
- [229] Pedro M Reis, Heinrich M Jaeger, and Martin Van Hecke. “Designer matter: A perspective”. In: *Extreme Mechanics Letters* 5 (2015), pp. 25–29 (cit. on p. 17).
- [230] Michael L. Rivera, Jack Forman, Scott E. Hudson, and Lining Yao. “Hydrogel-Textile Composites: Actuators for Shape-Changing Interfaces”. In: *Extended Abstracts of the 2020 CHI Conference on Human Factors in Computing Systems Extended Abstracts*. CHI ’20. Honolulu, HI, USA: Association for Computing Machinery, 2020, pp. 1–9. DOI: [10.1145/3334480.3382788](https://doi.org/10.1145/3334480.3382788) (cit. on pp. xxv, 112).
- [231] Michael L. Rivera and Scott E. Hudson. “Desktop Electrospinning: A Single Extruder 3D Printer for Producing Rigid Plastic and Electrospun Textiles”. In: *Proceedings of the 2019 CHI Conference on Human Factors in Computing Systems*. CHI ’19. Glasgow, Scotland Uk: ACM, 2019, 204:1–204:12. DOI: [10.1145/3290605.3300434](https://doi.org/10.1145/3290605.3300434) (cit. on p. xxv).
- [232] Michael L. Rivera, Melissa Moukperian, Daniel Ashbrook, Jennifer Mankoff, and Scott E. Hudson. “Stretching the Bounds of 3D Printing with Embedded Textiles”. In: *Proceedings of the 2017 CHI Conference on Human Factors in Computing Systems*. CHI ’17. Denver, Colorado, USA: ACM, 2017, pp. 497–508. DOI: [10.1145/3025453.3025460](https://doi.org/10.1145/3025453.3025460) (cit. on pp. xxv, 57, 82).
- [233] David Roedl, Shaowen Bardzell, and Jeffrey Bardzell. “Sustainable Making? Balancing Optimism and Criticism in HCI Discourse”. In: *ACM Trans. Comput.-Hum. Interact.* 22.3 (June 2015). ISSN: 1073-0516. DOI: [10.1145/2699742](https://doi.org/10.1145/2699742) (cit. on p. 91).
- [234] Orlando J Rojas. *Cellulose chemistry and properties: fibers, nanocelluloses and advanced materials*. Vol. 271. Springer, 2016 (cit. on pp. 91, 97).

- [235] Domenico Ronga, Catello Pane, Massimo Zaccardelli, and Nicola Pecchioni. “Use of Spent Coffee Ground Compost in Peat-Based Growing Media for the Production of Basil and Tomato Potting Plants”. In: *http://dx.doi.org/10.1080/00103624.2015.1122803* 47 (3 Feb. 2016), pp. 356–368. DOI: [10.1080/00103624.2015.1122803](https://doi.org/10.1080/00103624.2015.1122803). URL: <https://www.tandfonline.com/doi/abs/10.1080/00103624.2015.1122803> (cit. on pp. 97, 102, 113).
- [236] Thijs Jan Roumen, Willi Müller, and Patrick Baudisch. “Grafter: Remixing 3D-Printed Machines”. In: *Proceedings of the 2018 CHI Conference on Human Factors in Computing Systems*. CHI ’18. Montreal QC, Canada: Association for Computing Machinery, 2018, pp. 1–12. DOI: [10.1145/3173574.3173637](https://doi.org/10.1145/3173574.3173637) (cit. on p. 16).
- [237] Elizabeth Royte. “Corn plastic to the rescue”. In: *Smithsonian Magazine* 37.5 (2006), pp. 84–88 (cit. on p. 93).
- [238] Daniela Rus and Michael T Tolley. “Design, fabrication and control of soft robots”. In: *Nature* 521.7553 (2015), pp. 467–475 (cit. on p. 27).
- [239] Lilia Sabantina, Franziska Kinzel, Andrea Ehrmann, and Karin Finsterbusch. “Combining 3D printed forms with textile structures-mechanical and geometrical properties of multi-material systems”. In: *IOP Conference Series: Materials Science and Engineering*. Vol. 87. 1. IOP Publishing, 2015, p. 012005 (cit. on p. 35).
- [240] Mohammad Saberian, Jie Li, Anita Donnoli, Ethan Bonderenko, Paolo Oliva, Bailey Gill, Simon Lockrey, and Rafat Siddique. “Recycling of spent coffee grounds in construction materials: A review”. In: *Journal of Cleaner Production* 289 (Mar. 2021), p. 125837. ISSN: 0959-6526. DOI: [10.1016/J.JCLEPRO.2021.125837](https://doi.org/10.1016/J.JCLEPRO.2021.125837) (cit. on p. 97).
- [241] T. Scott Saponas, Chris Harrison, and Hrvoje Benko. “PocketTouch: Through-fabric Capacitive Touch Input”. In: *Proceedings of the 24th Annual ACM Symposium on User Interface Software and Technology*. UIST ’11. Santa Barbara, California, USA: ACM, 2011, pp. 303–308. DOI: [10.1145/2047196.2047235](https://doi.org/10.1145/2047196.2047235) (cit. on pp. 28, 72).
- [242] John Sargent Jr and R.X. Schwartz. “3D Printing: Overview, Impacts, and the Federal Role. CRS Report R45852, Version 15. Updated.” In: *Congressional Research Service* (Aug. 2019). URL: <https://crsreports.congress.gov/product/pdf/R/R45852> (cit. on pp. 1, 2, 92).
- [243] John Sarik, Alex Butler, James Scott, Steve Hodges, and Nicolas Villar. “Combining 3D printing and printable electronics”. In: (2012) (cit. on p. 24).
- [244] Greg Saul, Manfred Lau, Jun Mitani, and Takeo Igarashi. “SketchChair: an all-in-one chair design system for end users”. In: *Proceedings of the fifth international conference on Tangible, embedded, and embodied interaction*. 2010, pp. 73–80 (cit. on p. 15).
- [245] Valkyrie Savage, Colin Chang, and Björn Hartmann. “Sauron: Embedded Single-Camera Sensing of Printed Physical User Interfaces”. In: *Proceedings of the 26th Annual ACM Symposium on User Interface Software and Technology*. UIST ’13. St. Andrews, Scotland, United Kingdom: Association for Computing Machinery, 2013, pp. 447–456. DOI: [10.1145/2501988.2501992](https://doi.org/10.1145/2501988.2501992) (cit. on p. 25).
- [246] Valkyrie Savage, Sean Follmer, Jingyi Li, and Björn Hartmann. “Makers’ Marks: Physical Markup for Designing and Fabricating Functional Objects”. In: *Proceedings of the 28th Annual ACM Symposium on User Interface Software & Technology*. UIST ’15. Charlotte, NC, USA: Association for Computing Machinery, 2015, pp. 103–108. DOI: [10.1145/2807442.2807508](https://doi.org/10.1145/2807442.2807508) (cit. on p. 24).
- [247] Valkyrie Savage, Andrew Head, Björn Hartmann, Dan B. Goldman, Gautham Mysore, and Wilmot Li. “Lamello: Passive Acoustic Sensing for Tangible Input Components”. In: *Proceedings of the 33rd Annual ACM Conference on Human Factors in Computing Systems*. CHI ’15. Seoul, Republic of Korea: Association for Computing Machinery, 2015, pp. 1277–1280. DOI: [10.1145/2702123.2702207](https://doi.org/10.1145/2702123.2702207) (cit. on p. 19).

- [248] Valkyrie Savage, Ryan Schmidt, Tovi Grossman, George Fitzmaurice, and Björn Hartmann. “A Series of Tubes: Adding Interactivity to 3D Prints Using Internal Pipes”. In: *Proceedings of the 27th Annual ACM Symposium on User Interface Software and Technology*. UIST ’14. Honolulu, Hawaii, USA: Association for Computing Machinery, 2014, pp. 3–12. DOI: [10.1145/2642918.2647374](https://doi.org/10.1145/2642918.2647374) (cit. on pp. 24, 25).
- [249] Martin Schmitz, Martin Herbers, Niloofar Dezfuli, Sebastian Günther, and Max Mühlhäuser. “Off-Line Sensing: Memorizing Interactions in Passive 3D-Printed Objects”. In: *Proceedings of the 2018 CHI Conference on Human Factors in Computing Systems*. CHI ’18. Montreal QC, Canada: Association for Computing Machinery, 2018. DOI: [10.1145/3173574.3173756](https://doi.org/10.1145/3173574.3173756) (cit. on p. 25).
- [250] Martin Schmitz, Mohammadreza Khalilbeigi, Matthias Balwierz, Roman Lissermann, Max Mühlhäuser, and Jürgen Steimle. “Capricate: A Fabrication Pipeline to Design and 3D Print Capacitive Touch Sensors for Interactive Objects”. In: *Proceedings of the 28th Annual ACM Symposium on User Interface Software & Technology*. UIST ’15. Charlotte, NC, USA: Association for Computing Machinery, 2015, pp. 253–258. DOI: [10.1145/2807442.2807503](https://doi.org/10.1145/2807442.2807503) (cit. on p. 21).
- [251] Martin Schmitz, Andreas Leister, Niloofar Dezfuli, Jan Riemann, Florian Müller, and Max Mühlhäuser. “Liquido: Embedding Liquids into 3D Printed Objects to Sense Tilting and Motion”. In: *Proceedings of the 2016 CHI Conference Extended Abstracts on Human Factors in Computing Systems*. CHI EA ’16. San Jose, California, USA: Association for Computing Machinery, 2016, pp. 2688–2696. DOI: [10.1145/2851581.2892275](https://doi.org/10.1145/2851581.2892275) (cit. on p. 25).
- [252] Martin Schmitz, Jürgen Steimle, Jochen Huber, Niloofar Dezfuli, and Max Mühlhäuser. “Flexibles: Deformation-Aware 3D-Printed Tangibles for Capacitive Touchscreens”. In: *Proceedings of the 2017 CHI Conference on Human Factors in Computing Systems*. CHI ’17. Denver, Colorado, USA: Association for Computing Machinery, 2017, pp. 1001–1014. DOI: [10.1145/3025453.3025663](https://doi.org/10.1145/3025453.3025663) (cit. on p. 21).
- [253] Martin Schmitz, Martin Stitz, Florian Müller, Markus Funk, and Max Mühlhäuser. “./Trilaterate: A Fabrication Pipeline to Design and 3D Print Hover-, Touch-, and Force-Sensitive Objects”. In: *Proceedings of the 2019 CHI Conference on Human Factors in Computing Systems*. CHI ’19. Glasgow, Scotland Uk: Association for Computing Machinery, 2019. DOI: [10.1145/3290605.3300684](https://doi.org/10.1145/3290605.3300684) (cit. on p. 21).
- [254] Christian Schüller, Roi Poranne, and Olga Sorkine-Hornung. “Shape representation by zippables”. In: *ACM Transactions on Graphics (TOG)* 37.4 (2018), pp. 1–13 (cit. on p. 15).
- [255] Adriana Schulz. “Computational design for the next manufacturing revolution”. PhD thesis. Massachusetts Institute of Technology, 2018 (cit. on p. 22).
- [256] Adriana Schulz, Harrison Wang, Eitan Grinspun, Justin Solomon, and Wojciech Matusik. “Interactive Exploration of Design Trade-Offs”. In: *ACM Trans. Graph.* 37.4 (July 2018). ISSN: 0730-0301. DOI: [10.1145/3197517.3201385](https://doi.org/10.1145/3197517.3201385) (cit. on p. 14).
- [257] Adriana Schulz, Jie Xu, Bo Zhu, Changxi Zheng, Eitan Grinspun, and Wojciech Matusik. “Interactive Design Space Exploration and Optimization for CAD Models”. In: *ACM Trans. Graph.* 36.4 (July 2017). ISSN: 0730-0301. DOI: [10.1145/3072959.3073688](https://doi.org/10.1145/3072959.3073688) (cit. on p. 14).
- [258] Christian Schumacher, Bernd Bickel, Jan Rys, Steve Marschner, Chiara Daraio, and Markus Gross. “Microstructures to Control Elasticity in 3D Printing”. In: *ACM Trans. Graph.* 34.4 (July 2015), 136:1–136:13. ISSN: 0730-0301. DOI: [10.1145/2766926](https://doi.org/10.1145/2766926) (cit. on pp. 16, 71).
- [259] Yuliy Schwartzburg and Mark Pauly. “Fabrication-aware design with intersecting planar pieces”. In: *Computer Graphics Forum*. Vol. 32. 2pt3. Wiley Online Library. 2013, pp. 317–326 (cit. on p. 15).
- [260] Julia Schwarz, Chris Harrison, Scott Hudson, and Jennifer Mankoff. “Cord Input: An Intuitive, High-accuracy, Multi-degree-of-freedom Input Method for Mobile Devices”. In: *Proceedings of the SIGCHI Conference on Human Factors in Computing Systems*. CHI ’10. Atlanta, Georgia, USA: ACM, 2010, pp. 1657–1660. DOI: [10.1145/1753326.1753573](https://doi.org/10.1145/1753326.1753573) (cit. on pp. 28, 72).
- [261] Ashish Kumar Sen. *Coated textiles: principles and applications*. Crc Press, 2007 (cit. on p. 34).

- [262] Dietmar Seyferth. *Pre-ceramic polymers: Past, present and future*. Tech. rep. MASSACHUSETTS INST OF TECH CAMBRIDGE DEPT OF CHEMISTRY, 1992 (cit. on p. 8).
- [263] Corey Shemelya, Angel De La Rosa, Angel R Torrado, Kevin Yu, Jennifer Domanowski, Peter J Bonacuse, Richard E Martin, Michael Juhasz, Frances Hurwitz, Ryan B Wicker, et al. “Anisotropy of thermal conductivity in 3D printed polymer matrix composites for space based cube satellites”. In: *Additive Manufacturing* 16 (2017), pp. 186–196 (cit. on p. 20).
- [264] Jennifer J Shen. “Comparative life cycle assessment of polylactic acid (PLA) and polyethylene terephthalate (PET)”. In: *Comparative Assessment of PLA and PET* (2011) (cit. on p. 93).
- [265] Madlaina Signer, Alexandra Ion, and Olga Sorkine-Hornung. “Developable Metamaterials: Mass-Fabricable Metamaterials by Laser-Cutting Elastic Structures”. In: *Proceedings of the 2021 CHI Conference on Human Factors in Computing Systems*. New York, NY, USA: Association for Computing Machinery, 2021 (cit. on p. 17).
- [266] Michael Sivetz and Norman W. Desrosier. “Coffee technology”. In: (1979) (cit. on p. 97).
- [267] Mélina Skouras, Bernhard Thomaszewski, Bernd Bickel, and Markus Gross. “Computational design of rubber balloons”. In: *Computer Graphics Forum*. Vol. 31. 2pt4. Wiley Online Library. 2012, pp. 835–844 (cit. on p. 15).
- [268] Mélina Skouras, Bernhard Thomaszewski, Stelian Coros, Bernd Bickel, and Markus Gross. “Computational design of actuated deformable characters”. In: *ACM Transactions on Graphics (TOG)* 32.4 (2013), pp. 1–10 (cit. on p. 16).
- [269] Mélina Skouras, Bernhard Thomaszewski, Peter Kaufmann, Akash Garg, Bernd Bickel, Eitan Grinspun, and Markus Gross. “Designing inflatable structures”. In: *ACM Transactions on Graphics (TOG)* 33.4 (2014), pp. 1–10 (cit. on p. 15).
- [270] Mark A Skylar-Scott, Jochen Mueller, Claas W Visser, and Jennifer A Lewis. “Voxelated soft matter via multimaterial multinozzle 3D printing”. In: *Nature* 575.7782 (2019), pp. 330–335 (cit. on pp. 11, 26).
- [271] Haichuan Song, Jonàs Martínez, Pierre Bedell, Noémie Vennin, and Sylvain Lefebvre. “Colored Fused Filament Fabrication”. In: *ACM Trans. Graph.* 38.5 (June 2019). ISSN: 0730-0301. DOI: [10.1145/3183793](https://doi.org/10.1145/3183793) (cit. on p. 18).
- [272] Katherine W Song and Eric Paulos. “Unmaking: Enabling and Celebrating the Creative Material of Failure, Destruction, Decay, and Deformation”. In: *Proceedings of the 2021 CHI Conference on Human Factors in Computing Systems*. CHI ’21. Yokohama, Japan: Association for Computing Machinery, 2021. DOI: [10.1145/3411764.3445529](https://doi.org/10.1145/3411764.3445529) (cit. on p. 100).
- [273] Peng Song, Bailin Deng, Ziqi Wang, Zhichao Dong, Wei Li, Chi-Wing Fu, and Ligang Liu. “Cofifab: Coarse-to-Fine Fabrication of Large 3D Objects”. In: *ACM Trans. Graph.* 35.4 (July 2016). ISSN: 0730-0301. DOI: [10.1145/2897824.2925876](https://doi.org/10.1145/2897824.2925876) (cit. on p. 23).
- [274] Peng Song, Zhongqi Fu, Ligang Liu, and Chi-Wing Fu. “Printing 3D objects with interlocking parts”. In: *Computer Aided Geometric Design* 35 (2015), pp. 137–148 (cit. on p. 16).
- [275] Ruoyu Song, Cassandra Telenko, and GW WOODRUFF. “Material waste of commercial FDM printers under realistic conditions”. In: *Solid Freeform Fabrication 2016: Proceedings of the 26th Annual International Solid Freeform Fabrication 2016: Proceedings of the 27th Annual International Solid Freeform Fabrication Symposium—An Additive Manufacturing Conference*. 2016, pp. 1217–1229 (cit. on pp. 92, 100).
- [276] Guido Sonnemann and Sonia Valdivia. “The UNEP/SETAC life cycle initiative”. In: *Background and Future Prospects in Life Cycle Assessment*. Springer, 2014, pp. 107–144 (cit. on p. 114).
- [277] Ondrej Stava, Juraj Vanek, Bedrich Benes, Nathan Carr, and Radomír Měch. “Stress relief: improving structural strength of 3D printable objects”. In: *ACM Transactions on Graphics (TOG)* 31.4 (2012), pp. 1–11 (cit. on p. 15).

- [278] Lingyun Sun, Jiaji Li, Yu Chen, Yue Yang, Ye Tao, Guanyun Wang, and Lining Yao. “4DTexture: A Shape-Changing Fabrication Method for 3D Surfaces with Texture”. In: *Extended Abstracts of the 2020 CHI Conference on Human Factors in Computing Systems Extended Abstracts*. CHI ’20. Honolulu, HI, USA: Association for Computing Machinery, 2020, pp. 1–7. DOI: [10.1145/3334480.3383053](https://doi.org/10.1145/3334480.3383053) (cit. on pp. 20, 21).
- [279] Ivan E. Sutherland. “Sketchpad: A Man-Machine Graphical Communication System”. In: AFIPS ’63 (Spring) (1963), pp. 329–346. DOI: [10.1145/1461551.1461591](https://doi.org/10.1145/1461551.1461591) (cit. on p. 14).
- [280] Ryo Suzuki, Junichi Yamaoka, Daniel Leithinger, Tom Yeh, Mark D. Gross, Yoshihiro Kawahara, and Yasuaki Kakehi. “Dynablock: Dynamic 3D Printing for Instant and Reconstructable Shape Formation”. In: *Proceedings of the 31st Annual ACM Symposium on User Interface Software and Technology*. UIST ’18. Berlin, Germany: Association for Computing Machinery, 2018, pp. 99–111. DOI: [10.1145/3242587.3242659](https://doi.org/10.1145/3242587.3242659) (cit. on p. 25).
- [281] Ryo Suzuki, Koji Yatani, Mark D. Gross, and Tom Yeh. “Tabby: Explorable Design for 3D Printing Textures”. In: *Pacific Graphics Short Papers*. Ed. by Hongbo Fu, Abhijeet Ghosh, and Johannes Kopf. The Eurographics Association, 2018. DOI: [10.2312/pg.20181273](https://doi.org/10.2312/pg.20181273) (cit. on p. 21).
- [282] Saiganesh Swaminathan, Kadri Bugra Ozutemiz, Carmel Majidi, and Scott E. Hudson. “FiberWire: Embedding Electronic Function into 3D Printed Mechanically Strong, Lightweight Carbon Fiber Composite Objects”. In: *Proceedings of the 2019 CHI Conference on Human Factors in Computing Systems*. CHI ’19. Glasgow, Scotland Uk: Association for Computing Machinery, 2019. DOI: [10.1145/3290605.3300797](https://doi.org/10.1145/3290605.3300797) (cit. on p. 24).
- [283] Hiroko Tabuchi. *Cardboard Box Composting*. 2020. URL: <https://docs.google.com/document/d/1DpkZ6a8rpuWYRgtKbHZ19ijzz078F6QG0Hw2-8S0jjpg/mobilebasic> (cit. on p. 109).
- [284] Hiroko Tabuchi. *The Compost by My Couch: How (and Why) I Started an Odorless Bin at Home - The New York Times*. 2020. URL: <https://www.nytimes.com/2020/05/06/climate/new-york-coronavirus-composting.html> (cit. on p. 109).
- [285] Yasaman Tahouni, Tiffany Cheng, Dylan Wood, Renate Sachse, Rebecca Thierer, Manfred Bischoff, and Achim Menges. “Self-Shaping Curved Folding: A 4D-Printing Method for Fabrication of Self-Folding Curved Crease Structures”. In: *Symposium on Computational Fabrication*. SCF ’20. Virtual Event, USA: Association for Computing Machinery, 2020. DOI: [10.1145/3424630.3425416](https://doi.org/10.1145/3424630.3425416) (cit. on p. 112).
- [286] Haruki Takahashi and Jeeun Kim. “3D Printed Fabric: Techniques for Design and 3D Weaving Programmable Textiles”. In: *Proceedings of the 32nd Annual ACM Symposium on User Interface Software and Technology*. UIST ’19. New Orleans, LA, USA: Association for Computing Machinery, 2019, pp. 43–51. DOI: [10.1145/3332165.3347896](https://doi.org/10.1145/3332165.3347896) (cit. on p. 28).
- [287] Alexander Teibrich, Stefanie Mueller, François Guimbretière, Robert Kovacs, Stefan Neubert, and Patrick Baudisch. “Patching physical objects”. In: *Proceedings of the 28th Annual ACM Symposium on User Interface Software & Technology*. UIST ’15. Daegu, Kyungpook, Republic of Korea: ACM, 2015, pp. 83–91. DOI: [10.1145/2807442.2807467](https://doi.org/10.1145/2807442.2807467) (cit. on pp. 23, 94).
- [288] *The world’s leading, high performance, open source Life Cycle Assessment software*. Green Delta, 2021. URL: <https://www.openlca.org/> (cit. on p. 114).
- [289] Chloé Thomas, Cécile Grémy-Gros, Aurélie Perrin, Ronan Symoneaux, and Isabelle Maître. “Implementing LCA early in food innovation processes: Study on spirulina-based food products”. In: *Journal of Cleaner Production* 268 (2020) (cit. on p. 114).
- [290] Bernhard Thomaszewski, Stelian Coros, Damien Gauge, Vittorio Megaro, Eitan Grinspun, and Markus Gross. “Computational design of linkage-based characters”. In: *ACM Transactions on Graphics (TOG)* 33.4 (2014), pp. 1–9 (cit. on pp. 15, 16).
- [291] Skylar Tibbits, Carrie McKnelly, Carlos Olguin, Daniel Dikovsky, and Shai Hirsch. “4D Printing and universal transformation”. In: (2014) (cit. on p. 20).

- [292] Cesar Torres, Tim Campbell, Neil Kumar, and Eric Paulos. “HapticPrint: Designing Feel Aesthetics for Digital Fabrication”. In: *Proceedings of the 28th Annual ACM Symposium on User Interface Software & Technology*. UIST ’15. Charlotte, NC, USA: Association for Computing Machinery, 2015, pp. 583–591. DOI: [10.1145/2807442.2807492](https://doi.org/10.1145/2807442.2807492) (cit. on p. 21).
- [293] Cesar Torres, Jasper O’Leary, Molly Nicholas, and Eric Paulos. “Illumination Aesthetics: Light as a Creative Material within Computational Design”. In: *Proceedings of the 2017 CHI Conference on Human Factors in Computing Systems*. CHI ’17. Denver, Colorado, USA: Association for Computing Machinery, 2017, pp. 6111–6122. DOI: [10.1145/3025453.3025466](https://doi.org/10.1145/3025453.3025466) (cit. on p. 25).
- [294] Phylis G Tortora and Billie J Collier. *Understanding textiles*. 1997 (cit. on p. 34).
- [295] Nancy M. Trautmann and Marianne E. Krasny. *Composting in the classroom: Scientific inquiry for high school students*. Kendall/Hunt Publishing Company, 1998. ISBN: 0-7872-4433-3. URL: <https://ecommons.cornell.edu/bitstream/handle/1813/3338/?sequence=1> (cit. on pp. 108, 113).
- [296] Thibault Tricard, Vincent Tavernier, Cédric Zanni, Jonàs Martínez, Pierre-Alexandre Hugron, Fabrice Neyret, and Sylvain Lefebvre. *Freely orientable microstructures for designing deformable 3D prints*. Research Report. Université de Lorraine, CNRS, Inria, LORIA ; Université Grenoble Alpes, CNRS, Laboratoire Jean Kuntzmann, Inria, Mar. 2020 (cit. on pp. 16, 29).
- [297] Steve Tsang, Ravin Balakrishnan, Karan Singh, and Abhishek Ranjan. “A suggestive interface for image guided 3D sketching”. In: *Proceedings of the SIGCHI conference on Human Factors in Computing Systems*. 2004, pp. 591–598 (cit. on p. 14).
- [298] John R Tumbleston, David Shirvanyants, Nikita Ermoshkin, Rima Januszewicz, Ashley R Johnson, David Kelly, Kai Chen, Robert Pinschmidt, Jason P Rolland, Alexander Ermoshkin, et al. “Continuous liquid interface production of 3D objects”. In: *Science* 347.6228 (2015), pp. 1349–1352 (cit. on pp. 8, 26).
- [299] Edidiong Nseowo Udofia and Wenchao Zhou. “3D printed optics with a soft and stretchable optical material”. In: *Additive Manufacturing* 31 (2020), p. 100912 (cit. on pp. 27, 29).
- [300] Erva Ulu, Emrullah Korkmaz, Kubilay Yay, O Burak Ozdoganlar, and Levent Burak Kara. “Enhancing the structural performance of additively manufactured objects through build orientation optimization”. In: *Journal of Mechanical Design* 137.11 (2015) (cit. on p. 15).
- [301] Nobuyuki Umetani, Danny M Kaufman, Takeo Igarashi, and Eitan Grinspun. “Sensitive couture for interactive garment modeling and editing.” In: *ACM Trans. Graph.* 30.4 (2011), p. 90 (cit. on p. 15).
- [302] Nobuyuki Umetani and Ryan Schmidt. “Cross-sectional structural analysis for 3D printing optimization.” In: *SIGGRAPH Asia Technical Briefs*. Citeseer. 2013, pp. 5–1 (cit. on p. 15).
- [303] Francisca Gil Ureta, Chelsea Tymms, and Denis Zorin. “Interactive modeling of mechanical objects”. In: *Computer Graphics Forum*. Vol. 35. 5. Wiley Online Library. 2016, pp. 145–155 (cit. on p. 16).
- [304] Ben Utela, Duane Storti, Rhonda Anderson, and Mark Ganter. “A review of process development steps for new material systems in three dimensional printing (3DP)”. In: *Journal of Manufacturing Processes* 10.2 (2008), pp. 96–104 (cit. on pp. 9, 10).
- [305] Tatyana Vasilevitsky and Amit Zoran. “Steel-Sense: Integrating Machine Elements with Sensors by Additive Manufacturing”. In: *Proceedings of the 2016 CHI Conference on Human Factors in Computing Systems*. CHI ’16. San Jose, California, USA: Association for Computing Machinery, 2016, pp. 5731–5742. DOI: [10.1145/2858036.2858309](https://doi.org/10.1145/2858036.2858309) (cit. on p. 25).
- [306] Eldy S Lazaro Vasquez, Hao-Chuan Wang, and Katia Vega. “The Environmental Impact of Physical Prototyping: a Five-Year CHI Review”. In: *SelfSustainableCHI 2020* (2020) (cit. on p. 92).
- [307] Joshua Vasquez, Hannah Twigg-Smith, Jasper Tran O’Leary, and Nadya Peek. “Jubilee: An Extensible Machine for Multi-Tool Fabrication”. In: *Proceedings of the 2020 CHI Conference on Human Factors in Computing Systems*. CHI ’20. Honolulu, HI, USA: Association for Computing Machinery, 2020, pp. 1–13. DOI: [10.1145/3313831.3376425](https://doi.org/10.1145/3313831.3376425) (cit. on pp. 11, 26, 29, 117).

- [308] Marynel Vázquez, Eric Brockmeyer, Ruta Desai, Chris Harrison, and Scott E. Hudson. “3D Printing Pneumatic Device Controls with Variable Activation Force Capabilities”. In: *Proceedings of the 33rd Annual ACM Conference on Human Factors in Computing Systems*. CHI ’15. Seoul, Republic of Korea: Association for Computing Machinery, 2015, pp. 1295–1304. DOI: [10.1145/2702123.2702569](https://doi.org/10.1145/2702123.2702569) (cit. on p. 21).
- [309] J Venugopal and S Ramakrishna. “Applications of polymer nanofibers in biomedicine and biotechnology”. In: *Applied biochemistry and biotechnology* 125.3 (2005), pp. 147–157 (cit. on p. 72).
- [310] Kiril Vidimče, Alexandre Kaspar, Ye Wang, and Wojciech Matusik. “Foundry: Hierarchical Material Design for Multi-Material Fabrication”. In: *Proceedings of the 29th Annual Symposium on User Interface Software and Technology*. UIST ’16. Tokyo, Japan: Association for Computing Machinery, 2016, pp. 563–574. DOI: [10.1145/2984511.2984516](https://doi.org/10.1145/2984511.2984516) (cit. on p. 22).
- [311] Kiril Vidimče, Szu-Po Wang, Jonathan Ragan-Kelley, and Wojciech Matusik. “OpenFab: A Programmable Pipeline for Multi-Material Fabrication”. In: *ACM Trans. Graph.* 32.4 (July 2013). ISSN: 0730-0301. DOI: [10.1145/2461912.2461993](https://doi.org/10.1145/2461912.2461993) (cit. on p. 22).
- [312] Anita Vogl, Patrick Parzer, Teo Babic, Joanne Leong, Alex Olwal, and Michael Haller. “StretchEBand: Enabling Fabric-based Interactions Through Rapid Fabrication of Textile Stretch Sensors”. In: *Proceedings of the 2017 CHI Conference on Human Factors in Computing Systems*. CHI ’17. Denver, Colorado, USA: ACM, 2017, pp. 2617–2627. DOI: [10.1145/3025453.3025938](https://doi.org/10.1145/3025453.3025938) (cit. on pp. 28, 57, 71).
- [313] Ludwig Wilhelm Wall, Alec Jacobson, Daniel Vogel, and Oliver Schneider. “Scrappy: Using Scrap Material as Infill to Make Fabrication More Sustainable”. In: *Proceedings of the 2021 CHI Conference on Human Factors in Computing Systems*. New York, NY, USA: Association for Computing Machinery, 2021 (cit. on p. 94).
- [314] Guanyun Wang, Tingyu Cheng, Youngwook Do, Humphrey Yang, Ye Tao, Jianzhe Gu, Byoungkwon An, and Lining Yao. “Printed Paper Actuator: A Low-cost Reversible Actuation and Sensing Method for Shape Changing Interfaces”. In: *Proceedings of the 2018 CHI Conference on Human Factors in Computing Systems*. ACM, 2018, p. 569 (cit. on p. 60).
- [315] Guanyun Wang, Ye Tao, Ozguc Bertug Capunaman, Humphrey Yang, and Lining Yao. “A-line: 4D Printing Morphing Linear Composite Structures”. In: *Proceedings of the 2019 CHI Conference on Human Factors in Computing Systems*. 2019, pp. 1–12 (cit. on p. 20).
- [316] Guanyun Wang, Humphrey Yang, Zeyu Yan, Nurcan Gecer Ulu, Ye Tao, Jianzhe Gu, Levent Burak Kara, and Lining Yao. “4DMesh: 4D Printing Morphing Non-Developable Mesh Surfaces”. In: *The 31st Annual ACM Symposium on User Interface Software and Technology*. ACM, 2018, pp. 623–635 (cit. on pp. 20, 112).
- [317] Guanyun Wang, Lining Yao, Wen Wang, Jifei Ou, Chin-Yi Cheng, and Hiroshi Ishii. “XPrint: A Modularized Liquid Printer for Smart Materials Deposition”. In: *Proceedings of the 2016 CHI Conference on Human Factors in Computing Systems*. New York, NY, USA: Association for Computing Machinery, 2016, pp. 5743–5752. DOI: [10.1145/2858036.2858281](https://doi.org/10.1145/2858036.2858281) (cit. on pp. 27, 29, 117).
- [318] Lifeng Wang, Jacky Lau, Edwin L Thomas, and Mary C Boyce. “Co-continuous composite materials for stiffness, strength, and energy dissipation”. In: *Advanced Materials* 23.13 (2011), pp. 1524–1529 (cit. on p. 16).
- [319] Lingfeng Wang and Emily Whiting. “Buoyancy optimization for computational fabrication”. In: *Computer Graphics Forum*. Vol. 35. 2. Wiley Online Library, 2016, pp. 49–58 (cit. on p. 15).
- [320] Weiming Wang, Tuanfeng Y Wang, Zhouwang Yang, Ligang Liu, Xin Tong, Weihua Tong, Jiansong Deng, Falai Chen, and Xiuping Liu. “Cost-effective printing of 3D objects with skin-frame structures”. In: *ACM Transactions on Graphics (TOG)* 32.6 (2013), pp. 1–10 (cit. on p. 15).
- [321] Wen Wang, Lining Yao, Teng Zhang, Chin-Yi Cheng, Daniel Levine, and Hiroshi Ishii. “Transformative Appetite: Shape-Changing Food Transforms from 2D to 3D by Water Interaction through Cooking”. In: *Proceedings of the 2017 CHI Conference on Human Factors in Computing Systems*. CHI ’17. Denver, Colorado, USA: Association for Computing Machinery, 2017, pp. 6123–6132. DOI: [10.1145/3025453.3026019](https://doi.org/10.1145/3025453.3026019) (cit. on p. 58).

- [322] Xifan Wang, Franziska Schmidt, Dorian Hanaor, Paul H Kamm, Shuang Li, and Aleksander Gurlo. “Additive manufacturing of ceramics from preceramic polymers: A versatile stereolithographic approach assisted by thiol-ene click chemistry”. In: *Additive Manufacturing* 27 (2019), pp. 80–90 (cit. on p. 8).
- [323] Ya Nan Wang, Yun Xuan Weng, and Lei Wang. “Characterization of interfacial compatibility of polylactic acid and bamboo flour (PLA/BF) in biocomposites”. In: *Polymer Testing* 36 (June 2014), pp. 119–125. ISSN: 0142-9418. DOI: [10.1016/J.POLYMERTESTING.2014.04.001](https://doi.org/10.1016/j.polymeresting.2014.04.001) (cit. on p. 94).
- [324] Michael Wessely, Theophanis Tsandilas, and Wendy E. Mackay. “Shape-Aware Material: Interactive Fabrication with ShapeMe”. In: *Proceedings of the 31st Annual ACM Symposium on User Interface Software and Technology*. UIST ’18. Berlin, Germany: Association for Computing Machinery, 2018, pp. 127–139. DOI: [10.1145/3242587.3242619](https://doi.org/10.1145/3242587.3242619) (cit. on p. 117).
- [325] Irmandy Wicaksono and Joseph A. Paradiso. “Fabrickeyboard: multimodal textile sensate media as an expressive and deformable musical interface”. In: *17th International Conference on New Interfaces for Musical Expression, NIME 2017, Aalborg University, Copenhagen, Denmark, May 15-18, 2017*. 2017, pp. 348–353 (cit. on pp. 28, 57, 71).
- [326] Kelly Widdicks, Mike Hazas, Oliver Bates, and Adrian Friday. “Streaming, Multi-Screens and YouTube: The New (Unsustainable) Ways of Watching in the Home”. In: *Proceedings of the 2019 CHI Conference on Human Factors in Computing Systems*. New York, NY, USA: Association for Computing Machinery, 2019, pp. 1–13. ISBN: 9781450359702 (cit. on p. 91).
- [327] Kelly Widdicks and Daniel Pargman. “Breaking the Cornucopian Paradigm: Towards Moderate Internet Use in Everyday Life”. In: *Proceedings of the Fifth Workshop on Computing within Limits*. LIMITS ’19. Lappeenranta, Finland: Association for Computing Machinery, 2019. ISBN: 9781450372817. DOI: [10.1145/3338103.3338105](https://doi.org/10.1145/3338103.3338105) (cit. on p. 91).
- [328] John T. Williams. *Textiles for cold weather apparel*. Elsevier, 2009 (cit. on p. 35).
- [329] Kristin Williams, Rajitha Pulivarthy, Scott E. Hudson, and Jessica Hammer. “Understanding Family Collaboration Around Lightweight Modification of Everyday Objects in the Home”. In: *Proc. ACM Hum.-Comput. Interact.* 3.CSCW (Nov. 2019). DOI: [10.1145/3359287](https://doi.org/10.1145/3359287) (cit. on p. 118).
- [330] Kristin Williams, Rajitha Pulivarthy, Scott E. Hudson, and Jessica Hammer. “The Upcycled Home: Removing Barriers to Lightweight Modification of the Home’s Everyday Objects”. In: *Conference on Human Factors in Computing Systems - Proceedings* (Apr. 2020). DOI: [10.1145/3313831.3376314](https://doi.org/10.1145/3313831.3376314) (cit. on p. 118).
- [331] Karl Willis, Eric Brockmeyer, Scott Hudson, and Ivan Poupyrev. “Printed Optics: 3D Printing of Embedded Optical Elements for Interactive Devices”. In: *Proceedings of the 25th Annual ACM Symposium on User Interface Software and Technology*. UIST ’12. Cambridge, Massachusetts, USA: Association for Computing Machinery, 2012, pp. 589–598. DOI: [10.1145/2380116.2380190](https://doi.org/10.1145/2380116.2380190) (cit. on p. 18).
- [332] Karl D. D. Willis and Andrew D. Wilson. “InfraStructs: Fabricating Information inside Physical Objects for Imaging in the Terahertz Region”. In: *ACM Trans. Graph.* 32.4 (July 2013). ISSN: 0730-0301. DOI: [10.1145/2461912.2461936](https://doi.org/10.1145/2461912.2461936) (cit. on p. 18).
- [333] Terry Wohlers and Tim Gornet. “History of additive manufacturing”. In: *Wohlers report 2018: 3D printing and additive manufacturing state of the industry: annual worldwide progress report*. (2018) (cit. on p. 7).
- [334] Rundong Wu, Huaishu Peng, François Guimbretière, and Steve Marschner. “Printing Arbitrary Meshes with a 5DOF Wireframe Printer”. In: *ACM Trans. Graph.* 35.4 (July 2016). ISSN: 0730-0301. DOI: [10.1145/2897824.2925966](https://doi.org/10.1145/2897824.2925966) (cit. on p. 15).
- [335] Shanel Wu and Laura Devendorf. “Unfabricate: Designing Smart Textiles for Disassembly”. In: *Proceedings of the 2020 CHI Conference on Human Factors in Computing Systems*. New York, NY, USA: Association for Computing Machinery, 2020, pp. 1–14 (cit. on p. 91).
- [336] Sung-Yueh Wu, Chen Yang, Wensyang Hsu, and Liwei Lin. “3D-printed microelectronics for integrated circuitry and passive wireless sensors”. In: *Microsystems & Nanoengineering* 1 (2015), p. 15013 (cit. on p. 24).

- [337] Yingwei Wu, Dmitry Isakov, and Patrick S Grant. “Fabrication of composite filaments with high dielectric permittivity for fused deposition 3D printing”. In: *Materials* 10.10 (2017), p. 1218 (cit. on pp. 27, 29).
- [338] Xin Yan, Cong Rao, Lin Lu, Andrei Sharf, Haisen Zhao, and Baoquan Chen. “Strong 3D Printing by TPMS Injection”. In: *IEEE transactions on visualization and computer graphics* (2019) (cit. on p. 23).
- [339] Sang Ho Yoon, Ke Huo, Yunbo Zhang, Guiming Chen, Luis Paredes, Subramanian Chidambaram, and Karthik Ramani. “iSoft: A Customizable Soft Sensor with Real-time Continuous Contact and Stretching Sensing”. In: *Proceedings of the 30th Annual ACM Symposium on User Interface Software and Technology*. UIST ’17. Quebec City, QC, Canada: ACM, 2017, pp. 665–678. DOI: [10.1145/3126594.3126654](https://doi.org/10.1145/3126594.3126654) (cit. on pp. 28, 71).
- [340] Lauren D. Zarzar, Philseok Kim, and Joanna Aizenberg. “Bio-inspired Design of Submerged Hydrogel-Actuated Polymer Microstructures Operating in Response to pH”. In: *Advanced Materials* 23.12 (2011), pp. 1442–1446. DOI: [10.1002/adma.201004231](https://doi.org/10.1002/adma.201004231) (cit. on p. 58).
- [341] Jonas Zehnder, Espen Knoop, Moritz Bächer, and Bernhard Thomaszewski. “Metasilicone: Design and Fabrication of Composite Silicone with Desired Mechanical Properties”. In: *ACM Trans. Graph.* 36.6 (Nov. 2017), 240:1–240:13. ISSN: 0730-0301. DOI: [10.1145/3130800.3130881](https://doi.org/10.1145/3130800.3130881) (cit. on pp. 16, 29, 71).
- [342] Li-Hua Zhang, Xiao-Peng Duan, Xu Yan, Miao Yu, Xin Ning, Yong Zhao, and Yun-Ze Long. “Recent advances in melt electrospinning”. In: *RSC Advances* 6.58 (2016), pp. 53400–53414 (cit. on pp. 79, 80).
- [343] Quan Zhang, Dong Yan, Kai Zhang, and Gengkai Hu. “Pattern transformation of heat-shrinkable polymer by three-dimensional (3D) printing technique”. In: *Scientific reports* 5 (2015), p. 8936 (cit. on p. 20).
- [344] Ran Zhang, Thomas Auzinger, Duygu Ceylan, Wilmot Li, and Bernd Bickel. “Functionality-Aware Retargeting of Mechanisms to 3D Shapes”. In: *ACM Trans. Graph.* 36.4 (July 2017). ISSN: 0730-0301. DOI: [10.1145/3072959.3073710](https://doi.org/10.1145/3072959.3073710) (cit. on p. 16).
- [345] Clement Zheng, Jeeun Kim, Daniel Leithinger, Mark D. Gross, and Ellen Yi-Luen Do. “Mechamagnets: Designing and Fabricating Haptic and Functional Physical Inputs with Embedded Magnets”. In: *Proceedings of the Thirteenth International Conference on Tangible, Embedded, and Embodied Interaction*. TEI ’19. Tempe, Arizona, USA: Association for Computing Machinery, 2019, pp. 325–334. DOI: [10.1145/3294109.3295622](https://doi.org/10.1145/3294109.3295622) (cit. on p. 25).
- [346] Zhihan Clement Zheng. “Everyday Materials for Physical Interactive Systems”. PhD thesis. University of Colorado at Boulder, 2020 (cit. on p. 2).
- [347] Eduard Zhmayev, Daehwan Cho, and Yong Lak Joo. “Modeling of melt electrospinning for semi-crystalline polymers”. In: *Polymer* 51.1 (2010), pp. 274–290 (cit. on p. 76).
- [348] Amit Zoran and Leah Buechley. “Hybrid reassemblage: an exploration of craft, digital fabrication and artifact uniqueness”. In: *Leonardo* 46.1 (2013), pp. 4–10 (cit. on p. 23).
- [349] Amit Zoran and Dror Cohen. “Digital Konditorei: Programmable Taste Structures Using a Modular Mold”. In: *Proceedings of the 2018 CHI Conference on Human Factors in Computing Systems*. CHI ’18. Montreal QC, Canada: Association for Computing Machinery, 2018. DOI: [10.1145/3173574.3173974](https://doi.org/10.1145/3173574.3173974) (cit. on p. 21).